The Interactions of Biogenic and Anthropogenic Gaseous Emissions with Respect to Aerosol Formation in the United States

by

Alexandra Karambelas

A Master's Thesis submitted in partial fulfillment of the requirements for the degree of

Master of Science

Department of Atmospheric and Oceanic Sciences

at the

University of Wisconsin, Madison

December, 2013

Abstract

Fine particulate matter less than 2.5 microns in diameter ($PM_{2.5}$) is composed of primary and secondary aerosols and are harmful to human health. Both anthropogenic and biogenic sources contribute to $PM_{2.5}$. Recent studies of aerosol formation in the southeast U.S. have investigated the interactions between precursor gases emitted from the aforementioned sources with respect to the formation of biogenic secondary organic aerosol (SOA). However, little work has been done on the reverse influence to understand how inorganic aerosol formation is affected by biogenic precursors. In this two-part study, model results from the U.S EPA Community Multi-scale Air Quality (CMAQ) Model are used to evaluate current understanding of aerosol formation and the change in dry deposition over the continental U.S.

Although biogenic emissions contribute to $PM_{2.5}$ via SOA, sensitivity simulations using CMAQ for July 2007 predict that the contribution of biogenic gases to total $PM_{2.5}$ is surprisingly negative. By "zeroing out" biogenic emissions, total $PM_{2.5}$ increases by approximately 10% due to large increases in both particulate sulfate and particulate nitrate. This increase occurs despite a near total elimination of SOA, which is known to contribute significantly to total summertime organic carbon. These simulated results are supported by known atmospheric chemical mechanisms that initiate the gas-phase oxidation of biogenic and anthropogenic precursors in the formation of secondary aerosols. However, the aerosol mechanism fails to capture hydroxyl radical recycling, which is important for the formation of secondary aerosols. The removal of biogenic emissions is shown to yield greater amounts of nucleation and accumulation mode inorganic aerosols, which are subject to reduced dry

deposition. Understanding the non-linear chemical processes represented in CMAQ can support air quality management and model evaluation.

As the second component of this study, continuous real-time measurements of organic aerosols (OA) in Atlanta, GA were analyzed in summer 2011. These observations indicate about 30% of the total OA results from isoprene epoxydiol (IEPOX), an isoprene-derived compound unique to low-NO_X environments. Reactive uptake of gas-phase IEPOX into the aerosol phase is dependent on the availability of IEPOX and aerosol water, as well as the aerosol acidity as determined by anthropogenic gases. Model results indicate the known pathways are represented accurately, though resulting aerosol concentrations are largely under-predicted.

Results from both studies indicate a complex relationship exists between anthropogenic and biogenic emissions and the formation of inorganic and secondary organic aerosols. In Chapter 2, biogenic emissions appear to indirectly prohibit aerosol formation in the eastern U.S. through the preferential gas-phase oxidation reactions of biogenic VOCs. Additionally, the dry deposition of inorganic aerosols is also influenced by biogenic emissions. Chapter 3 results suggest recent updates to the CMAQ isoprene-derived aerosol mechanism improve simulations of isoprene-derived aerosol formation comparatively to ground-based measurements. Overall, the results from this thesis enhance the current understanding of aerosol formation over the continental U.S. and confirm the complexity associated with secondary aerosols.

Acknowledgements

My first round of "Thanks!" goes to my undergraduate, Master's, and soon-to-be Ph.D. advisor, Professor Tracey Holloway. Without her guidance and steady support I would have never had the chance to work with CMAQ and become excited about putting together new modeling experiments. I feel very lucky to have been able to work with and learn from Tracey, and I look forward to having her as my Ph.D. advisor over the next few years.

I especially am grateful for the opportunity to be a member of her research team, as I have had the opportunity to work alongside some wonderful people, including but not limited to Dr. Erica Bickford, Jacob Oberman, Erica Scotty, Dr. Monica Harkey, Arber Rrushaj, Ryan Kladar, and many more. I have been able to learn a lot from the other members of the Holloway Research group, and I definitely know I wouldn't be the researcher I am today without their help and knack for helping me talk through problems.

I thank several amazing scientists at the EPA in Research Triangle Park, NC for introducing me to the detailed world of aerosol chemistry in a whirlwind 12-weeks: Drs. Robert Pinder, Havala Pye, and Shannon Capps. Without the research experience I gained working there, I would not know what IEPOX is or how ISORROPIA works (among other things), and I was grateful to have the opportunity.

I would also like to thank my thesis readers, both official and unofficial: Drs. Ankur Desai, Frank Keutsch, and Robert Pinder, for providing helpful insight into the final edition of this thesis. In addition, I acknowledge and am grateful for the organizations that funded this research: NASA Air Quality Applied Sciences Team, EPA, and the National Center for Freight and Infrastructure Research and Education.

Finally, I dedicate this thesis to my parents for their continued love and support through my educational endeavors, and my younger brother, Matthew, in hopes that he one day will have a career he enjoys as much as I do mine.

Table of Contents

Chapter 1.
Introduction

The United States (U.S.) Environmental Protection Agency (EPA) regulates fine particulate matter less than 2.5 μm in diameter ($PM_{2.5}$) and coarse particulate matter less than 10 μm in diameter (PM_{10}) under the National Ambient Air Quality Standards (NAAQS). Air quality regulations have been in place since the Clean Air Act (CAA) was enacted in the 1970s, which has resulted in significant improvements in the air quality conditions in the U.S. However, air quality from criteria pollutants, especially $PM_{2.5}$, still poses a significant concern.

Particulates, also known as aerosols, are liquids and solids suspended in the atmosphere, and they come in a broad range of sizes, from nucleated Aitken size particles less than 1 μm in diameter, to larger coarse particles greater than 2.5 μm. Larger particles do not remain suspended for very long, but fine particulates have an average lifetime of ~5 days with rainout as the main removal mechanism. $PM_{2.5}$ including both directly emitted (primary) aerosols and those formed in the atmosphere (secondary aerosols). These in turn come from a variety of sources, both anthropogenic and biogenic. Particulates have implications for health, air quality, and climate change, but the processes by which secondary aerosols form are not fully understood, something that can hinder mitigation strategies.

The work presented in this thesis analyzes the complex atmospheric chemistry associated with aerosol formation processes. Understanding how aerosols form in the atmosphere is necessary for improving air quality mitigation techniques, implementing accurate chemistry in air quality models, and understanding links between climate change and aerosol concentrations. Both anthropogenic and biogenic emissions can contribute to

aerosol formation, but interactions between man-made and naturally emitted compounds introduce complexity into the secondary aerosol formation process. In this thesis, the connections between biogenic and anthropogenic emissions with respect to aerosol formation are evaluated spatially across the U.S. and temporally in Atlanta, Georgia, a location subject to large amounts of both local anthropogenic and nearby biogenic emissions. Air quality model simulations are used in conjunction with ground-based measurements and satellite observations of the gas-phase precursor nitrogen dioxide (NO_2) to evaluate the model and the current understanding of aerosol formation. Ultimately, this thesis aims to answer how and to what extent these interactions influence aerosol concentration in the U.S.

Two distinct experiments are presented that use model simulations to improve the understanding of biogenic and anthropogenic interactions with respect to aerosol formation. First, a model sensitivity study is used to target the biogenic contribution to total $PM_{2.5}$. To accomplish this, a model simulation without biogenic emissions included is compared to a base case simulation that includes all emission sectors. The difference between the two scenarios represents the bulk contribution to total $PM_{2.5}$ solely from biogenic emissions. In a second experiment, explicit isoprene-derived secondary organic aerosol (SOA) formation is investigated using model simulations with an updated aerosol pathway. A sensitivity simulation with the same pathway aims to produce isoprene-derived SOA concentrations comparable to measurements with the assumption that additional unknown aerosol species exist. The conclusions of these experiments have implications for atmospheric chemistry and air quality management.

Particulate Pollution Regulation

Fine particulate matter contributes negatively to human health, visibility, cloud processes, and the radiative balance of the earth. The smallest aerosols can cause detrimental health effects to both the respiratory and the cardiovascular systems, leading to hearth disease, lung disease, asthma, chronic bronchitis, and premature death (Burgan et al., 2010; Norris et al., 1999; Risom et al., 2005). Studies have found that a disproportionate increase in the number of hospital visits and deaths associated with very small increases in particulate pollution (Abbey et al., 1999; Brunekreef & Holgate, 2002). Accumulation of $PM_{2.5}$ in urban and rural areas can also cause disruptions due to decreased visibility, most noticeable in pristine regions of the U.S. such as national parks where influxes of increased $PM_{2.5}$ can lead to extremely low visibility. Aerosols also have a profound effect on cloud processes. Fine particulates may act as cloud condensation nuclei (CCN), where cloud particles can form on the surface of aerosols (Ervens et al., 2011). More CCN leads to a cloud made of many small droplets that are less likely to precipitate out of the cloud and yield brighter clouds that are more reflective, thus having a negative impact on local radiative balance and can cause short-term cooling (Albrecht, 1989). Other particulates such as black carbon are absorbing particles and can contribute to warming (Jacobson, 2010). The complexity of aerosols and the uncertainty of their influence on climate change is reported by the Intergovernmental Panel on Climate Change (IPCC, 2013) in assessment reports, where the need for further research is emphasized.

Air pollution regulations enforced by the U.S. EPA NAAQS are established based on both primary and secondary standards. Primary standards are in place to regulate pollution with respect to human health, and secondary standards are set to ensure the protection of

public welfare, including visibility as well as crop, livestock, and building protection. Current $PM_{2.5}$ primary standards are an annual average not to exceed 12 $\mu g/m^3$, with secondary standards enforcing an annual average of 15 $\mu g/m^3$. Additionally, a second primary and secondary standard of 35 $\mu g/m^3$ daily average is set to ensure minimal repercussions from short-term exposure to aerosols. These standards were most recently revised in December of 2012.

Counties that cannot meet these regulation standards are designated as non-attainment regions and are required to develop air pollution mitigation strategies through State Implementation Plans (SIPs). A map of counties designated as non-attainment according the most recent 2006 1-day average standard of 35 $\mu g/m^3$ is shown in Figure 1.1. Most non-attainment areas are located near highly populated regions such as the northeastern U.S. and much of central California. Regions are designated as non-attainment through measurements taken by ground-based monitors.

Air quality monitoring occurs through the use of ground-based monitors dispersed across the U.S. Ground-based monitors are mostly located in highly populated regions due to their installation requirements (e.g. US EPA, 2013a), and thus they may not be not representative of the entire county. Instead, they provide a snapshot of the air quality conditions in a localized area. Certain monitor networks, like the Clean Air Status and Trends Network (CASTNet) are specifically in place to monitor long-term background air quality trends in rural locations (US EPA, 2013b). Although ground-based monitors are the best available source of air quality data, ambient measurements alone do not identify individual sources that may be contributing to poor air quality conditions. However, observations can be used in tandem with air quality modeling to identify large-contributing

sources. Additionally, satellite observations provide greater spatial coverage but are not able to provide high temporal resolution over the U.S.

Fine Particulate Matter Formation Characteristics

Sources of $PM_{2.5}$ include emissions of primary aerosols from combustion processes, electricity generators, biomass burning, dust, as well as the formation of secondary particulates from the oxidation of gaseous precursor species. The wide variety of sources will yield different contributions to total $PM_{2.5}$ across the U.S., where cars and electricity generators are known to contribute more in urban areas and natural sources will contribute more in rural areas (Kleindienst et al., 2010). Figure 1.2 depicts the variety in $PM_{2.5}$ composition at urban sites across the U.S. The eastern U.S. exhibits greater influence from sulfate (SO_4^{2-}) pollution than does the western U.S., due mostly to the large amount of coal-fired electricity generating units in the Ohio River Valley. In contrast, nitrate (NO_3^-) is prominent in all urban areas due to emissions from on-road motor vehicles. Notably, organic carbon makes up a large component of total $PM_{2.5}$ across the U.S. but most significantly in the urban areas surrounded by densely forested regions, like Birmingham, Atlanta, and Seattle. Both biogenic and anthropogenic sources contribute to primary emissions of $PM_{2.5}$ constituents such as black and organic carbon through biomass burning and incomplete combustion, though here we are concerned more so with natural and man-made gaseous precursor emissions that lead to aerosol formation.

Inorganic particulates form in the atmosphere through oxidation reactions involving oxidants and gaseous precursor emissions. Gas-phase precursors include species such as nitrogen oxides (NO_X) that predominantly come from motor vehicles and combustion

processes and sulfur dioxide (SO_2) that is largely emitted from coal-fired power plants. These species can undergo gas-phase oxidation in the atmosphere, however they may also react with oxidants in the aqueous phase to yield aerosol NO_3^- and SO_4^{2-} (Seinfeld & Pandis, 2006). Abundant tropospheric oxidants include the hydroxyl radical (OH) and hydrogen peroxide (H_2O_2) that come from photolytic reactions that break apart oxygen (O_2) and ozone (O_3) (Jacob, 1999a). Aerosol SO_4^{2-} and NO_3^- are highly correlated with the locations of their precursor species (Clarke et al., 1997) and largely contribute to total $PM_{2.5}$ in these regions.

It is also well understood that biogenic emissions contribute heavily to $PM_{2.5}$ through the formation of SOA (Tsigaridis & Kanakidou, 2003; Zhang et al., 2007). Biogenic sources emit volatile organic compounds (VOCs) to the atmosphere that can contribute to the O_3 formation (Jacob, 1999b) or undergo oxidation reactions leading to SOA formation. Compounds contributing to SOA formation include terpenes (Kavouras et al., 1998) and isoprene (Guenther et al., 2006). These compounds contribute significantly to SOA in the summertime (Kleindienst et al., 2007), when biogenic sources are most active. SOA is a large fraction of the total aerosol budget, however SOA formation is not entirely understood (Kanakidou et al., 2005).

With increasing interest in atmospheric chemistry and the role aerosols play in human health and climate change, recent research has investigated aerosols and the anthropogenic connection with biogenic SOA formation (e.g. Carlton et al., 2010; de Gouw & Jimenez, 2009; Weber et al., 2007). Both laboratory and field experiments have made significant advances in isoprene-derived aerosol formation (Claeys et al., 2004; Kleindienst, Edney, Lewandowski, Offenberg, & Jaoui, 2006; Lin et al., 2013) and additionally have studied how acidified aerosol in the vicinity of BVOCs significantly enhances organic aerosol (OA) in the

atmosphere (Shilling et al., 2013; Surratt et al., 2007). Further, model analysis has aimed to understand how reductions in anthropogenic or "controllable" emissions influence biogenic SOA formation (Carlton et al., 2010). While these studies have sought to understand the role anthropogenic emissions play in biogenic SOA formation, however, the influence biogenic emissions have on inorganic aerosols has received less attention.

Research Overview

This thesis will examine aerosol formation and removal processes as simulated by the U.S. EPA Community Multi-scale Air Quality (CMAQ) model. Simulation specific meteorology, emissions, and lateral boundary conditions are used to create the model environment. Chapter 2 examines the reverse interactions in an attempt to understand the influence biogenic emissions play on the formation of inorganic aerosols and total $PM_{2.5}$. A base case model simulation is validated with *in situ* measurements from a rural monitoring network and satellite observations. In this chapter, the connection between anthropogenic emissions, biogenic emissions, and aerosol formation is linked to gas-phase oxidation processes of aerosol precursors. Chapter 3 presents and discusses results from two model simulations with the purpose of evaluating the current knowledge of isoprene-derived aerosol formation pathway. Base case model simulations from late summer 2011 are compared with a unique measurement dataset of one group of isoprene-derived aerosols from Atlanta, GA. A sensitivity simulation increases mass concentrations to be within a factor of two of the measurements. Finally, the overall conclusions and connections between the chapter results are presented, and future work is considered.

Figures

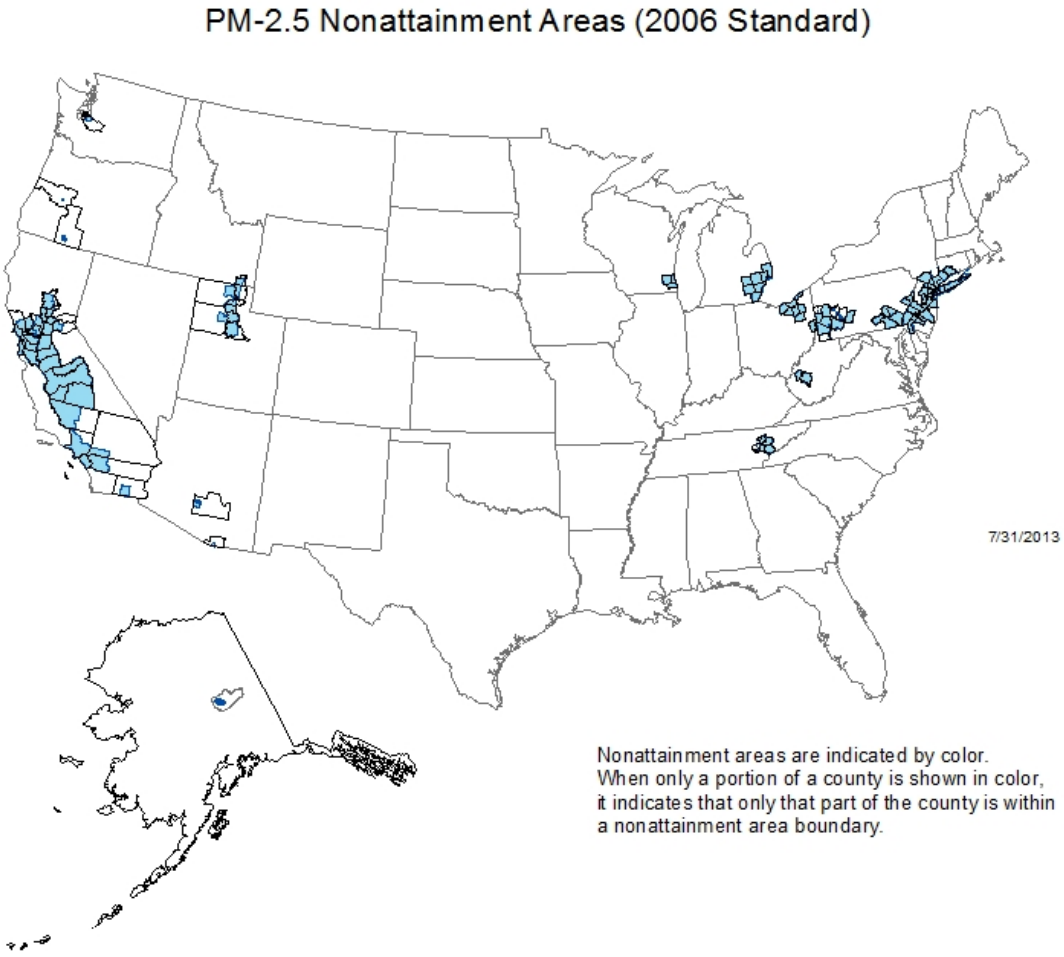

Figure 1.1 U.S. counties designated as non-attainment for the previous $PM_{2.5}$ NAAQS secondary standard of 35 $\mu g/m^3$. *Source: epa.gov*

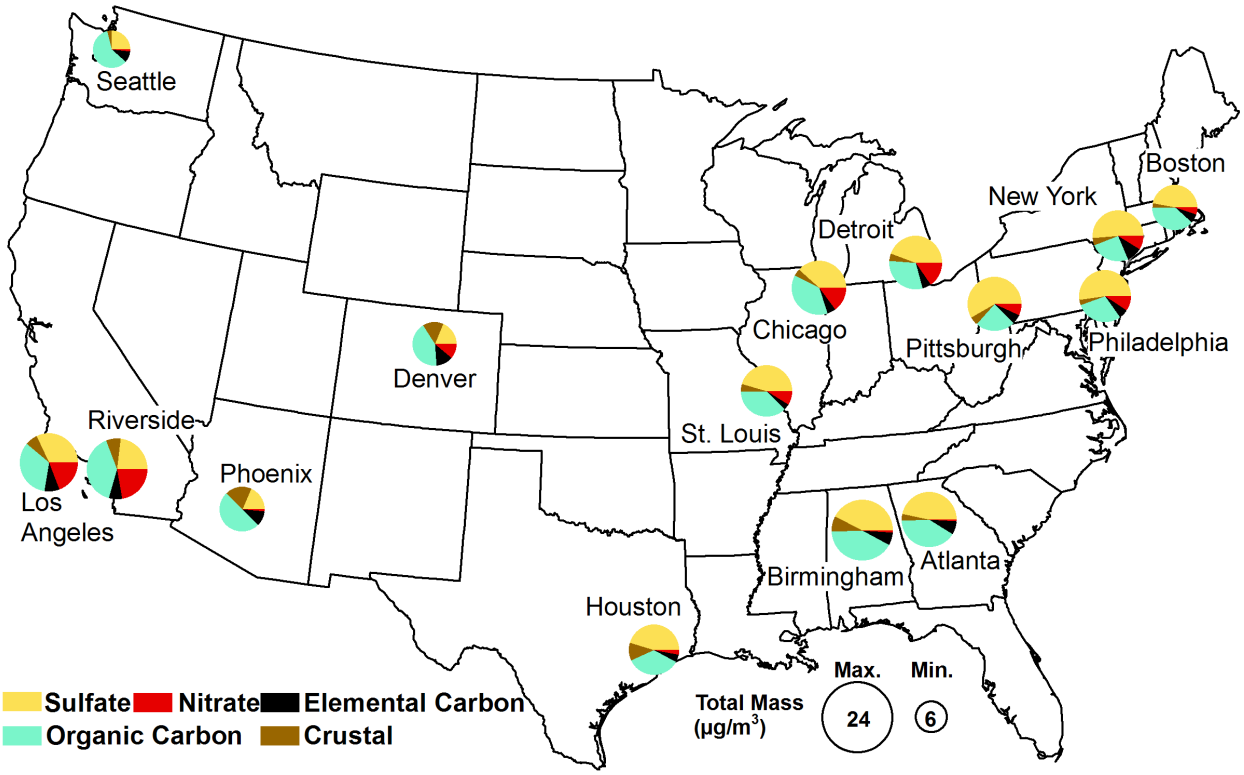

Figure 1.2 U.S. map depicting contributions of various species to total $PM_{2.5}$ and total $PM_{2.5}$ mass averaged over the annual 2008 year. Note the variety in sources contributing to total $PM_{2.5}$ at select urban locations during the course of the year. *Source: epa.gov*

References

Abbey, D. E., Nishino, N., McDonnell, W. F., Burchette, R. J., Knutsen, S. F., Lawrence Beeson, W., & Yang, J. X. (1999). Long-term inhalable particles and other air pollutants related to mortality in nonsmokers. *American journal of respiratory and critical care medicine*, *159*(2), 373–82. doi:10.1164/ajrccm.159.2.9806020

Albrecht, B. A. (1989). Aerosols, Cloud Microphysics, and Fractional Cloudiness. *Science*, *245*, 1227–1230.

Brunekreef, B., & Holgate, S. (2002). Air pollution and health. *The Lancet*, *360*(9341), 1233–1242. doi:10.1016/S0140-6736(02)11274-8

Burgan, O., Smargiassi, A., Perron, S., & Kosatsky, T. (2010). Cardiovascular effects of sub-daily levels of ambient fine particles: a systematic review. *Environmental health : a global access science source*, *9*, 26. doi:10.1186/1476-069X-9-26

Carlton, A. G., Pinder, R. W., Bhave, P. V, Pouliot, G. A., Alexander, T. W., Park, T., & Carolina, N. (2010). To What Extent Can Biogenic SOA be Controlled ? *Environmental Science & Technology*, *44*(9), 3376–3380.

Claeys, M., Graham, B., Vas, G., Wang, W., Vermeylen, R., Pashynska, V., … Maenhaut, W. (2004). Formation of secondary organic aerosols through photooxidation of isoprene. *Science*, *303*(5661), 1173–6. doi:10.1126/science.1092805

Clarke, J., Edgerton, E., & Martin, B. (1997). Dry Deposition Calculations for the Clean Air Status and Trends Network. *Science*, *31*(21), 3667–3678.

De Gouw, J., & Jimenez, J. L. (2009). Organic Aerosols in the Earth's Atmosphere. *Environmental Science & Technology Feature*, *43*(20), 7614–7618.

Ervens, B., Turpin, B. J., & Weber, R. J. (2011). Secondary organic aerosol formation in cloud droplets and aqueous particles (aqSOA): a review of laboratory, field and model studies. *Atmospheric Chemistry and Physics*, *11*(21), 11069–11102. doi:10.5194/acp-11-11069-2011

Guenther, A., Karl, T., Harley, P., Wiedinmyer, C., Palmer, P. I., & Geron, C. (2006). Estimates of global terrestrial isoprene emissions using MEGAN (Model of Emissions of Gases and Aerosols from Nature). *Atmospheric Chemistry and Physics Discussions*, *6*(1), 107–173. doi:10.5194/acpd-6-107-2006

IPCC. (2013). *CLIMATE CHANGE 2013 The Physical Science Basis*.

Jacob, D. J. (1999a). CHAPTER 11 . OXIDIZING POWER OF THE. In *Introduction to Atmospheric Chemistry* (Vol. 3, pp. 199–219).

Jacob, D. J. (1999b). CHAPTER 12 . OZONE AIR POLLUTION. In *Introduction to Atmospher* (pp. 232–243).

Jacobson, M. Z. (2010). Short-term effects of controlling fossil-fuel soot, biofuel soot and gases, and methane on climate, Arctic ice, and air pollution health. *Journal of Geophysical Research*, *115*(D14), D14209. doi:10.1029/2009JD013795

Kanakidou, M., Seinfeld, J. H., Pandis, S. N., Barnes, I., Dentener, F. J., Facchini, M. C., … Wilson, J. (2005). Organic aerosol and global climate modelling: a review. *Atmospheric Chemistry and Physics*, *5*(4), 1053–1123. doi:10.5194/acp-5-1053-2005

Kavouras, I. G., Mihalopoulos, N., & Stephanou, E. G. (1998). Formation of atmospheric particles from organic acids produced by forests. *Nature*, *372*(3), 683–686.

Kleindienst, T. E., Edney, E. O., Lewandowski, M., Offenberg, J. H., & Jaoui, M. (2006). Secondary Organic Carbon and Aerosol Yields from the Irradiations of Isoprene and a-Pinene in the Presence of NOx and SO2. *Environmental Science & Technology*, *40*(12), 3807–3812.

Kleindienst, T. E., Jaoui, M., Lewandowski, M., Offenberg, J. H., Lewis, C. W., Bhave, P. V., & Edney, E. O. (2007). Estimates of the contributions of biogenic and anthropogenic hydrocarbons to secondary organic aerosol at a southeastern US location. *Atmospheric Environment*, *41*(37), 8288–8300. doi:10.1016/j.atmosenv.2007.06.045

Kleindienst, T. E., Lewandowski, M., Offenberg, J. H., Edney, E. O., Jaoui, M., Zheng, M., … Edgerton, E. S. (2010). Contribution of Primary and Secondary Sources to Organic Aerosol and PM2.5 at SEARCH Network Sites. *Journal of Air & Waste Management Association*, *60*, 1388–1399. doi:10.3155/1047-3289.60.11.1388

Lin, Y., Zhang, H., Pye, H. O. T., Zhang, Z., Marth, W. J., Park, S., & Arashiro, M. (2013). Epoxide as a precursor to secondary organic aerosol formation from isoprene photooxidation in the presence of nitrogen oxides. *Proceedings of the National Academy of Sciences*, *110*(17), 6718–6723. doi:10.1073/pnas.1221150110/-/DCSupplemental.www.pnas.org/cgi/doi/10.1073/pnas.1221150110

Norris, G., YoungPong, S. N., Koenig, J. Q., Larson, T. V, Sheppard, L., & Stout, J. W. (1999). An association between fine particles and asthma emergency department visits for children in Seattle. *Environmental health perspectives*, *107*(6), 489–93. Retrieved from http://www.pubmedcentral.nih.gov/articlerender.fcgi?artid=1566574&tool=pmcentrez&rendertype=abstract

Risom, L., Møller, P., & Loft, S. (2005). Oxidative stress-induced DNA damage by particulate air pollution. *Mutation research*, *592*(1-2), 119–37. doi:10.1016/j.mrfmmm.2005.06.012

Seinfeld, J. H., & Pandis, S. N. (2006). *Atmospheric Chemistry and Physics: From Air Pollution to Climate Change*. New York: John Wiley & Sons, Inc.

Shilling, J. E., Zaveri, R. A., Fast, J. D., Kleinman, L., Alexander, M. L., Canagaratna, M. R., … Zhang, Q. (2013). Enhanced SOA formation from mixed anthropogenic and biogenic emissions during the CARES campaign. *Atmospheric Chemistry and Physics*, *13*, 2091–2113. doi:10.5194/acp-13-2091-2013

Surratt, J. D., Kroll, J. H., Kleindienst, T. E., Edney, E. O., Claeys, M., Sorooshian, A., … Seinfeld, J. H. (2007). Evidence for organosulfates in secondary organic aerosol. *Environmental Science & Technology*, *41*(2), 517–27. Retrieved from http://www.ncbi.nlm.nih.gov/pubmed/17969680

Tsigaridis, K., & Kanakidou, M. (2003). Global modelling of secondary organic aerosol in the troposphere: A sensitivity analysis. *Atmospheric Chemistry and Physics Discussions*, *3*(3), 2879–2929. doi:10.5194/acpd-3-2879-2003

US EPA. (2013a). *SO2 NAAQS Designations Source-Oriented Monitoring Technical Assistance Document*.

US EPA. (2013b). *Clean Air Status and Trends Network 2011 Annual Report*. Washington, DC.

Weber, R. J., Sullivan, A. P., Peltier, R. E., Russell, A., Yan, B., Zheng, M., … Edgerton, E. (2007). A study of secondary organic aerosol formation in the anthropogenic-influenced southeastern United States. *Journal of Geophysical Research*, *112*(D13), D13302. doi:10.1029/2007JD008408

Zhang, Y., Huang, J.-P., Henze, D. K., & Seinfeld, J. H. (2007). Role of isoprene in secondary organic aerosol formation on a regional scale. *Journal of Geophysical Research*, *112*(D20), 1–13. doi:10.1029/2007JD008675

Chapter 2.
Simulated Response of Inorganic Aerosol to Biogenic Emissions

Chapter adapted from Karambelas, A., T. Holloway, and E. Bickford. *Simulated response of inorganic aerosol to biogenic emissions*. In preparation for submission.

Introduction

Total fine particulate matter less than 2.5 μm in diameter ($PM_{2.5}$) is composed of a variety of subspecies including sulfate (SO_4^{2-}), nitrate (NO_3^-), organic carbon (OC), elemental carbon, and ammonium (NH_4^+). Carbon particulate compounds are both directly emitted from man-made sources and are formed in the atmosphere from the oxidation of volatile organic compounds (VOCs) emitted from biogenic sources (Kanakidou et al., 2005; Kavouras et al., 1999). Anthropogenic emissions of sulfur dioxide (SO_2) and nitrogen oxides (NO_X) oxidize and react with ammonia (NH_3) to form ammonium salts and contribute to particulate matter in this way (e.g. Gaydos et al., 2005). The composition of $PM_{2.5}$ is unique to local sources of emissions and varies spatially. This study explores the response of total $PM_{2.5}$ and the inorganic subspecies SO_4^{2-} and NO_3^- to the removal of biogenic emissions in the continental U.S.

The influence of SO_2 and NO_x on the formation of SOA has been the subject of previous studies (e.g. Edney et al., 2005; Lin et al., 2013; Surratt et al., 2007, 2008). However, less is known about the role of biogenic VOCs on the formation and growth of particulate SO_4^{2-} and NO_3^-. Here, we employ the U.S. Environmental Protection Agency Community Multi-scale Air Quality (CMAQ) Model to characterize the contributions and the net impact of biogenic emissions on total $PM_{2.5}$, including SO_4^{2-}, NO_3^-, SOA, and other species. First, how SOA and inorganic aerosols contribute to $PM_{2.5}$ will be presented.

Secondary Organic Aerosol Formation

SOA contributes significantly to total $PM_{2.5}$ across the U.S., but is most prevalent in regions with high biogenic emissions. Anthropogenic sources also contribute to SOA formation, although they contribute just a small fraction of total SOA. Both observational analyses (Kleindienst et al., 2010; Lewandowski et al., 2008) and a chemical mass balance modeling approach (Zheng et al., 2007) have shown SOA to contribute more to $PM_{2.5}$ in rural regions than urban areas due to the availability of biogenic sources. Biogenic VOCs that contribute most substantially to SOA include isoprene (Claeys et al., 2004; Surratt et al., 2006) and mono- and sesquiterpene species (Jaoui et al., 2007).

Much of total SOA formation is attributed to the aerosol partitioning of semi-volatile biogenic VOC emissions, as estimated in global model experiments (Henze & Seinfeld, 2006; Tsigaridis & Kanakidou, 2003), filter measurements in the Sierra Nevada Mountains (Cahill et al., 2006), gas chromatography-mass spectrometry in the Amazon rainforest (Claeys et al., 2004) and outdoor chamber experiments (Griffin et al., 1999). Recent research has identified that isoprene aerosol forms via reactive uptake into the aerosol phase (Y. Lin et al., 2013; Surratt et al., 2010).

It is estimated that 50-70% of total SOA is derived from the oxidation of biogenic VOCs under the influence of anthropogenic emissions (Carlton et al., 2010; Shilling et al., 2013; Spracklen et al., 2011). In chamber experiments, the presence of SO_2 and subsequent acidified aerosol increased the amount of isoprene-derived aerosol produced by a factor of 7 (Kleindienst et al., 2006). Recent work in California shows that organic aerosol concentrations are enhanced in the presence of combined anthropogenic and biogenic emissions (Shilling et al., 2013). Despite the exact formation mechanisms remaining unclear,

the transformation from gaseous VOC to SOA begins with the gas-phase oxidation of VOCs by oxidants such as ozone (O_3) and the hydroxyl radical (OH), and nitrate radicals, all of which are known to be influenced by the NO_x emissions (Hurley et al., 2001; Nøjgaard et al., 2006). Therefore, higher emissions of anthropogenic SO_2 and NO_X, and associated increases in SO_4^{2-} and NO_3^-, would be expected to increase SOA.

Inorganic Aerosol Formation and Dry Deposition

Primarily anthropogenic in origin, SO_4^{2-} contributes more than 25% of total $PM_{2.5}$ in the Eastern U.S. (Edgerton et al., 2005). The SO_4^{2-} aerosol formation process is best explained in Seinfeld and Pandis (2006), but a brief explanation is included here. Sulfate production is initiated from the oxidation of anthropogenic-emitted SO_2 to yield sulfuric acid (H_2SO_4). From there, gaseous H_2SO_4 in the presence of water vapor preferentially condenses onto existing particles, or it may nucleate and form new particles from gas-phase H_2SO_4. Dissolved sulfur (IV) can undergo aqueous-phase oxidation to higher order and less volatile sulfur (VI) by hydrogen peroxide (H_2O_2) or O_3 through another sulfate aerosol formation mechanism. The sulfur (IV) to sulfur (VI) conversion pathway becomes important for in-cloud processes or environments of high relative humidity. Atmospheric NH_3 acts to neutralize gas-phase H_2SO_4 to ammonium sulfate, a source of SO_4^{2-} aerosol. The degree to which H_2SO_4 is neutralized influences aerosol acidity, which is important for certain SOA formation pathways (See Chapter 3). Growth of SO_4^{2-} aerosol occurs through vapor condensation onto particles in the accumulation mode.

Another anthropogenic contributor to total $PM_{2.5}$ is NO_3^-, which contributes about 3-7% of the total $PM_{2.5}$ on average annually in rural to urban regions of the southeast U.S.

(Edgerton et al., 2005). Nitrate aerosol forms through both homogenous gas-phase oxidation and heterogeneous aqueous phase reaction and is best explained in Orel and Seinfeld (1977). Daytime oxidation of NO_2 by OH yields HNO_3 vapor, which reacts with NH_3 leftover from H_2SO_4 neutralization to form ammonium nitrate. In the evening, HNO_3 is formed from the reaction of VOCs and NO_3 radical, and HNO_3 proceeds to behave the same as it does in the daytime. Homogenous nucleation of HNO_3 to particle phase is unlikely in normal atmospheric conditions due to its high vapor pressure, and thus most HNO_3 will condense on to existing particles. Similar to SO_4^{2-}, growth of NO_3^- aerosols occurs mainly through the condensation of HNO_3 vapor onto existing particles.

Aerosols are subject to removal by wet deposition through precipitation processes that "clean out" suspended particulates. However, dry deposition should not be ignored as a removal process. Sulfate aerosol, in particular, is heavily impacted by dry deposition, which accounts for 40% of the total sulfur deposition on average (Baumgardner et al., 2002; Butler & Likens, 1995) and up to 55% of total sulfur deposition in forested regions (Linderg & Lovett, 1992). Aerosol dry deposition depends on wind speed, solar radiation, and the type and condition of ground cover (Sheih et al., 1979). Although total sulfur dry deposition has been shown to spatially correlate with gaseous SO_2 precursor concentrations (Clarke et al., 1997), SO_4^{2-} was the major component in sulfur dry deposition in rural areas (Meyers et al., 1991). Annual estimates of SO_4^{2-} dry deposition are much less than SO_2 (Table 2.1), and the same trend holds true for NO_3^- and HNO_3. Total sulfur ($SO_2 + SO_4^{2-}$) and nitrogen ($HNO_3 + NO_3^-$) dry deposition is typically highest in the Ohio River Valley and the eastern U.S. with annual fluxes up to 12 kg/ha and 3.3 kg/ha respectively (Baumgardner et al., 2002). Similarly, highest dry deposition fluxes of SO_4^{2-} and NO_3^- are estimated in the eastern U.S.

(1.5 kg/ha and less than 0.5 kg/ha respectively) (Baumgardner et al., 2002; Meyers et al., 1991).

Interconnectivity of Anthropogenic and Biogenic Aerosol Formation

Past studies have found that reductions of anthropogenic emissions yields significant reductions of SOA, up to 50% compared to base case simulations (Carlton et al., 2010; Stein & Saylor, 2012), and additional studies have examined the influence atmospheric acidity plays in isoprene-derived gas-phase precursor uptake into the aerosol phase (Edney et al., 2005; Lin et al., 2012; Surratt et al., 2007, 2008). However, the reverse influence of biogenic emissions on aerosol formation has not been characterized. While biogenic emissions directly contribute to the $PM_{2.5}$ budget through SOA formation, they may have an influence on both the formation of inorganic aerosols that contribute to $PM_{2.5}$ and the dry deposition removal of inorganic $PM_{2.5}$ subspecies.

In this chapter, we evaluate simulated concentrations and dry deposition fluxes of SO_4^{2-} and NO_3^- from the U.S. EPA Community Multi-scale Air Quality (CMAQ) model against independent estimates from the Clean Air Status and Trends Network (CASTNet) for July 2007. We compare a sensitivity simulation in which biogenic emissions are removed from the model inputs with a base case scenario to characterize how the biogenic sensitivity of SO_4^{2-} and NO_3^- dry deposition affects the total $PM_{2.5}$ budget over the eastern U.S. Simulations presented indicate that there is a preference to oxidize biogenic VOCs in the atmosphere, affecting inorganic aerosol processes. The removal of biogenic compounds is shown in this study to *increase* $PM_{2.5}$ conditions through an indirect relationship between inorganic aerosols and SOA. We evaluate the response of inorganic aerosols to changes in

biogenic emissions, as simulated by CMAQ over the continental U.S. (CONUS). Interestingly, although SOA contributes positively to total $PM_{2.5}$, removing VOCs from a simulated environment causes total $PM_{2.5}$, SO_4^{2-}, and NO_3^- to increase in concentration.

Model Overview

Air Quality Modeling

Model simulations are performed using CMAQ v4.7.1 to quantify the impact of biogenic emissions on SOA, particulate SO_4^{2-} and NO_3^-, and total $PM_{2.5}$. CMAQ is a 3-dimensional grid-based photochemical model that simulates emissions, gas-phase chemistry, aerosol thermodynamics, advection, and deposition. The model is used for policy analysis by researchers and air quality managers when developing SIPs to qualify attainment with the EPA NAAQS. The “base case” scenario includes all emissions sectors and the "no biogenic" scenarios has biogenic emissions set to zero. We use the chemical bond V (CB05) gas-phase chemistry mechanism and the AERO5 aerosol module included with the model and run on a 36 km x 36 km grid over the CONUS domain for July 2007. Ten days of model spin-up are discarded from the analysis.

Dynamic boundary conditions were generated for July 2007 from the global Model for Ozone and Related Chemical Tracers (MOZART) (Emmons et al., 2010) at the National Center for Atmospheric Research (NCAR), which were downloaded for use at acd.ucar.edu/wrf-chem/mozart.shtml. Meteorology inputs for CMAQ are created using the Weather Research and Forecasting (WRF) model version 3.2 with historic NCEP North American Regional Reanalysis (NARR) data from the NCEP Eta-model (Mesinger et al., 2006) and retrieved from rda.ucar.edu/datasets/. Data from WRF is simulated using Grell

cumulus parameterization (Grell & Devenyi, 2002) with 27 vertical sigma layers from the surface to approximately 150hPa. WRF data is pre-processed for CMAQ using the Meteorology-Chemistry Interface Processor (MCIP). Collaborator Dr. Erica Bickford prepared data from WRF simulations used in the CMAQ simulations presented in this chapter.

The Lake Michigan Air Director's Consortium (LADCO) provided hourly sector-specific anthropogenic and biogenic emissions data on a 36 km x 36 km CONUS grid. Emissions data are separated into individual sectors that are combined using a merge tool from the EPA's Sparse Matrix Operator Kernel Emissions (SMOKE). Biogenic emissions were processed by LADCO using a combination of land cover variables including leaf area index, plant functional types, emission factors, and satellite measurement constraints (Millet et al., 2010) in the Model for Emissions of Gases and Aerosols from Nature (MEGAN) v2.0 (Guenther et al., 2006). These inputs are processed with MCIP-preprocessed meteorology during the simulation time period to predict emissions from natural sources. Although results from CMAQ-MEGAN analysis show overestimates of isoprene and other VOC emissions in comparison to other biogenic emissions model frameworks (Carlton & Baker, 2011), no adjustments to the emissions are included in these simulations.

Aerosol Properties in CMAQ

Gas-phase chemistry initiates inorganic and organic secondary aerosol formation in CMAQ. Anthropogenic emissions of NO_2 and SO_2 oxidize to gaseous HNO_3 and H_2SO_4 respectively. In CMAQ, only H_2SO_4 nucleates to form new particles of an assumed diameter of 3.5 nanometers (Binkowski & Roselle, 2003). Concentrations of HNO_3 and H_2SO_4 are

used along with modeled relative humidity, temperature, and concentrations of Na, HCl, and NH_3 to determine aerosol partitioning in the thermodynamic equilibrium model ISORROPIA (Nenes, 1998), which is run in-line and models the SO_4^{2-}-NO_3^--Cl^--Na^+-NH_4^+ ion system. Equilibrium reactions between the gas, solid, and aqueous phases determine the amount of inorganic aerosol in the system using temperature-dependent thermodynamic properties including equilibrium constants and activity coefficients which determine the volatility of a compound.

Quantifying the acidity in the model environment is important for nitrate formation through the reaction with NH_3. Through ISORROPIA, Na and NH_3 are used to neutralize H_2SO_4, and any leftover NH_3 reacts with HNO_3 to form ammonium nitrate (NH_4NO_3). In acidic conditions, deficient NH_3 concentrations are unable to react with HNO_3 in order to form NO_3^- aerosol. In a highly neutralized environment, this reaction occurs and yields NH_4NO_3 that equilibrates with aqueous NH_4^+ and NO_3^- ions. However, the availability of both nitric and sulfuric acids depends first and foremost on the gas-phase oxidation of their gaseous precursors.

The CB05 chemical mechanism used here includes the oxidation of 19 different VOC species including isoprene, mono- and sesqui-terpenes, and anthropogenic VOCs (Carlton et al., 2010). Gas-phase isoprene oxidation only occurs by OH radical to form semi-volatile compounds, while mono- and sesqui-terpernes undergo oxidation by either the OH, O_3 or NO_3 radicals to form semi-volatile species. The partitioning behavior of oxidized isoprene (Henze & Seinfeld, 2006), a weighted set of the lump-sum of five monoterpenes (Bian & Bowman, 2002), and sesquiterpenes (Griffin et al., 1999) are specific to each species. Semi-volatile compounds may undergo oligomerization reactions to form low-volatility aerosols

(Dommen et al., 2006; Kroll et al., 2006). Additionally, CB05 includes the acid-catalyzed formation of non-volatile aerosols from semi-volatile isoprene oxidation products. Concentrations of aerosol acidity are calculated using ion concentrations from ISORROPIA, and although existing semi-volatile isoprene-derived aerosol is removed to compensate for the acid-catalyzed aerosol formation, inorganic aerosols are not removed from the system by this process.

Aerosol growth in CMAQ is mode-dependent, and both intramodal and intermodal coagulation contribute to growth. Mass concentrations for Aitken ($\varphi_{i,n}$) and accumulation ($\varphi_{j,n}$) modes, including new particle formation, condensational growth, coagulation, and primary emissions, are shown in equations (1) and (2) (Binkowski & Roselle, 2003)

(1) $$\frac{\partial \varphi_{i,n}}{\partial t} = P_{i,n} - L_i \varphi_{i,n} = \varphi'_{i,n} + E_{i,n} + R_n \Omega_i - L_i \varphi_{i,n}$$

(2) $$\frac{\partial \varphi_{j,n}}{\partial t} = P_{j,n} = E_{j,n} + R_n \Omega_j + L_i \varphi_{i,n}$$

where *i* represents the Aitken mode particles and *j* represents accumulation mode particles. The Aitken mode, aerosols with a diameter less than 0.1 um, experiences growth ($P_{i,n}$) from change in mass over time ($\varphi'_{i,n}$), primary emissions ($E_{i,n}$), and condensational growth ($R_n\Omega_i$) where R_n is the gas-phase production rate of species *n* and Ω_i is the fractional apportionment of the condensing species (equation (1)). New particle growth in CMAQ only occurs via nucleation from H_2SO_4, and these new particles have an assumed initial diameter of 3.5 nanometers (Binkowski & Roselle, 2003). Aitken loss processes (L_i) include moderate intramodal coagulation loss and large intermodal coagulation losses to the accumulation mode, particles with diameters ranging between 0.1 and 2.5 um, with every time step. Growth ($P_{j,n}$) in the accumulation regime (equation (2)) includes primary emissions ($E_{j,n}$),

condensational growth ($R_n\Omega_j$), and what was lost from Aitken intermodal coagulation ($L_i\varphi_{i,n}$). Losses through both intramodal and intermodal coagulation in the accumulation mode are miniscule.

Dry depositional losses are calculated separately for each aerosol regime and are dependent on modeled concentrations and dry deposition velocities. Quantifying the dry deposition of aerosol species is a difficult and uncertain process (Baumgardner et al., 1999). The dry deposition velocity relies on knowledge of a variety of characteristics about the aerosol, the particulate size, and the surface the aerosol is depositing onto. Dry deposition of mono-disperse particles of the same particle diameter in CMAQ is governed by both Brownian particle diffusivity (D_p),

(3) $$D_{\mathrm{p}} = \left(\frac{k_b T}{3\pi v \rho_{\mathrm{air}} D}\right) Cc$$

and gravitational settling velocity (v_G),

(4) $$v_{\mathrm{G}} = \left[\frac{g}{18v}\left(\frac{\rho_{\mathrm{p}}}{\rho_{\mathrm{air}}}\right) D^2\right] Cc$$

each applied with the same linearized correction factor, *Cc* (Binkowski & Shankar, 1995). In equations 3 and 4, k_b is the Boltzmann constant, T is temperature, ρ_{air} is the air pressure, ρ_p is the particle pressure, D is diameter, v is the particle's velocity, and g is gravity. For poly-disperse particles that encompass a broad range of particle diameters, both equations (3) and (4) are averaged over particle size distributions. Ultimately, the dry deposition velocity (v_d) of a poly-disperse particle is calculated as

(5) $$v_d = \frac{1}{r_a + r_b + v_s r_a r_b} + v_s$$

And is dependent on the gravitational settling velocity (v_s), surface layer resistance (r_b), and the aerodynamic particle resistance (r_a). Dry depositional flux is then calculated from the multiplication of the concentration and the dry deposition velocity,

$$F = C(z) * v_d, \quad (6)$$

where dry depositional losses are calculated separately for each aerosol regime. Therefore, it is expected that with increasing concentration, the dry deposition flux will also increase.

Accurate dry deposition measurement is one of the more uncertain aspects of the $PM_{2.5}$ budget due to discrepancies in deposition velocity estimates (Nicholson, 1988), and the relationship between biogenic emissions, inorganic aerosols, and dry deposition has yet to be documented. Further, most dry deposition analyses have focused on monitor network measurements and have not included air quality model simulations in their analysis (e.g. Baumgardner et al., 2002; Raymond et al., 2004 and others). From these uncertainties, modeled dry deposition flux results presented in this chapter may be indicative of atmospheric processes or sensitivities in the model system.

Model Evaluation

CASTNet Measurements and Comparisons with CMAQ

Model simulations are compared with measurements and independently calculated deposition from nationwide Clean Air Status and Trends Network (CASTNet) locations for July 2007. Monitors take weekly concentration measurements of a variety of gases and particulates. Measurements of SO_2 and SO_4^{2-} are sampled at a 10m-reference height using a three-stage, open-faced filter pack method as outlined in Baumgardner et al. (1999). This technique offers adequate sensitivity in the presence of very low SO_2 and SO_4^{2-} concentrations

like those found in rural areas and the western U.S. (Baumgardner et al., 1999). Dry deposition fluxes are calculated using equation (6) with CASTNet weekly concentrations and model-estimated values for v_d. The multi-layer model (MLM) (Meyers et al., 1998) calculates v_d with the following equation (Baumgardner et al., 2002)

(7) $$v_d = \frac{1}{r_a + r_b + r_c}$$

r_a and r_b are equivalent to r_a and r_b from equation (5) respectively, and r_c is the surface uptake resistance. This calculation differs from the one employed in CMAQ, in that (5) uses more aerosol characteristics in solving for v_d. The MLM uses radiative transfer and wind profile observations taken at the measurement location to determine surface uptake resistances (T.P. Meyers et al., 1998), and has been shown to have a slightly low bias for SO_2 deposition velocities when compared to measurements (Finkelstein et al., 2000; T.P. Meyers et al., 1998). Other dry deposition velocity correlations are unknown because dry deposition is very difficult to measure directly. Additionally, semi-volatile gas-phase compounds may partition onto the filter, yielding a greater aerosol mass than might be representative of the measurement location (e.g. Mader & Pankow, 2001). From the complexity associated with making dry deposition measurements from model-determined deposition velocity and observed concentrations, these methods result in highly uncertain fluxes. Therefore, although they provide a comparison for CMAQ evaluation, neither CASTNet measurements nor model are precisely accurate in measuring dry deposition.

Weekly averaged model results are compared with weekly CASTNet measurements and dry deposition fluxes at 82 monitor locations across the U.S. for July 2007. Predicted SO_4^{2-} concentrations correlate well with CASTNet observations and have a positive spatial

average correlation coefficient of r=0.898 with measurements across the continental U.S. (Figure 2.1). Sulfate correlations are strongly positive in the eastern half of the U.S. and weakly positive closer to the Atlantic Ocean (Supplemental Figure 2.1). Predicted NO_3^- concentrations show a considerably worse correlation of an r-value less than 0.1 (Figure 2.2). These results are consistent with past CMAQ evaluation, in which the model generally estimates SO_4^{2-} significantly better than NO_3^- (Spak & Holloway, 2009). Across the U.S. most CASTNet monitors exhibit strong negative correlations with CMAQ-predicted NO_3^- concentrations (Supplemental Figure 2.2). Few strongly positive correlations exist scattered across the upper Midwest and the Southwest geographic regions, as well as east of the Ohio River Valley.

In the western half of the U.S., SO_4^{2-} and NO_3^- exhibit both strongly positive and strongly negative correlations. This is an effect of the Rocky Mountain topography in CMAQ, which makes it difficult to accurately predict atmospheric conditions (e.g. Kim et al., 2010). The measurement-comparable CMAQ-predicted SO_4^{2-} and NO_3^- concentrations are 2.31 $\mu g/m^3$ and 0.472 $\mu g/m^3$, respectively whereas the average CASTNet concentrations are 3.52 $\mu g/m^3$ and 0.326 $\mu g/m^3$. CMAQ under predicts SO_4^{2-} concentrations with an average low bias of approximately 1.22 $\mu g/m^3$ and over predicts NO_3^- with a high bias of 0.15 $\mu g/m^3$. Larger concentrations of both SO_4^{2-} and NO_3^- are predicted with a low bias in CMAQ. Smaller concentrations of NO_3^- however are overpredicted by CMAQ. However, lower SO_4^{2-} concentrations are predicted with the most accuracy.

Predicted monthly averages of the dry deposition fluxes of SO_4^{2-} and NO_3^- individually in $\mu g/m^2$ are compared with calculated fluxes at the CASTNet locations. Correlation coefficients of r=0.590 for SO_4^{2-} (Figure 2.3) and r=0.34 for NO_3^- (Figure 2.4) suggest CMAQ predicts deposition moderately well, and significantly better than expected given the difficulty in accurate deposition measurements. Generally, predicted SO_4^{2-} dry deposition values exhibit a strong positive correlation with CASTNet values around the Ohio River Valley and the Northeast U.S. where SO_4^{2-} concentrations are highest, and correlations weaken and in some cases reverse to a negative correlation at some CASTNet sites farther south and closer to the Atlantic Ocean where SO_4^{2-} concentrations are smaller (Supplemental Figure 2.3). The opposite is true with NO_3^- dry deposition, where nearly all of the CASTNet locations in the Ohio River Valley exhibit negative correlations with CMAQ and few positively correlated sites exist east of the Ohio River Valley and scattered in the southeast and western U.S. (Supplemental Figure 2.4). Both SO_4^{2-} and NO_3^- exhibit negative mean fractional biases indicating that CMAQ will tend to under-predict dry deposition values in the summer (Table 2.1). Correlations between CMAQ and CASTNet estimated fluxes are better when SO_4^{2-} concentrations are high; thus correlations are better in the eastern U.S. than in the west. Nitrate dry deposition flux correlations are overall very weak, and only get worse as CASTNet NO_3^- flux observations get larger.

Model Evaluation with OMI NO_2 Observations

Additional CMAQ model evaluation is conducted using NO_2 measurements from the Ozone Monitoring Instrument. Retrievals were processed using the Wisconsin Horizontal Interpolation Program for Satellites (WHIPS)

(http://www.sage.wisc.edu/download/WHIPS/WHIPS.html). This program re-grids level 2 satellite data to the model grid for better comparison. Model data is compared with time-specific OMI NO_2 overpasses, at approximately 2PM EST time, and an averaging kernel is applied to the model data.

Comparisons of CMAQ NO_2 concentrations (a) and OMI NO_2 observations (b) for July 2007 are shown in Figure 2.5. Gas-phase NO_2 is presented to give an understanding of how CMAQ predicts a prominent gas-phase precursor that contributes to $PM_{2.5}$. Although NO_2 is not unique to $PM_{2.5}$ formation, comparing CMAQ NO_2 to OMI NO_2 measurements provides an indication of the accuracy of the gas-phase chemical mechanism in CMAQ.

From the two panels, CMAQ overpredicts NO_2 concentrations in regions of high concentrations, while underpredicting in regions of low concentrations. This is most prominent in Los Angeles, where CMAQ predicts very high concentrations greater than $15x10^{15}$ molecules/cm^2 but OMI observes around $10x10^{15}$ molecules/cm^2. The opposite occurs across much of the rural U.S., where CMAQ predicts just about half of what OMI measures. These urban overestimate and rural underestimates are comparable to what is seen in other studies when other NO_2 retrieval methods are compared with CMAQ simulation results (Stockwell et al., 2007; Zhang et al., 2009). Spatially, CMAQ does a fairly good job of simulating NO_2 concentrations when compared with OMI NO_2 observations.

Sensitivity Simulation Analysis

Net Sensitivity of $PM_{2.5}$ to Biogenic Emissions

Across the U.S., the largest average $PM_{2.5}$ concentrations for July 2007 are seen in highly populated regions such as the eastern half of the U.S. and urban centers such as

Houston and Los Angeles (Figure 2.6a). The largest concentrations are seen in and near the Ohio River Valley, known for large emissions of SO_2 from coal-fired power plants. In this region, average $PM_{2.5}$ concentrations exceed 10 $\mu g/m^3$. Localized regions of high $PM_{2.5}$ like Houston and Los Angeles experience similar concentrations. Moving outward from the Ohio River Valley, concentrations decline, and much of the eastern half of the U.S. experiences concentrations beyond 5 $\mu g/m^3$. The western U.S. is particularly clean in comparison, with total $PM_{2.5}$ concentrations around 1 $\mu g/m^3$ on average.

To quantify the contribution of biogenic emissions to total $PM_{2.5}$, the "base case" simulation is compared with the "no biogenic" sensitivity simulation. In the latter model simulation, all biogenic emissions are removed from the inputs and the model is run as normal. Through this method, we are able to evaluate what contribution biogenic emissions have on air quality. The difference between the "no biogenic" and "base case" simulations indicate that biogenic emissions contribute *negatively* to total $PM_{2.5}$ concentrations in the eastern U.S.

Concentrations of total $PM_{2.5}$ increase substantially in the eastern U.S. but decrease in the western U.S. with the removal of biogenic emissions (Figure 2.6b). Differences between the eastern and western U.S. are due to the types of emissions. In the western U.S. $PM_{2.5}$ concentrations are positively contributed to by SOA (Supplemental Figure 2.5) but $PM_{2.5}$ concentrations in the eastern U.S. are largely determined by anthropogenic aerosol formation (Supplemental Figures 2.6, 2.7). Largest positive changes are localized and include regions near the Ohio River Valley, central Pennsylvania and Virginia, and between the Appalachians and the Carolina coastlines. In these regions $PM_{2.5}$ increases by 25% and more without the presence of biogenic emissions. However, the same is not true in the western

U.S. West of the Rocky Mountains, $PM_{2.5}$ concentrations decrease in most of the region very slightly between 0 and 10% of the original values. Regions where decreases exceed 10% include northern California and the Northern Rockies near the U.S.-Canada border, regions where biogenic aerosols make up the majority of $PM_{2.5}$ in CMAQ (Supplemental Figure 2.5). From this, it seems that biogenic emissions in the base case simulation contribute strongly to total $PM_{2.5}$ in the western U.S. in the form of SOA, while biogenic emissions decrease total $PM_{2.5}$ in the eastern U.S.

Total $PM_{2.5}$ is the sum of SOA and inorganic aerosols including SO_4^{2-} and NO_3^-. In removing biogenic emissions from CMAQ, the resulting simulation reveals the connection that biogenic emissions have with the formation of inorganic aerosols. Without biogenic sources, the formation of SOA is limited, however the formation of inorganic SO_4^{2-} and NO_3^- is shown to increase, leading to the increase in total $PM_{2.5}$ concentrations.

Production Sensitivity of SOA

In the base case simulation, clear spatial patterns are evident for SOA (Figure 2.7a). SOA is higher in the eastern half of the U.S. than the western half, similar to the distribution of total $PM_{2.5}$ (Figure 2.6a). In the eastern U.S. SOA averages 0.75 $\mu g/m^3$ whereas the western U.S. averages less than 0.25 $\mu g/m^3$. There are areas of heightened SOA concentration at the border of Ohio and West Virginia, southeast Missouri, and parts of the northern Rocky Mountains and northern California in the western U.S. However, SOA contributes less than 30% to total $PM_{2.5}$ in the eastern U.S. and more than 30% in the west (Supplemental Figure 2.5).

As expected, the removal of biogenic emissions in the sensitivity case reduces SOA concentrations across the U.S. (Figure 2.7b). Remaining SOA in these simulations indicate anthropogenic VOC. Without biogenic emissions, SOA is effectively reduced to near zero across the majority of the U.S. Only the Great Lakes and the northeastern U.S. coast are affected by anthropogenic SOA production. Even in these areas, the concentrations are minimal, less than 0.20 $\mu g/m^3$ over Lake Michigan and along the coast from Washington, D.C. to Boston, Massachusetts (up to 10% of total SOA). Most of the anthropogenic SOA is likely due to large amounts of vehicle emissions of *n*-alkanes that contribute to SOA (Yan et al., 2009).

Sensitivity of Inorganic Formation to Biogenic Emission Removal

Maximum concentrations of $PM_{2.5}$ and SO_4^{2-} are found along the Ohio River Valley with concentrations greater than 15 $\mu g/m^3$ and 5 $\mu g/m^3$ respectively (Figure 2.8a). Correlations between predicted SO_4^{2-} concentrations and observations are strongest in this region, indicating CMAQ's ability to correctly estimate high SO_4^{2-} concentrations. The eastern U.S. experiences SO_4^{2-} concentrations between 2.5 and 4 $\mu g/m^3$ while the estimated concentration rarely reaches values greater than 0.5 $\mu g/m^3$ in much of the Rocky Mountains. The average monthly SO_4^{2-} concentration in the U.S. is about 0.65 $\mu g/m^3$. Higher concentrations of SO_4^{2-} and $PM_{2.5}$ are predicted in the eastern U.S. than in the west because there are more urban centers and sources of anthropogenic particulates. Across the U.S., SO_4^{2-} contributes more than 50% to total $PM_{2.5}$ downwind of the Ohio River Valley and approximately 30% on average elsewhere (Supplemental Figure 2.6).

Nitrate concentrations are strongly related to population density and NO_2 emissions (Figure 2.8b). Although low in magnitude, concentrations of NO_3^- can contribute extensively to $PM_{2.5}$ at the local scale where other sources are less prominent. Large contributions of NO_3^- to $PM_{2.5}$ occur in and nearby large urban areas co-located with large emissions of NH_3, for example near New York City, Los Angeles, and southern Lake Michigan. Regions of high NO_3^- comprise approximately 20% of total $PM_{2.5}$ (Supplemental Figure 2.7), in comparison to countrywide SO_4^{2-} contributions of around 40% on average. Heaviest contributions of NO_3^- to $PM_{2.5}$ occur in the northern Midwest through the I-90 corridor, the Northeastern coast, Los Angeles and Yosemite National Park. These regions are all similarly influenced by the relative abundance of NO_2, NH_3, and SO_4^{2-} concentrations, which lead to NO_3^- formation. Overall, even though SO_4^{2-} particles are a larger portion of $PM_{2.5}$, NO_3^- is as important at the local scale.

The CMAQ simulation with no biogenic emissions shows a surprising increase in SO_4^{2-} and NO_3^- aerosols. Sulfate concentrations increase by more than 40% in some regions of the U.S. (Figure 2.8c), and NO_3^- concentrations increase by up to 100% in some regions (Figure 2.8d). The largest increases in SO_4^{2-} concentrations occur along the Ohio River Valley, from Pennsylvania westward through Missouri. On average, the SO_4^{2-} concentration over the U.S. changes by positive 12%. Increased concentrations over the Atlantic Ocean off the east coast are observed and occur because the increased SO_4^{2-} over land is carried in the zonal flow across the continent. Much of the U.S. east of the Great Plains also experiences an increase in SO_4^{2-} concentrations by 25% or more. In the southeastern U.S. and the northern Great Lakes into Canada, NO_3^- increases a considerable amount under the no-

biogenic emissions scenario. NO_3^- concentrations in regions outside of the Ohio River Valley double or triple when biogenic emissions are removed in the simulation.

Western states and coastal areas along the Gulf of Mexico experience comparatively weaker increases of SO_4^{2-} and NO_3^- concentrations less than 15% and 60% respectively on average. In the west, CMAQ predicts SO_4^{2-} concentrations to increase slightly in the Rocky Mountain region as well, with concentrations increasing by about 15% when biogenics are not included in the simulation. Disregarding the mountainous region and focusing to the west, large increases in NO_3^- concentrations occur throughout much of the coastal western U.S. as well as highway corridors in the Pacific Northwest. The desert southwest is largely insensitive to biogenic removal, and NO_3^- concentrations remain pretty consistent. Los Angeles and northern Nevada NO_3^- concentrations decrease in response to removing biogenic emissions, something not evident in the SO_4^{2-} changes anywhere in the U.S. Concentrations increase by about 20% and 30% on average for SO_4^{2-} and NO_3^- respectively.

Given that both NO_2 and SO_2 are predominant anthropogenic emissions, it is interesting that NO_3^- increases the most where SO_4^{2-} increases the least. In the Ohio River Valley, SO_4^{2-} concentrations increase substantially but NO_3^- increases minimally. Extreme NO_3^- concentration growth occurs outside of this area, in the general southeastern U.S. as well as in the northern Great Lakes and Canada. Overall, removing biogenic emissions influences all regions of the U.S., especially rural areas. We note that certain areas, like Yosemite National Park, exhibit an *increase* in NO_3^- concentrations under the sensitivity case, suggesting local heterogeneity in nitrate aerosol formation processes.

In urban areas, however, both SO_4^{2-} and NO_3^- increase less than neighboring rural areas under the "no biogenic" scenario. Urban areas are less influenced by biogenic

contributions to $PM_{2.5}$ aerosol in the base case simulation. As such, cities are less influenced by the removal of these sources in comparison to nearby rural areas that experience an abundance of biogenic emissions. For example, whereas most of Illinois exhibits 20-40% increased SO_4^{2-}, the Chicago area exhibits increases of ~15%. Similar phenomena are observed in the case of NO_3^- aerosol, with cities like Minneapolis, Atlanta, and New York City experiencing simulated increases of NO_3^- approximately 10-15% less than neighboring rural areas. Removing biogenic emissions has a more prominent influence on inorganic aerosol formation in rural areas than urban, comparatively.

Sensitivity of Inorganic Dry Deposition to Biogenic Emission Removal

Since dry deposition is directly related to the concentration, speciated $PM_{2.5}$ dry deposition fluxes are generally coincident spatially with species concentration. Base case SO_4^{2-} dry deposition fluxes are fairly constant across much of the interior U.S. with values of 10 $\mu g/m^2$ or less (Figure 2.9a). Downwind of the Ohio River Valley there are significantly higher dry deposition fluxes that are double or triple what the rest of the U.S. experiences on average, with fluxes beyond 30 $\mu g/m^2$ in this region. The heightened dry deposition fluxes stretch from the central Southeast north through much of the eastern U.S. Predicted dry deposition fluxes have a strong positive correlation of 0.775 with predicted SO_4^{2-} concentrations in the eastern U.S. (Table 2.2). Strongest correlations are found in the Southeast, Ohio River Valley, Great Plains, Southwest and northern Rocky Mountains. For comparison, correlations of SO_4^{2-} with SO_4^{2-} wet deposition are sporadic across the U.S., ranging from -1 to +1 within distinct regions, indicating a stronger and more consistent relationship between SO_4^{2-} concentrations and dry deposition processes.

Base case dry deposition fluxes of NO_3^- are more of a local phenomenon than that of SO_4^{2-}. Nitrate fluxes are also a fraction of SO_4^{2-} fluxes, and most of the U.S. exhibits less than 0.5 $\mu g/m^3$ of NO_3^- dry deposition (Figure 2.9b). However, localized regions of heavy NO_3^- dry deposition greater than 3 $\mu g/m^3$ exist in both the eastern and western U.S. Most areas are urban, like New York, Philadelphia, Toronto, Cincinnati, and Los Angeles, though strong fluxes greater than 4 $\mu g/m^3$ are also seen along the eastern border of Lake Michigan as well as Yosemite National Park. All of these areas are coincident with localized regions of high NO_3^- concentrations, and other urban areas like Chicago or Dallas and forested areas like Yellowstone National Park do not exhibit similar NO_3^- concentrations or dry deposition fluxes. Similar to SO_4^{2-}, predicted NO_3^- concentrations correlated more strongly with predicted dry deposition than wet deposition values. Only in the southeast U.S. is NO_3^- wet deposition a more prominent removal process than dry deposition, which remains a strong and fairly consistent removal process across the U.S.

Removing biogenic emissions inadvertently impacts the dry deposition flux of inorganic aerosols, and their removal impacts dry deposition in region-specific ways. Changes in SO_4^{2-} dry deposition fluxes vary despite strong positive concentration changes across the U.S. as a result of removing biogenic emissions (Figure 2.8c). Large increases in SO_4^{2-} dry deposition greater than 20% are seen across the Mississippi basin and north into the lower Great Lakes region (Figure 2.9c), coinciding with a substantial increase in SO_4^{2-} concentrations. Strong negative changes are seen east of the Appalachians where the largest SO_4^{2-} dry deposition fluxes existed in the base case. In the western half of the U.S., areas of increased deposition are found along major interstates, like I-15 through Idaho, I-80 in Wyoming, and I-90 in Wyoming and Montana. Much of the northwest Pacific experiences

increased dry deposition of SO_4^{2-} but only by a few percent, while the lower mountain west and southwest sees decreases in dry deposition fluxes of up to 10%. Yosemite National Park experiences a regionally-unique increase in SO_4^{2-} dry deposition flux of more than 10%, while the rest of the southwestern U.S. experiences mainly negative changes. Changes to SO_4^{2-} dry deposition fluxes vary spatially across the U.S. and generally are not consistent with changes in concentrations resulting from a lack of biogenic emissions.

Nitrate dry deposition increases across the U.S., with substantial positive changes across the southeast, the Upper Great Lakes region, and the western U.S. (Figure 2.9d). Changes in NO_3^- fluxes are significant, reaching 75% to 100% in some regions of the eastern U.S. However, there are some scattered local areas that exhibit low sensitivity compared to the region-wide changes. Nitrate dry deposition fluxes in the Cincinnati area of the Ohio River Valley and the Chicago and the Northeastern U.S. change by less than 10% while nearby areas change by more than 20%. These areas also exhibit similar sensitivities to changes in NO_3^- concentrations. In the west, NO_3^- dry deposition fluxes increase significantly in Yosemite National Park and the Pacific Northwest due to biogenic emissions removal, while NO_2-polluted Los Angeles experiences a slight decrease of about 10% in NO_3^- dry deposition flux. Similar to changes in SO_4^{2-} dry deposition, I-15 stretching across Idaho exhibits a strong increase in NO_3^- dry deposition. These changes in dry deposition flux are directly related to the changes in NO_3^- concentrations induced from the removal of biogenic emissions.

Discussion

Fine particulate matter may be either directly emitted as primary $PM_{2.5}$, or formed in the atmosphere through the oxidation of anthropogenic and biogenic gaseous precursors. Among the largest contributing gaseous precursor species are SO_2, NO_X, and VOCs, yielding SO_4^{2-}, NO_3^-, and SOA. When biogenic emissions are removed from CMAQ, total $PM_{2.5}$ concentrations increase in the eastern half of the U.S. while decreasing west of the Rocky Mountains. Increased $PM_{2.5}$ occurs because of large increases in particulate SO_4^{2-}, NO_3^-, and NH_4^+ (not shown) despite near total elimination of SOA in the sensitivity simulation. The removal of biogenic emissions allows for increased concentrations of particulate species indicative of a complex relationship between anthropogenic and biogenic emissions.

Both SOA (Kleindienst et al., 2010) and inorganic aerosols like SO_4^{2-} and NO_3^- (Edgerton et al., 2005; M. Kim et al., 2007; Zhang et al., 2004) contribute to total $PM_{2.5}$ across the U.S. Biogenic emissions contribute to $PM_{2.5}$ by the formation of SOA through oxidation reactions involving VOCs such as isoprene. Smaller contributions to SOA come from the oxidation of anthropogenic gaseous precursors, yet these are insignificant compared to the contribution through biogenic sources. The largest emissions of VOCs including isoprene are in the southeastern U.S., but interestingly SOA contributes more to total $PM_{2.5}$ in the western U.S. Concentrations of $PM_{2.5}$ are significantly less in the west, and therefore SOA makes up a larger fraction of total aerosol mass, whereas the eastern U.S. experiences larger $PM_{2.5}$ fractional components from particulate SO_4^{2-} and NO_3^-.

Base case contributions of SO_4^{2-} and NO_3^- to total $PM_{2.5}$ vary according to local and regional source emissions of SO_2, NO_X, and NH_3. Sulfate tends to be highest in the Ohio River Valley region, where there are significant emissions of SO_2, whereas NO_3^- is largest

near of urban areas and highways, coincident with large sources of precursor NO_2. Downwind of the Ohio River Valley, SO_4^{2-} aerosol contributes ~50% to total $PM_{2.5}$ in this region coincident with substantial emissions of SO_2 from coal-fired power plants (Zhao et al., 2007). Interestingly, larger contributions of SO_4^{2-} (~30%) are seen in much of the rural and suburban U.S. versus in urban centers (<20%). In order to form SO_4^{2-}, SO_2 emissions must undergo oxidation and reaction with NH_3, which neither occurs immediately nor directly at the emission source. As such, SO_4^{2-} is more of a regional aerosol that affects the air quality across broad areas.

Nitrate concentrations, however, contribute to $PM_{2.5}$ in a less broad, more region-specific manner due to the availability of ingredients necessary for NO_3^- formation: NO_X and NH_3. Localized NO_X emissions from urban centers and near highways mix downwind with NH_3 emitted from rural livestock. Largest contributions of NO_3^- to total $PM_{2.5}$ are about 20% in the upper Midwest and the Great Lakes region, while elsewhere in the U.S. NO_3^- contributes only a few percent to total $PM_{2.5}$. Without both NO_X and NH_3, NO_3^- will not be able to form, which is why cities such as Houston, Dallas, and Denver without nearby sources of NH_3 do not experience large amounts of NO_3^- pollution. Absolute changes in particulate NO_3^- concentrations presented here are small compared to that of SO_4^{2-}, however, they are expected to be more dramatic in the winter when NO_3^- poses a large air pollution problem, contributing significantly to $PM_{2.5}$ (Heo et al., 2013). Additionally, the poor correlation that exists between simulated NO_3^- concentrations and ground observations indicates weak confidence in the model predictions, particularly in comparison to predicted SO_4^{2-}.

Gas-phase Oxidation Processes

The formation of both inorganic aerosol and SOA relies on the oxidation of gaseous precursors. Oxidants form through photolytic reactions of anthropogenic pollutants that also contribute to primary OA and act as sites for semi-volatile VOC condensation and aerosol growth. The connection between biogenic emissions and inorganic aerosol formation is indirect and is regulated by oxidation lifetimes of the gas-phase precursors isoprene, NO_2, and SO_2. Oxidation lifetimes vary between gas-phase species, but in general the oxidation of isoprene (Jacob et al., 1989) is significantly faster than that of NO_2 (Dentener & Crutzen, 1993) and especially that of SO_2 (Chin et al., 1996). In the atmosphere, isoprene is preferentially oxidized over anthropogenic inorganic gases, leading to SOA formation at a greater rate than inorganic aerosol formation. In addition, measurements have shown VOC oxidation, particularly that of isoprene, participate in OH-recycling and maintain OH concentrations in low-NO_X environments (Lelieveld et al., 2008). Implementing one variety of OH recycling mechanism (Peeters et al., 2009) into a global model has been shown to reduce SOA production globally through reducing certain isoprene oxidation pathways and increasing others (G. Lin et al., 2012). However, the CB05 chemical mechanism used in these CMAQ simulations does not include OH-recycling, and as such, simulated OH concentrations are not maintained as recent measurements have shown. Instead, the oxidation of isoprene by OH effectively removes OH from the model environment in the base case simulation, and inorganic aerosols are less readily formed through oxidation reactions. However, removing VOCs in the "no biogenic" simulation nearly eliminates SOA from the model environment, yet SO_4^{2-}, NO_3^-, and $PM_{2.5}$ increase. Oxidants like OH are now abundant because they were not removed in VOC oxidation (Supplemental Figure 2.8), and

they have the ability to react with inorganic emissions. Consequently, anthropogenic gases like SO_2 and NO_2 are subject to greater oxidation by OH radical and enhanced aerosol nucleation without biogenic gaseous emissions in the atmosphere.

From the comparison of the base case and no biogenic simulations, the changes in aerosol formation resulting from the removal of biogenic emissions are the result of an increased availability of oxidants. Increased SO_4^{2-} results from an increased amount of SO_2 oxidation through reaction with OH radical following gas-phase reaction (153) of the CB05 chemical mechanism (Yarwood et al., 2005) (Table 2.3). In the base case simulation, this reaction proceeds at a slower rate than reactions (142) and (150), the reaction of OH radical with isoprene or monoterpene respectively (Yu et al., 2010). Removing biogenic emissions reduced the ability for these reactions to take place, and reaction (153) can proceed without interference from the oxidation of biogenic gases. In this situation, a domain average of 29.4% (0.19 $\mu g/m^3$) more SO_4^{2-} was predicted from the excess nucleation of only 5% more SO_2 (0.015 ppb). Increased concentrations of NO_3^- arose from similarly enhanced gas-phase oxidation of NO_2 to yield HNO_3 that reacts with excess NH_3. From this, Aitken (Supplemental Figure 2.9) and accumulation (Supplemental Figure 2.10) mode particulates increase significantly due to enhanced gas-phase oxidation while coarse particulates remained similar to their base case concentration.

Response of Inorganic Aerosols

Changes in concentrations due to biogenic emission removal occur broadly across much of the U.S. The Ohio River Valley region is subject to large amounts of anthropogenic pollution of SO_2 from coal-fired power plants and others (M. Kim et al., 2007; Zhao et al.,

2007), and because there is already a substantial amount of SO_4^{2-} precursor in this region, a greater increase in concentration occurs here compared to elsewhere in the U.S. Concentrations of SO_2 across the western U.S. are on the order of 0.5 ppb or less, which is 4 to 5 times less than concentrations observed in the Ohio River Valley, suggesting smaller concentrations of SO_2 lead to smaller concentrations of SO_4^{2-}. Although significant increases in SO_4^{2-} concentrations are centralized around the Ohio River Valley, positive changes to NO_3^- concentrations are largely seen elsewhere: the southeast U.S., the upper Great Lakes, and along highways in the western U.S.

Urban regions experience noticeably smaller increases of both SO_4^{2-} and NO_3^- concentrations. In the base case simulation, the influence from biogenic emissions to total aerosol mass in large cities is considerably less than in surrounding rural areas, and the anthropogenic contribution outweighs the biogenic contribution. Biogenic emissions do not interfere with oxidation reactions in urban areas because VOC emissions are substantially less than SO_2 and NO_X emissions, and inorganic aerosols preferentially form over SOA. Therefore, removing biogenic sources does not alter the aerosol formation exhibited in urban areas as dramatically relative to nearby non-urban areas.

Changes in SO_4^{2-} concentrations correspond with changes in SO_4^{2-} dry deposition. The largest areas of base case dry deposition flux were downwind of the regions of highest SO_4^{2-} concentrations, southeast of the Ohio River Valley. This region is collocated with significant decreases in dry deposition flux on the order of 15% and more when there are zero biogenic emissions. Greater amounts of freshly nucleated SO_4^{2-} particulates are transported downwind where they fail to deposit, implying a lack of condensational growth of the particulates in the model (Binkowski & Shankar, 1995). Interestingly, increases on the

order of 20% and more are seen in the western portions of the Ohio River Valley, collocated with a region of substantial SO_4^{2-} concentration increases. Increasing SO_4^{2-} concentrations substantially is expected to increase the SO_4^{2-} dry deposition flux in this region. Similar changes are noted near highways in the Pacific Northwest, though changes to dry deposition flux in the western U.S. are only within ±5%, or a few ng/m^2 differences, and are not as significant as the changes predicted in the eastern U.S. Nitrate dry deposition enhancement is more linear and increases with increased concentration. This is attributed to the differences in the changes in aerosol mode concentrations, where CMAQ predicts more sulfate nucleation than accumulation mode aerosol. In the model, NO_3^- is not formed through nucleation, and all NO_3^- aerosol is collected in the accumulation mode. With the removal of biogenic emissions, changes are introduced to not only inorganic aerosol formation but dry deposition fluxes as well.

We have found that dry deposition removal of sulfate and nitrate aerosol is related to ambient biogenic VOCs and SOA formation, as simulated in the CMAQ model. From this evaluation, more gaseous SO_2 particles nucleate and form new aerosol particles due to the excess OH radical. Since more SO_2 is modeled to nucleate, less SO_2 is predicted to condense onto existing particles and fail to grow to sizes suitable for removal by dry deposition. Additionally, without biogenic VOCs, more emitted NO_X undergoes reactions with NH_3 to yield NO_3^- aerosol. Thus inorganic aerosol formation and growth is enhanced overall while SOA is effectively removed. Aerosol mass concentrations are shown to increase by the indirect relationship between biogenic VOCs, anthropogenic gases, and gas-phase oxidation processes. Biogenic gaseous emissions preferentially oxidize in the atmosphere to yield SOA products in subsequent reactions. With the removal of biogenic VOCs, inorganic

oxidation reactions occur with more prevalence. These results indicate that gaseous biogenic emissions play a dual role in contributing to total $PM_{2.5}$, where they help reduce overall concentrations of $PM_{2.5}$ while contributing significantly to total $PM_{2.5}$ in the form of biogenic SOA.

Figures

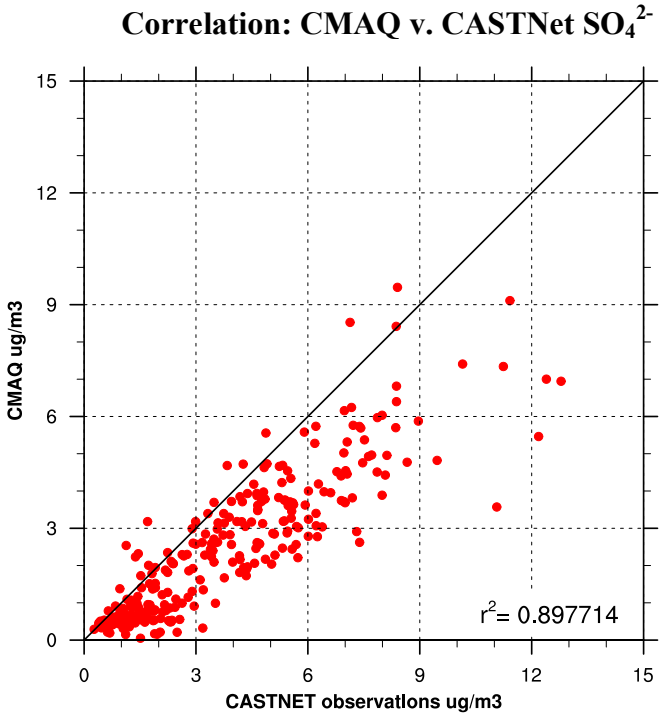

Figure 2.1 Scatterplot of CMAQ predicted sulfate concentrations compared with CASTNet sulfate observations for July 2007.

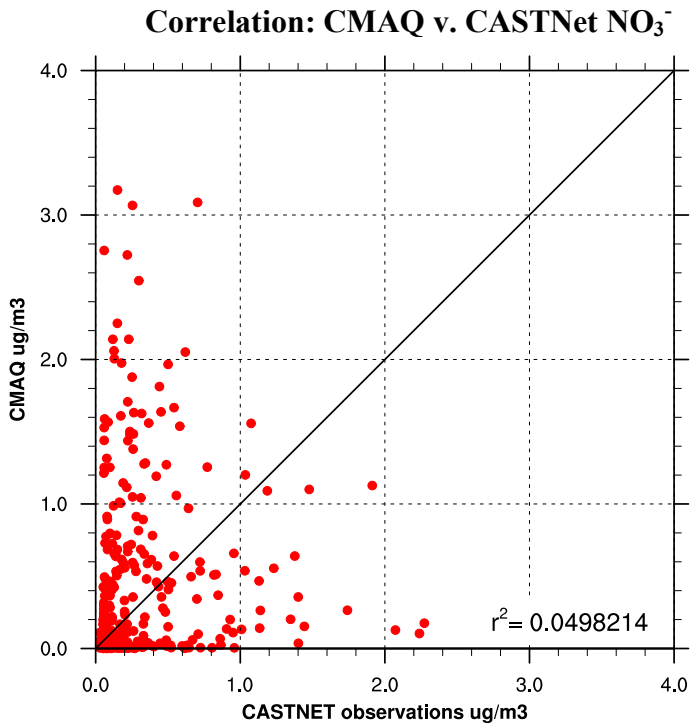

Figure 2.2 Same as Figure 2.1 except for nitrate concentrations.

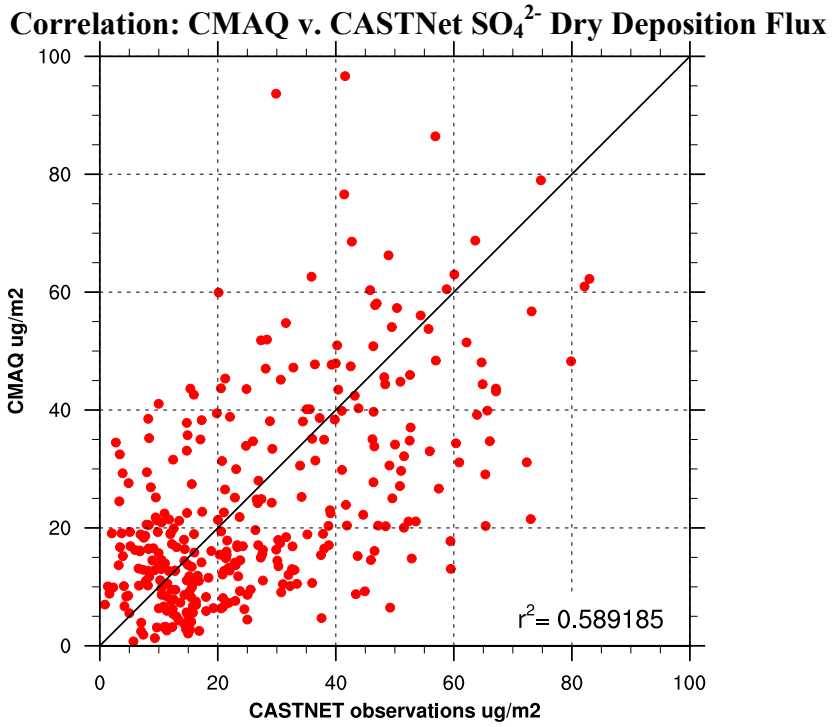

Figure 2.3 Scatterplot comparing CMAQ predicted dry deposition fluxes for sulfate to those measured by CASTNet monitors.

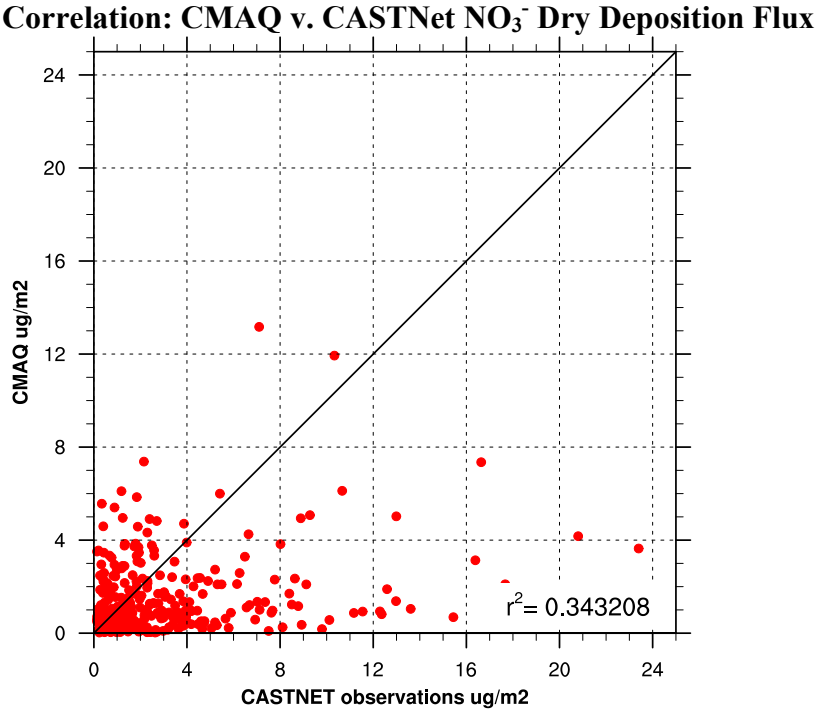

Figure 2.4 Same as Figure 2.3 except for nitrate dry deposition fluxes.

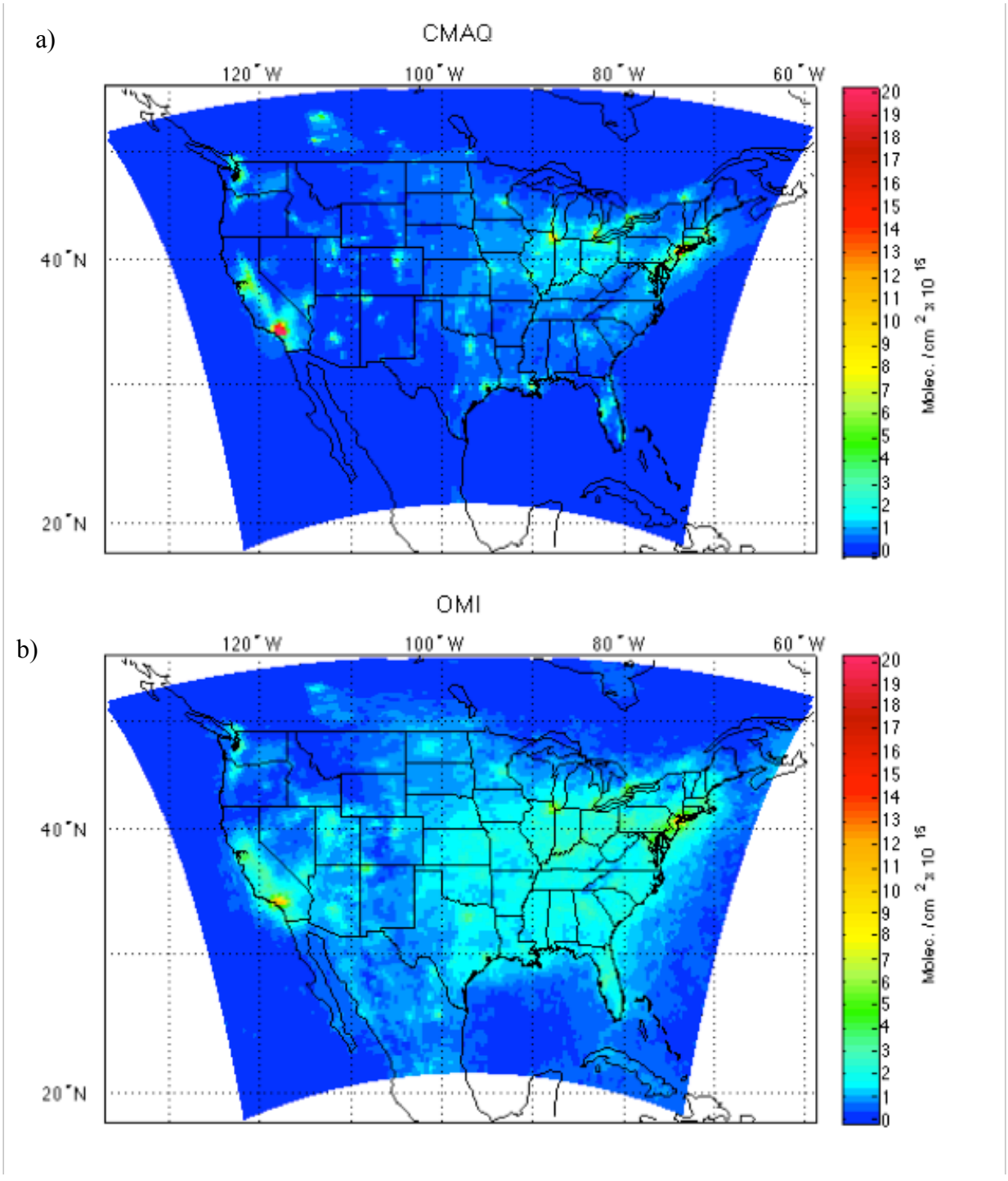

Figure 2.5 CMAQ NO_2 predicted concentrations (a) compared with OMI NO_2 observations (b).

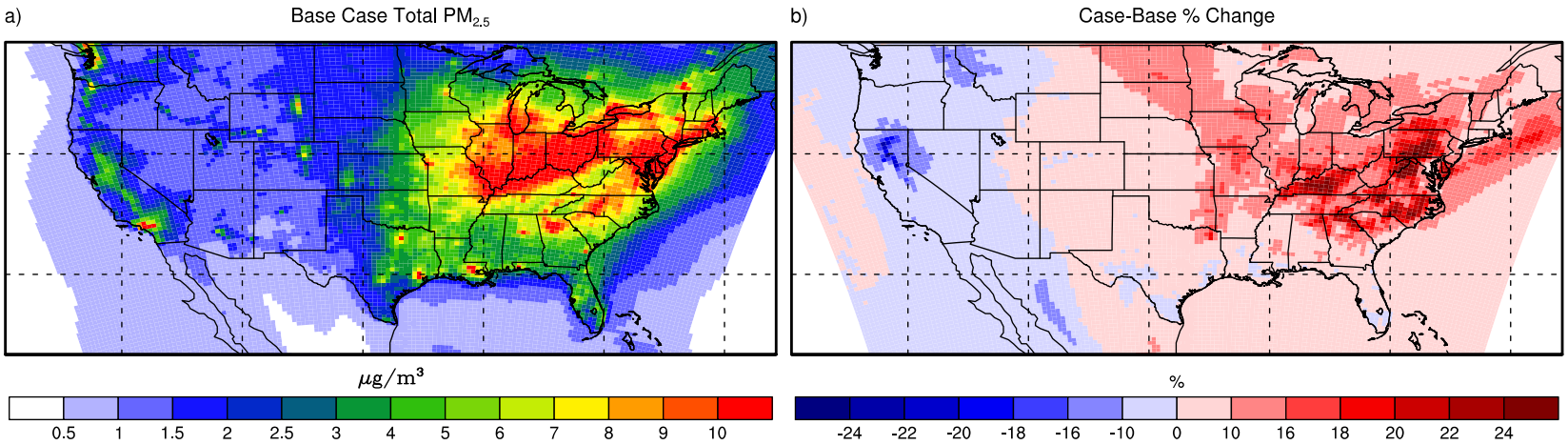

Figure 2.6 CMAQ plot of base case total PM2.5 concentrations (a) and no biogenic case minus base case percent change in concentration (b) for July 2007.

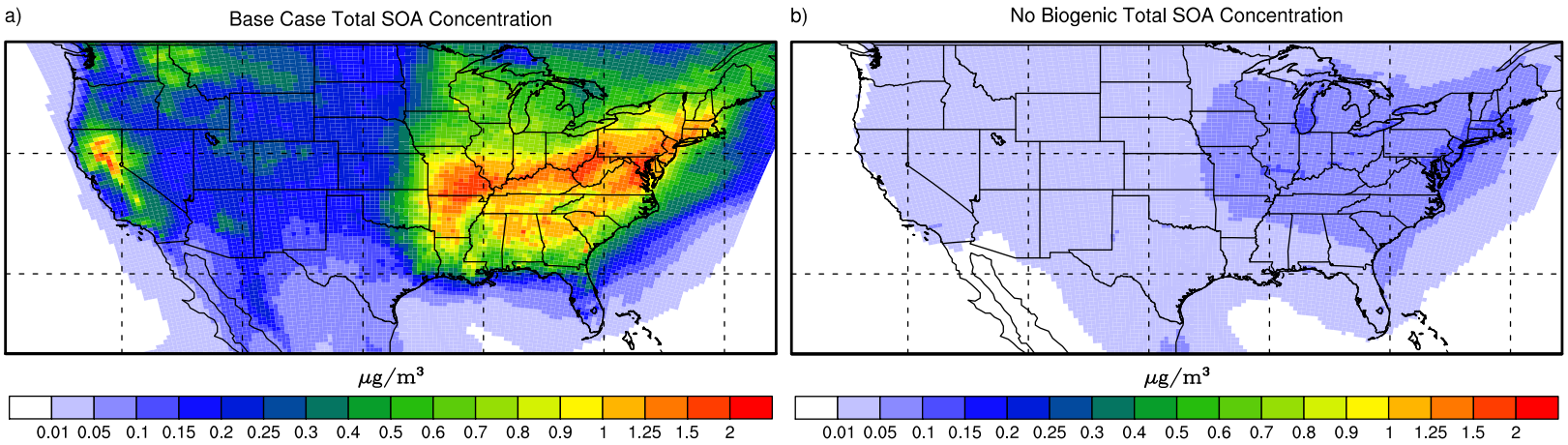

Figure 2.7 CMAQ plot of base case total SOA (a) and total SOA from the no biogenic simulation (b) averaged over July 2007.

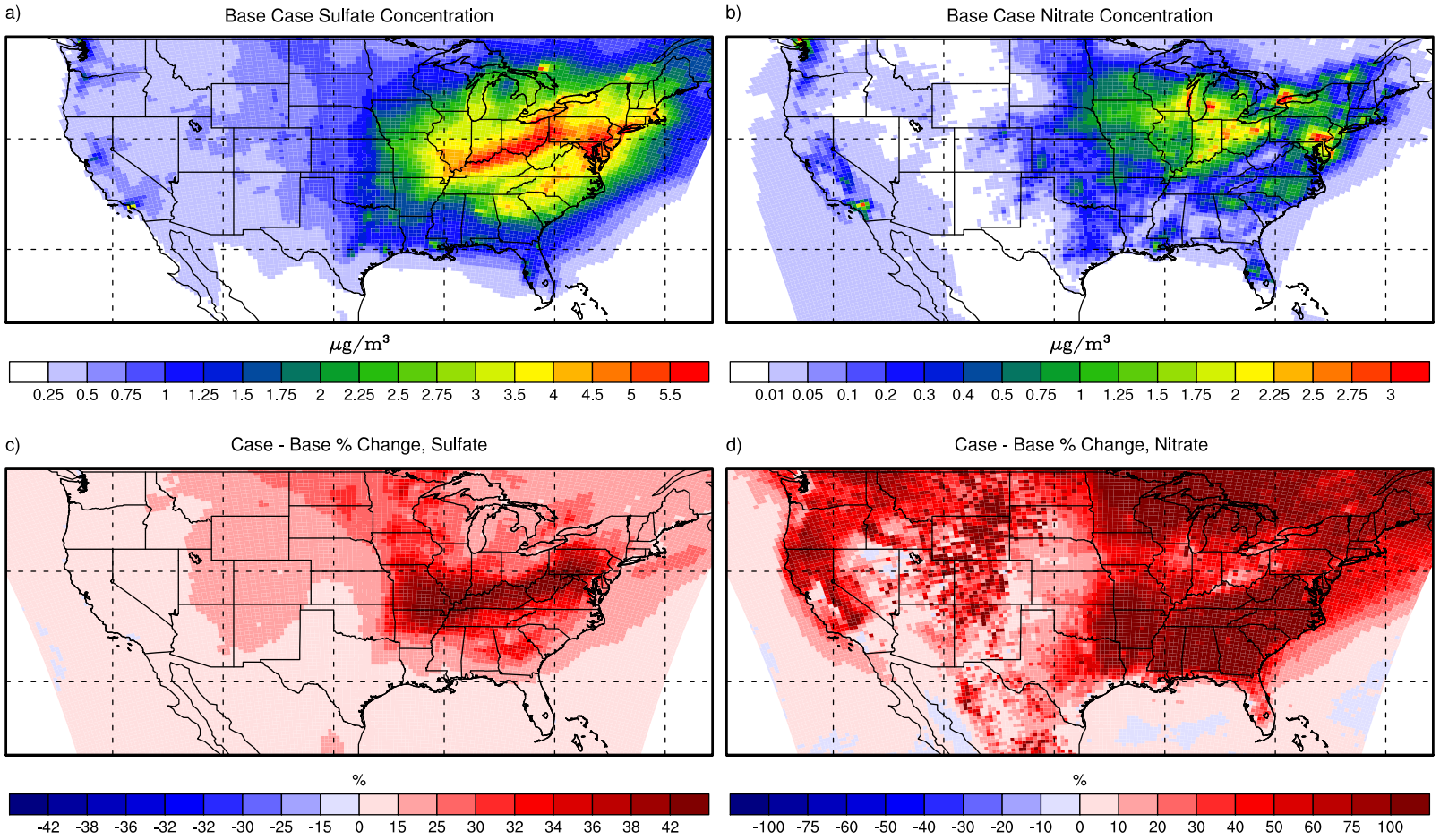

Figure 2.8 CMAQ plots of base case sulfate concentrations (a), nitrate concentrations (b), and no biogenic case minus base case percent differences for sulfate concentration (c) and nitrate concentration (d) averaged over July 2007.

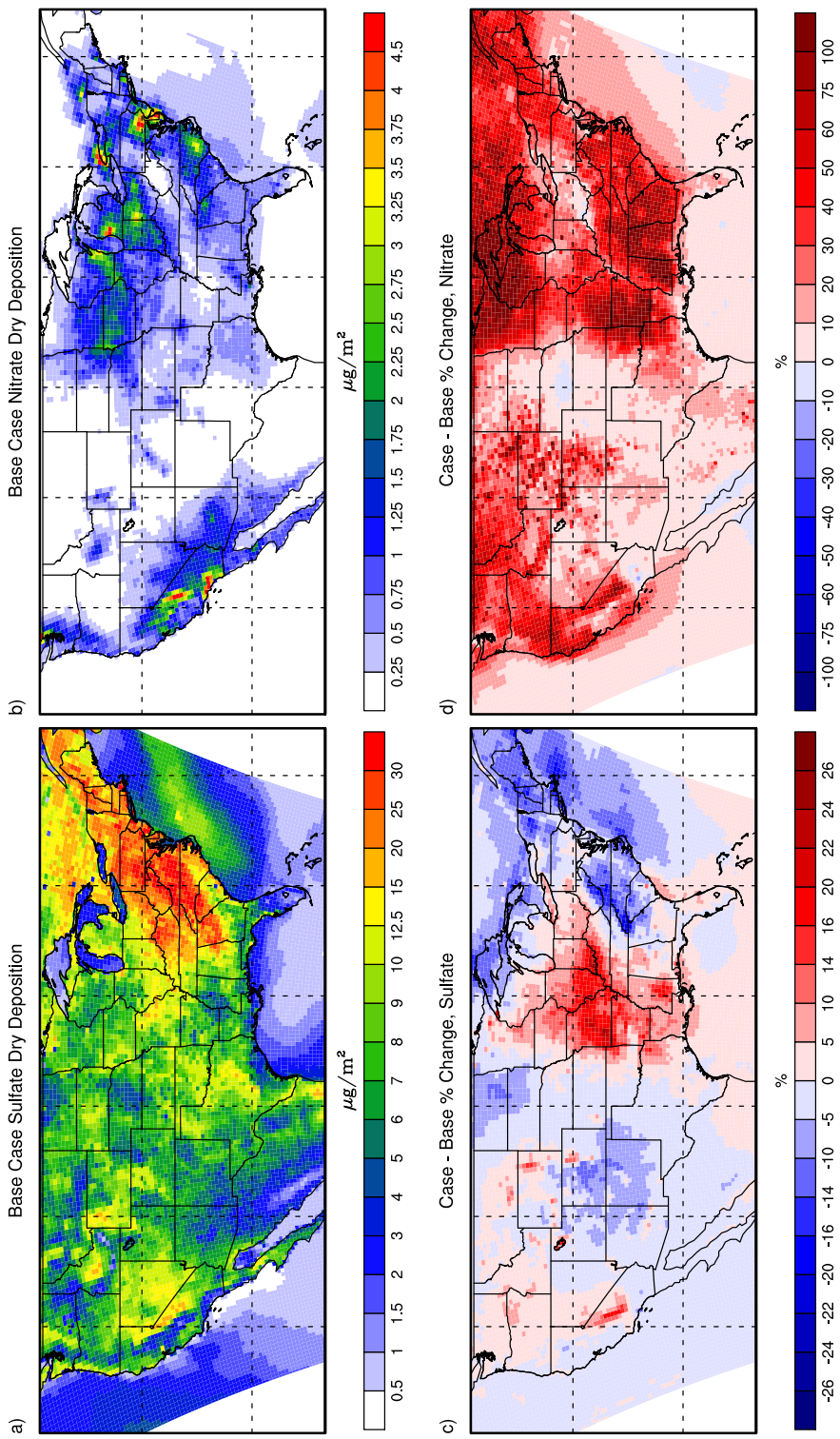

Figure 2.9 Same as Figure 2.8 except for dry deposition fluxes.

Tables

	Location	Dry Flux (kg/ha) annual	Source
Gases			
SO_2	Eastern U.S	7.0 7.17 5.39	Clarke et al 1997 Baumgardner et al 2002 Meyers et al 1991
HNO_3	Eastern U.S.	11.32 8.32 2.6	Clarke et al 1997 Baumgarder et al 2002 Meyers et al 1991
Particulates			
SO_4^{2-}	Eastern U.S.	1.52 1.5	Baumgardner et al 2002 Meyers et al 1991
NO_3^{2-}	Eastern U.S.	0.34 0.049	Baumgarder et al 2002 Meyers et al 1991

Table 2.1 Previous studies examining dry deposition of SO_2, HNO_3, SO_4^{2-}, and NO_3^-

	r^2	bias (ug/m^3)	mean bias (%)	error (ug/m^3)	mean error (%)
SO_4^{2-} Dry Deposition	0.59	-0.0031	0.013	-11.6	60.35
SO_4^{2-} Concentration	0.898	-1.22	-47.24	1.29	50.51
NO_3^- Dry Deposition	0.34	-0.0015	-43.4	0.0024	97.55
NO_3^- Concentration	0.05	0.146	-8.07	0.482	115.8

Table 2.2 Statistics comparing weekly averaged CMAQ predicted sulfate and nitrate concentration and dry deposition fluxes with CASTNet monitor observations.

Equation #	Reaction		Reaction Rate @ 298K, 1 atm
142	OH+ISOP→	0.91ISPD + 0629FORM + 0.25XO2 + 0.25HO2 + 0.25CXO3 + 0.25PAR	$9.97x10^{-11}$
150	TERP + OH →	0.750HO2 + 1.25XO2 + 0.25XO2N + 0.28FORM + 1.66PAR + 0.47ALDX	$6.77x10^{-11}$
153	SO_2 + OH →	SULF + HO2	$8.89x10^{-13}$

Table 2.3 Gas-phase chemical equations from the chemical bond V mechanism in the CMAQ model.

Supplemental Figures

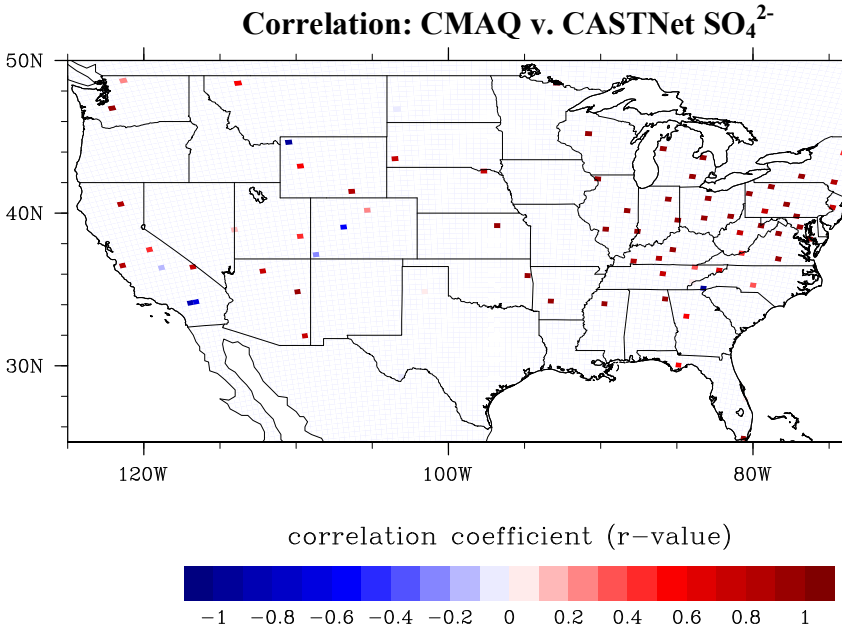

Supplemental Figure 2.1 Spatial correlation of weekly sulfate concentrations in CMAQ and from CASTNet monitors averaged over July 2007.

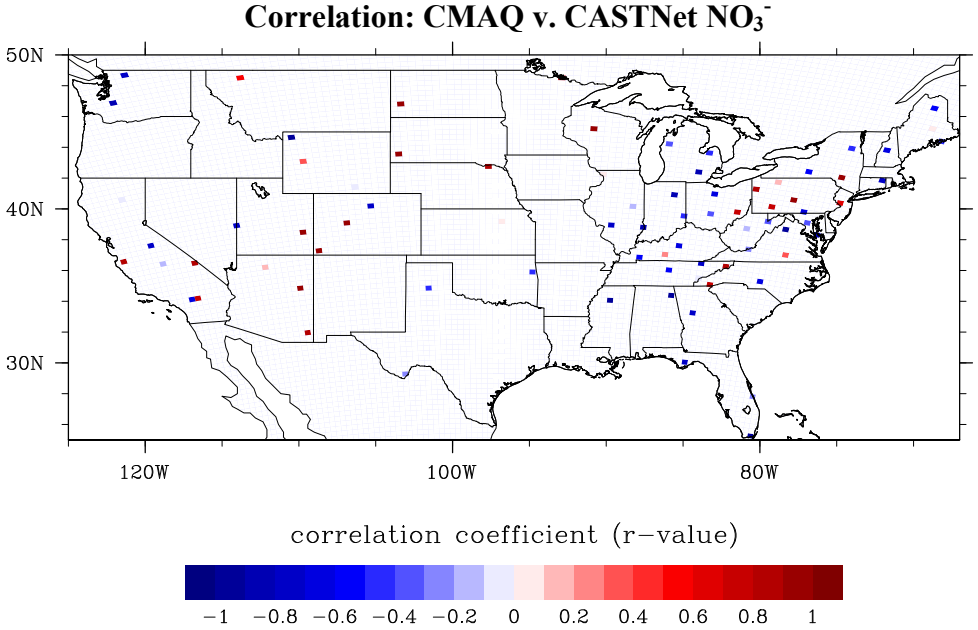

Supplemental Figure 2.2 Same as Supplemental Figure 2.1 but for nitrate concentrations.

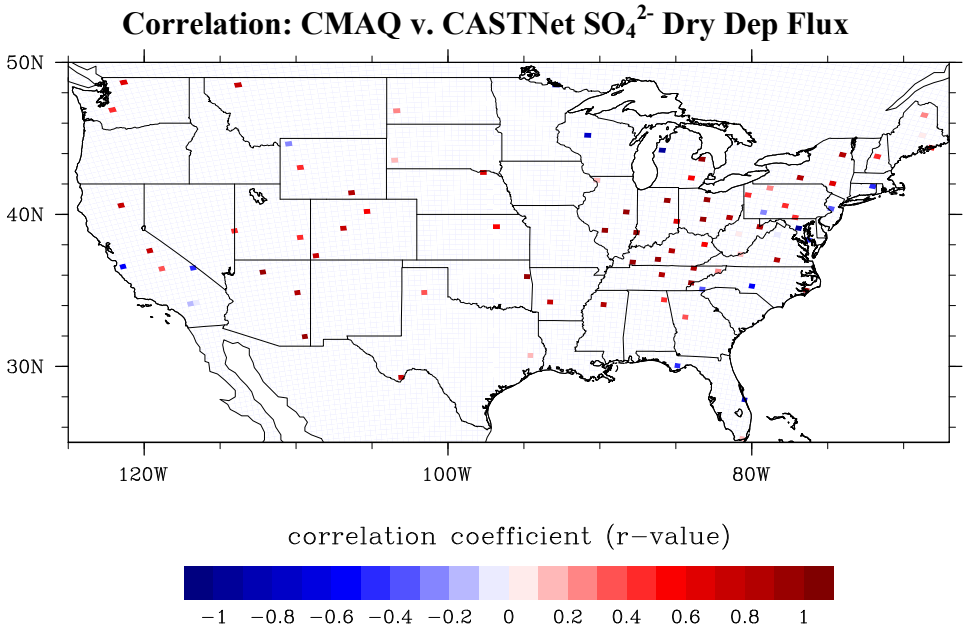

Supplemental Figure 2.3 Spatial correlation of weekly sulfate dry deposition fluxes in CMAQ and from CASTNet monitors averaged over July 2007.

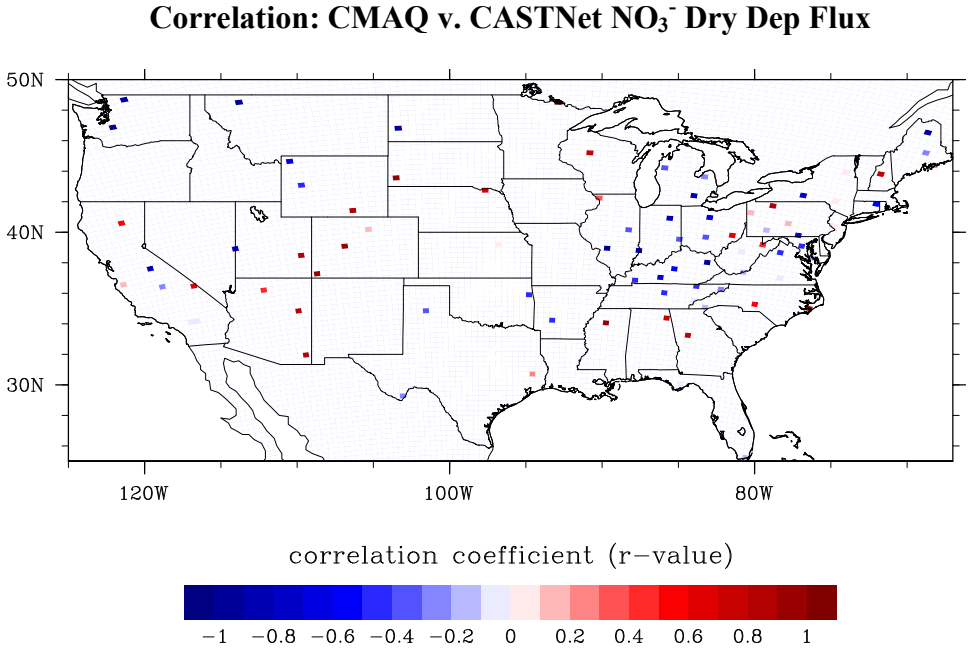

Supplemental Figure 2.4 Same as Supplemental Figure 2.3 except for nitrate dry deposition fluxes.

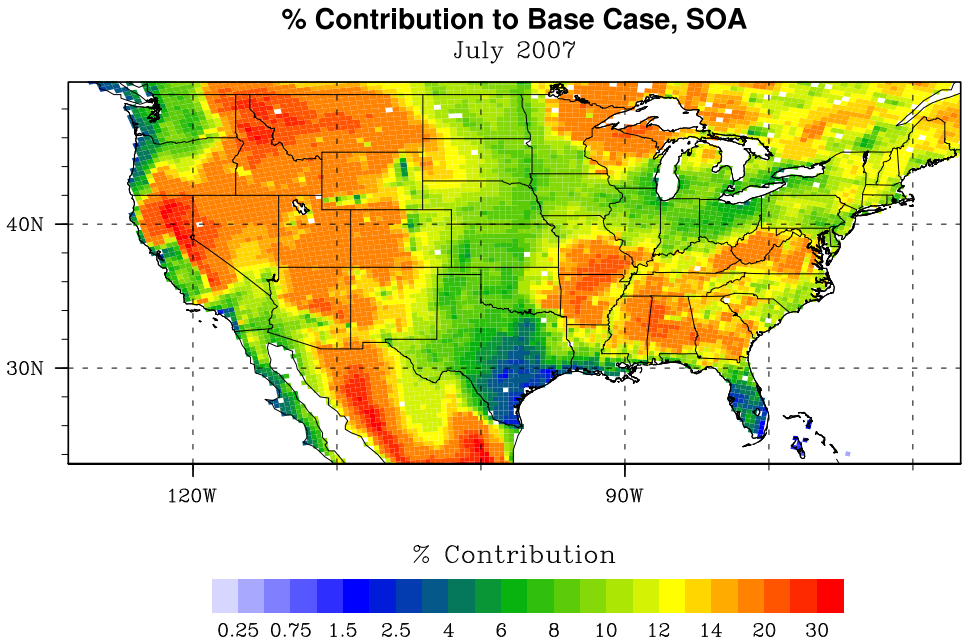

Supplemental Figure 2.5 Base case average percent contribution of SOA to total $PM_{2.5}$ for July 2007.

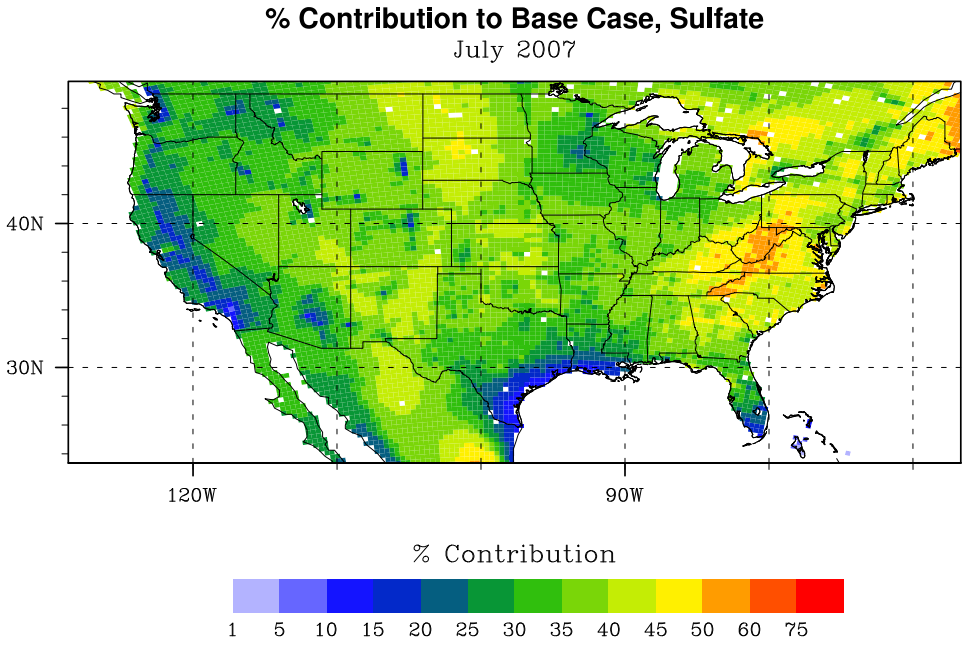

Supplemental Figure 2.6 Base case average percent contribution of SO_4^{2-} to total $PM_{2.5}$ for July 2007.

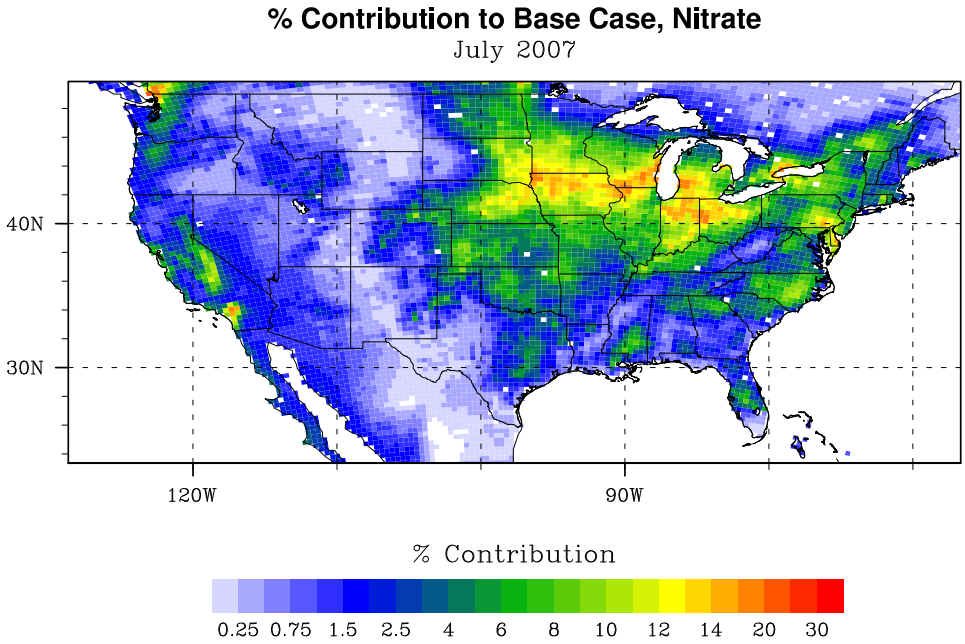

Supplemental Figure 2.7 Base case average percent contribution of NO_3^- to total $PM_{2.5}$ for July 2007.

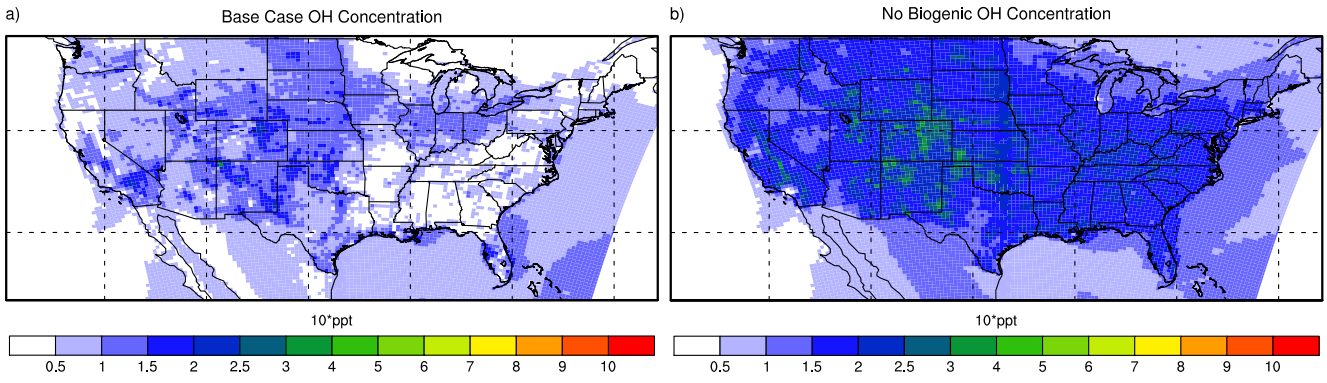

Supplemental Figure 2.8. Base Case (a) and No Biogenic (b) concentrations of OH in 10*ppt. Without biogenic emissions, the concentration of OH increases drastically. The low concentrations in the base case are due to the lack of OH-recycling in the CB05 chemical mechanism used in these simulations.

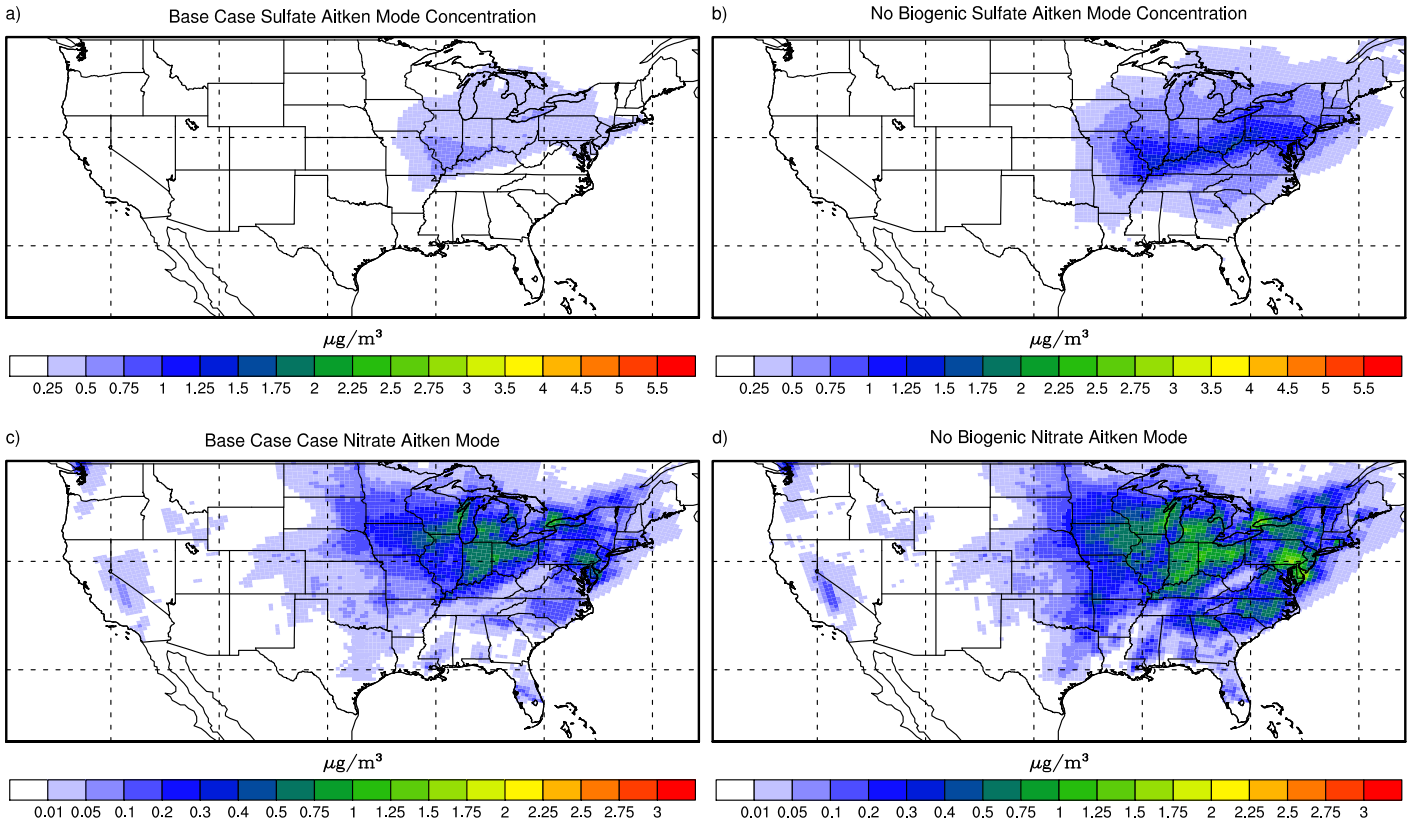

Supplemental Figure 2.9. (a) Base Case SO_4^{2-} Aitken mode concentration, (b) No Biogenic SO_4^{2-}Aitken mode concentration, (c) Base Case NO_3^- Aitken mode concentration, (d) No Biogenic NO_3^-Aitken mode concentration. Without biogenic emissions, $NO_3^-$and SO_4^{2-}Aitken and accumulation mode particles readily form via reaction with OH.

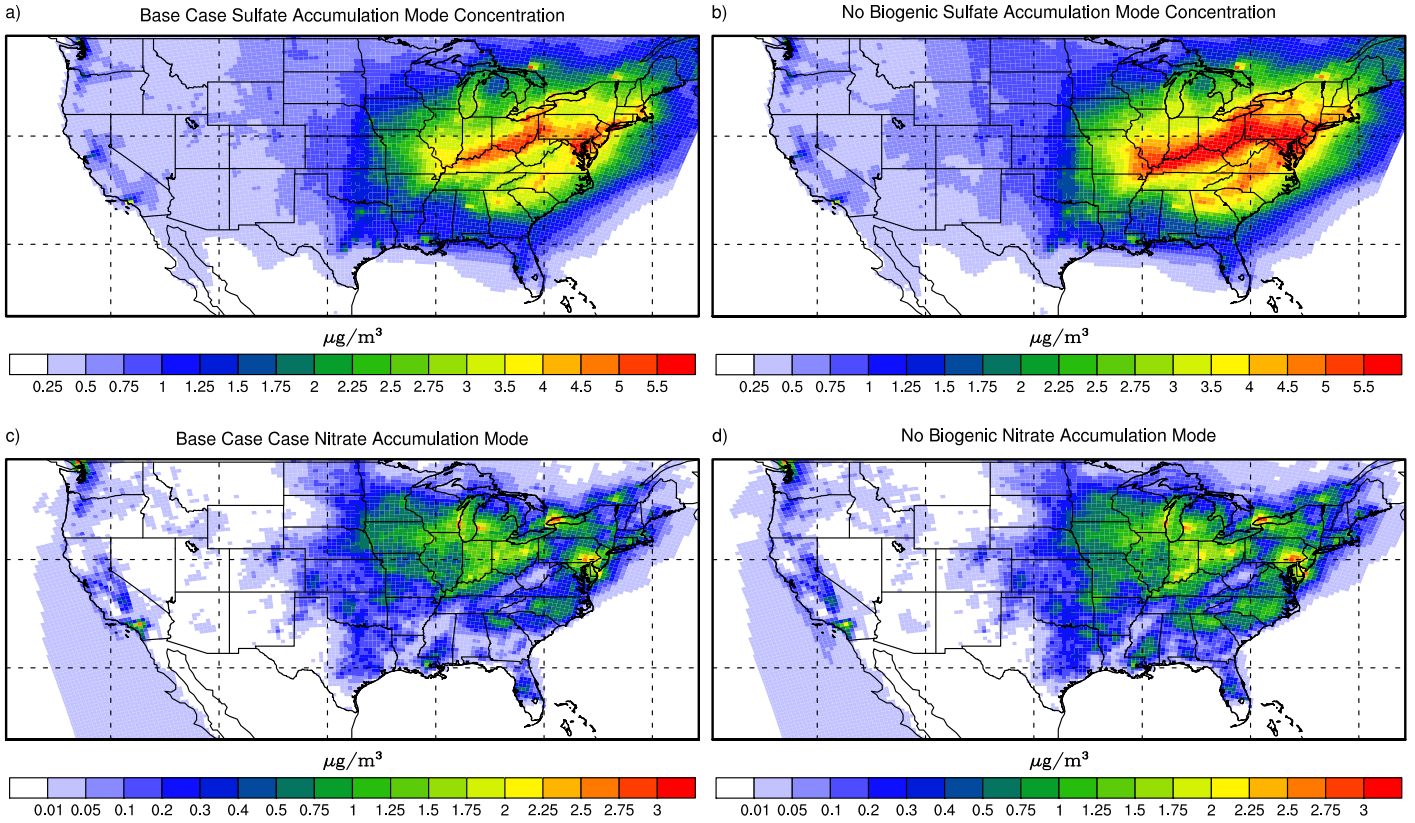

Supplemental Figure 2.10. Same as Supplemental Figure 2.9, except for accumulation mode SO_4^{2-} and NO_3^-.

References

Baumgardner, R. E., Isil, S. S., Bowser, J. J., & Fitzgerald, K. M. (1999). Measurements of Rural Sulfur Dioxide and Particle Sulfate: Analysis of CASTNet Data, 1987 through 1996. *Journal of the Air & Waste Management Association*, *49*(11), 1266–1279. doi:10.1080/10473289.1999.10463966

Baumgardner, R. E., Lavery, T. F., Rogers, C. M., & Isil, S. S. (2002). Estimates of the atmospheric deposition of sulfur and nitrogen species: Clean Air Status and Trends Network 1990-2000. *Environmental Science & Technology*, *36*(12), 2614–29. Retrieved from http://www.ncbi.nlm.nih.gov/pubmed/12099457

Bian, F., & Bowman, F. M. (2002). Theoretical method for lumping multicomponent secondary organic aerosol mixtures. *Environmental Science & Technology*, *36*(11), 2491–7. Retrieved from http://www.ncbi.nlm.nih.gov/pubmed/12075810

Binkowski, F. S., & Roselle, S. J. (2003). Models-3 Community Multiscale Air Quality (CMAQ) model aerosol component 1. Model description. *Journal of Geophysical Research*, *108*(D6), 4183. doi:10.1029/2001JD001409

Binkowski, F. S., & Shankar, U. (1995). The Regional Particulate Matter Model 1. Model description and preliminary results, *100*(95).

Butler, T. J., & Likens, G. E. (1995). A Direct Comparison of Throughfall Plus Stemflow to Estimates of Dry and Total Deposition for Sulfur and Nitrogen. *Atmospheric Environment*, *29*(11).

Cahill, T. M., Seaman, V. Y., Charles, M. J., Holzinger, R., & Goldstein, A. H. (2006). Secondary organic aerosols formed from oxidation of biogenic volatile organic compounds in the Sierra Nevada Mountains of California. *Journal of Geophysical Research*, *111*(D16), D16312. doi:10.1029/2006JD007178

Carlton, A. G., & Baker, K. R. (2011). Photochemical modeling of the Ozark isoprene volcano: MEGAN, BEIS, and their impacts on air quality predictions. *Environmental Science & Technology*, *45*(10), 4438–45. doi:10.1021/es200050x

Carlton, A. G., Bhave, P. V, Napelenok, S. L., Edney, E. O., Sarwar, G., Pinder, R. W., … Houyoux, M. (2010). Model representation of secondary organic aerosol in CMAQv4.7. *Environmental Science & Technology*, *44*(22), 8553–60. doi:10.1021/es100636q

Carlton, A. G., Pinder, R. W., Bhave, P. V, Pouliot, G. A., Alexander, T. W., Park, T., & Carolina, N. (2010). To What Extent Can Biogenic SOA be Controlled ? *Environmental Science & Technology*, *44*(9), 3376–3380.

Chin, M., Jacob, D. J., Gardner, G. M., Foreman-fowler, M. S., Spiro, P. A., & Savoie, D. L. (1996). A global three-dimensional model of tropospheric sulfate. *Journal of Geophysical Research*, *101*, 18667–18690.

Claeys, M., Graham, B., Vas, G., Wang, W., Vermeylen, R., Pashynska, V., … Maenhaut, W. (2004). Formation of secondary organic aerosols through photooxidation of isoprene. *Science*, *303*(5661), 1173–6. doi:10.1126/science.1092805

Clarke, J., Edgerton, E., & Martin, B. (1997). Dry Deposition Calculations for the Clean Air Status and Trends Network. *Science*, *31*(21), 3667–3678.

Dentener, F. J., & Crutzen, P. J. (1993). Reaction of N205 on Tropospheric Aerosols: Impact on the Global Distributions of NOx, O3, and OH. *Journal of Geophysical Research*, *98*(92), 7149–7163.

Dommen, J., Metzger, A., Duplissy, J., Kalberer, M., Alfarra, M. R., Gascho, A., … Baltensperger, U. (2006). Laboratory observation of oligomers in the aerosol from isoprene/NOx photooxidation. *Geophysical Research Letters*, *33*(13), L13805. doi:10.1029/2006GL026523

Edgerton, E. S., Hartsell, B. E., Saylor, R. D., Jansen, J. J., Hansen, D. A., & Hidy, G. M. (2005). The Southeastern Aerosol Research and Characterization Study: Part II. Filter-based measurements of fine and coarse particulate matter mass and composition. *Journal of the Air & Waste Management Association (1995)*, *55*(10), 1527–42. Retrieved from http://www.ncbi.nlm.nih.gov/pubmed/16295278

Edney, E. O., Kleindienst, T. E., Jaoui, M., Lewandowski, M., Offenberg, J. H., Wang, W., & Claeys, M. (2005). Formation of 2-methyl tetrols and 2-methylglyceric acid in secondary organic aerosol from laboratory irradiated isoprene/NOX/SO2/air mixtures and their detection in ambient PM2.5 samples collected in the eastern United States. *Atmospheric Environment*, *39*(29), 5281–5289. doi:10.1016/j.atmosenv.2005.05.031

Emmons, L. K., Walters, S., Hess, P. G., Lamarque, J.-F., Pfister, G. G., Fillmore, D., … Kloster, S. (2010). Description and evaluation of the Model for Ozone and Related chemical Tracers, version 4 (MOZART-4). *Geoscientific Model Development*, *3*(1), 43–67. doi:10.5194/gmd-3-43-2010

Finkelstein, P. L., Ellestad, T. G., Clarke, J. F., Meyers, T. P., Schwede, D. B., Hebert, E. O., & Neal, J. A. (2000). Ozone and sulfur dioxide dry deposition to forests : Observations and model evaluation. *Journal of Geophysical Research*, *105*.

Gaydos, T. M., Stanier, C. O., & Pandis, S. N. (2005). Modeling of in situ ultrafine atmospheric particle formation in the eastern United States. *Journal of Geophysical Research*, *110*, 1–12. doi:10.1029/2004JD004683

Grell, G. A., & Devenyi, D. (2002). A generalized approach to parameterizing convection combining ensemble and data assimilation techniques. *Geophyiscal Research Letters*, *29*(14), 10–13.

Griffin, R. J., Cocker, D. R., Seinfeld, J. H., & Dabdub, D. (1999). Estimate of global atmospheric organic aerosol from oxidation of biogenic hydrocarbons. *Geophysical Research Letters*, *26*(17), 2721–2724.

Guenther, A., Karl, T., Harley, P., Wiedinmyer, C., Palmer, P. I., & Geron, C. (2006). Estimates of global terrestrial isoprene emissions using MEGAN (Model of Emissions of Gases and Aerosols from Nature). *Atmospheric Chemistry and Physics Discussions*, *6*(1), 107–173. doi:10.5194/acpd-6-107-2006

Henze, D. K., & Seinfeld, J. H. (2006). Global secondary organic aerosol from isoprene oxidation. *Geophysical Research Letters*, *33*(9), L09812. doi:10.1029/2006GL025976

Heo, J., Mcginnis, J. E., Foy, B. De, & Schauer, J. J. (2013). Identification of potential source areas for elevated PM 2.5 , nitrate and sulfate concentrations. *Atmospheric Environment*, *71*(September 2006), 187–197. doi:10.1016/j.atmosenv.2013.02.008

Hurley, M. D., Sokolov, O., Wallington, T. J., Takekawa, H., Karasawa, M., Klotz, B., … Becker, K. H. (2001). Organic aerosol formation during the atmospheric degradation of toluene. *Environmental Science & Technology*, *35*(7), 1358–66. Retrieved from http://www.ncbi.nlm.nih.gov/pubmed/11348067

Jacob, D. J., Sillman, S., Logan, J. a., & Wofsy, S. C. (1989). Least independent variables method for simulation of tropospheric ozone. *Journal of Geophysical Research*, *94*(D6), 8497. doi:10.1029/JD094iD06p08497

Jaoui, M., Lewandowski, M., Kleindienst, T. E., Offenberg, J. H., & Edney, E. O. (2007). β -caryophyllinic acid: An atmospheric tracer for β -caryophyllene secondary organic aerosol. *Geophysical Research Letters*, *34*(5), L05816. doi:10.1029/2006GL028827

Kanakidou, M., Seinfeld, J. H., Pandis, S. N., Barnes, I., Dentener, F. J., Facchini, M. C., … Wilson, J. (2005). Organic aerosol and global climate modelling: a review. *Atmospheric Chemistry and Physics*, *5*(4), 1053–1123. doi:10.5194/acp-5-1053-2005

Kavouras, I. G., Mihalopoulos, N., & Stephanou, E. G. (1999). Secondary Organic Aerosol Formation vs Primary Organic Aerosol Emission: In Situ Evidence for the Chemical Coupling between Monoterpene Acidic Photooxidation Products and New Particle Formation over Forests. *Environmental Science & Technology*, *33*(7), 1028–1037. doi:10.1021/es9807035

Kim, M., Deshpande, S. R., & Crist, K. C. (2007). Source apportionment of fine particulate matter (PM2.5) at a rural Ohio River Valley site. *Atmospheric Environment*, *41*, 9231–9243. doi:10.1016/j.atmosenv.2007.07.061

Kim, Y., Fu, J. S., & Miller, T. L. (2010). Improving ozone modeling in complex terrain at a fine grid resolution – Part II: Influence of schemes in MM5 on daily maximum 8-h ozone concentrations and RRFs (Relative Reduction Factors) for SIPs in the non-attainment areas. *Atmospheric Environment*, *44*(17), 2116–2124. doi:10.1016/j.atmosenv.2010.02.038

Kleindienst, T. E., Edney, E. O., Lewandowski, M., Offenberg, J. H., & Jaoui, M. (2006). Secondary Organic Carbon and Aerosol Yields from the Irradiations of Isoprene and a-Pinene in the Presence of NOx and SO2. *Environmental Science & Technology*, *40*(12), 3807–3812.

Kleindienst, T. E., Lewandowski, M., Offenberg, J. H., Edney, E. O., Jaoui, M., Zheng, M., … Edgerton, E. S. (2010). Contribution of Primary and Secondary Sources to Organic Aerosol and PM2.5 at SEARCH Network Sites. *Journal of Air & Waste Management Association*, *60*, 1388–1399. doi:10.3155/1047-3289.60.11.1388

Kroll, J. H., Ng, N. L., Murphy, S. M., Flagan, R. C., & Seinfeld, J. H. (2006). Secondary organic aerosol formation from isoprene photooxidation. *Environmental Science & Technology*, *40*(6), 1869–77. Retrieved from http://www.pubmedcentral.nih.gov/articlerender.fcgi?artid=3637755&tool=pmcentrez&rendertype=abstract

Lelieveld, J., Butler, T. M., Crowley, J. N., Dillon, T. J., Fischer, H., Ganzeveld, L., … Williams, J. (2008). Atmospheric oxidation capacity sustained by a tropical forest. *Nature*, *452*(7188), 737–40. doi:10.1038/nature06870

Lewandowski, M., Jaoui, M., Offenberg, J. H., Kleindienst, T. E., Edney, E. O., Sheesley, R. J., & Schauer, J. J. (2008). Primary and Secondary Contributions to Ambient PM in the Midwestern United States. *Environmental Science & Technology*, *42*(9), 3303–3309.

Lin, G., Penner, J. E., Sillman, S., Taraborrelli, D., & Lelieveld, J. (2012). Global modeling of SOA formation from dicarbonyls, epoxides, organic nitrates and peroxides. *Atmospheric Chemistry and Physics*, *12*(10), 4743–4774. doi:10.5194/acp-12-4743-2012

Lin, Y., Zhang, H., Pye, H. O. T., Zhang, Z., Marth, W. J., Park, S., & Arashiro, M. (2013). Epoxide as a precursor to secondary organic aerosol formation from isoprene photooxidation in the presence of nitrogen oxides. *Proceedings of the National Academy of Sciences*, *110*(17), 6718–6723. doi:10.1073/pnas.1221150110/-/DCSupplemental.www.pnas.org/cgi/doi/10.1073/pnas.1221150110

Lin, Y., Zhang, Z., Docherty, K. S., Zhang, H., Budisulistiorini, S. H., Rubitschun, C. L., … Surratt, J. D. (2012). Isoprene Epoxydiols as Precursors to Secondary Organic Aerosol Formation : Acid-Catalyzed Reactive Uptake Studies with Authentic Compounds. *Environmental Science & Technology*, *46*, 250–258.

Lin, Y.-H., Knipping, E. M., Edgerton, E. S., Shaw, S. L., & Surratt, J. D. (2013). Investigating the influences of SO2 and NH3 levels on isoprene-derived secondary organic aerosol formation using conditional sampling approaches. *Atmospheric Chemistry and Physics*, *13*, 8457–8470. doi:10.5194/acp-13-8457-2013

Linderg, S. E., & Lovett, G. M. (1992). Deposition and Forest Canopy Interactions of Airborne Sulfur: Results from the Integrated Forest Study. *Atmospheric Environment*, *26A*(8), 1477–1492.

Mader, B. T., & Pankow, J. F. (2001). Gas/solid partitioning of semivolatile organic compounds (SOCs) to air filters. 3. An analysis of gas adsorption artifacts in measurements of atmospheric SOCs and organic carbon (OC). WHen using teflon membrane filters and quartz fiber filters. *Environmental science & technology*, *35*(17), 3422–32. Retrieved from http://www.ncbi.nlm.nih.gov/pubmed/11563642

Mesinger, F., DiMego, G., Kalnay, E., Mitchell, K., Shafran, P. C., Ebisuzaki, W., … Shi, W. (2006). North American Regional Reanalysis. *Bulletin of the American Meteorological Society*, *87*(3), 343–360. doi:10.1175/BAMS-87-3-343

Meyers, T.P., Finkelstein, P., Clarke, J., Ellestad, T. G., & Sims, P. F. (1998). A multilayer model for inferring dry deposition using standard meteorological measurements. *Journal of Geophysical Research*, *103*(98).

Meyers, Tilden P, Hicks, B. B., Hosker, R. P., Womack, J. D., & Satterfield, L. C. (1991). Dry Deposition Inferential Measurement Techniques II. Seasonal and Annual Deposition Rates of Sulfur and Nitrate. *Atmospheric Environment*, *25*(10), 2361–2370.

Millet, D. B., Guenther, A., Siegel, D. A., Nelson, N. B., Singh, H. B., Gouw, J. A. De, … Bakley, M. (2010). Global atmospheric budget of acetaldehyde : 3-D model analysis and constraints from in-situ and satellite observations. *Atmospheric Chemistry and Physics*, *10*, 3405–3425.

Nenes, A. (1998). ISORROPIA: A New Thermodynamic Equilibrium Model for Multiphase Multicomponent Inorganic Aerosols.

Nicholson, K. W. (1988). The Dry Deposition of Small Particles: A Review of Experimental Measurements. *Atmospheric Environment*, *22*(12), 2653–2666.

Nøjgaard, J. K., Bilde, M., Stenby, C., Nielsen, O. J., & Wolkoff, P. (2006). The effect of nitrogen dioxide on particle formation during ozonolysis of two abundant monoterpenes

indoors. *Atmospheric Environment*, *40*(6), 1030–1042. doi:10.1016/j.atmosenv.2005.11.029

Orel, A. E., & Seinfeld, J. H. (1977). Nitrate Formation in Atmospheric Aerosols. *Environmental Science & Technology*.

Peeters, J., Nguyen, T. L., & Vereecken, L. (2009). HOx radical regeneration in the oxidation of isoprene. *Physical Chemistry Chemical Physics*, *11*(28), 5935–9. doi:10.1039/b908511d

Raymond, H. a, Yi, S.-M., Moumen, N., Han, Y., & Holsen, T. M. (2004). Quantifying the dry deposition of reactive nitrogen and sulfur containing species in remote areas using a surrogate surface analysis approach. *Atmospheric Environment*, *38*(17), 2687–2697. doi:10.1016/j.atmosenv.2004.02.011

Seinfeld, J. H., & Pandis, S. N. (2006). *Atmospheric Chemistry and Physics: From Air Pollution to Climate Change*. New York: John Wiley & Sons, Inc.

Sheih, C. M., Wesley, M. L., & Hicks, B. B. (1979). Estimated Dry Deposition Velocities of Sulfur Over the Eastern United States and Surrounding Regions. *Atmospheric Environment*, *13*(2), 1361–1368.

Shilling, J. E., Zaveri, R. A., Fast, J. D., Kleinman, L., Alexander, M. L., Canagaratna, M. R., … Zhang, Q. (2013). Enhanced SOA formation from mixed anthropogenic and biogenic emissions during the CARES campaign. *Atmospheric Chemistry and Physics*, *13*, 2091–2113. doi:10.5194/acp-13-2091-2013

Spak, S. N., & Holloway, T. (2009). Seasonality of speciated aerosol transport over the Great Lakes region. *Journal of Geophysical Research*, *114*(D8), D08302. doi:10.1029/2008JD010598

Spracklen, D. V., Jimenez, J. L., Carslaw, K. S., Worsnop, D. R., Evans, M. J., Mann, G. W., … Forster, P. (2011). Aerosol mass spectrometer constraint on the global secondary organic aerosol budget. *Atmospheric Chemistry and Physics*, *11*(23), 12109–12136. doi:10.5194/acp-11-12109-2011

Stein, A. F., & Saylor, R. D. (2012). Sensitivities of sulfate aerosol formation and oxidation pathways on the chemical mechanism employed in simulations. *Atmospheric Chemistry and Physics*, *12*(18), 8567–8574. doi:10.5194/acp-12-8567-2012

Stockwell, W. R., Gonzalez, T., Fitzgerald, R. M., Lu, D., Zhang, Y., & Fuentes, J. D. (2007). Thoughts on modeling aerosol formation using examples from CMAQ and WRF-Chem. In *International Aerosol Modeling Algorithms (IAMA) Conference*.

Surratt, J. D., Chan, A. W. H., Eddingsaas, N. C., Chan, M., Loza, C. L., Kwan, A. J., … Seinfeld, J. H. (2010). Reactive intermediates revealed in secondary organic aerosol formation from isoprene. *Proceedings of the National Academy of Sciences of the United States of America*, *107*(15), 6640–5. doi:10.1073/pnas.0911114107

Surratt, J. D., Go, Y., Chan, A. W. H., Vermeylen, R., Shahgholi, M., Kleindienst, T. E., … Seinfeld, J. H. (2008). Organosulfate Formation in Biogenic Secondary Organic Aerosol. *Journal of Physical Chemistry A*, 8345–8378.

Surratt, J. D., Kroll, J. H., Kleindienst, T. E., Edney, E. O., Claeys, M., Sorooshian, A., … Seinfeld, J. H. (2007). Evidence for organosulfates in secondary organic aerosol. *Environmental Science & Technology*, *41*(2), 517–27. Retrieved from http://www.ncbi.nlm.nih.gov/pubmed/17969680

Surratt, J. D., Murphy, S. M., Kroll, J. H., Ng, N. L., Hildebrandt, L., Sorooshian, A., … Seinfeld, J. H. (2006). Chemical composition of secondary organic aerosol formed from the photooxidation of isoprene. *Journal of Physical Chemistry A*, *110*(31), 9665–90. doi:10.1021/jp061734m

Tsigaridis, K., & Kanakidou, M. (2003). Global modelling of secondary organic aerosol in the troposphere: A sensitivity analysis. *Atmospheric Chemistry and Physics Discussions*, *3*(3), 2879–2929. doi:10.5194/acpd-3-2879-2003

Yan, B. O., Zheng, M. E. I., Hu, Y., Weber, R. J., Baek, J., Edgerton, E. S., & Carolina, N. (2009). Roadside , Urban , and Rural Comparison of Primary and Secondary Organic Molecular Markers in Ambient PM 2 . 5. *Environmental Science & Technology*, *43*(12), 4287–4293.

Yarwood, G., Rao, S., Yocke, M., & Whitten, G. Z. (2005). *Updates to the Carbon Bond chemical mechanism: CB05 Final Report to the US EPA, RT-0400675*.

Yu, S., Mathur, R., Sarwar, G., Kang, D., Tong, D., Pouliot, G., & Pleim, J. (2010). Eta-CMAQ air quality forecasts for O_3 and related species using three different photochemical mechanisms (CB4, CB05, SAPRC-99): comparisons with measurements during the 2004 ICARTT study. *Atmospheric Chemistry and Physics*, *10*(6), 3001–3025. doi:10.5194/acp-10-3001-2010

Zhang, Y., Pun, B., Wu, S.-Y., Vijayaraghavan, K., & Seigneur, C. (2004). Application and evaluation of two air quality models for particulate matter for a southeastern U.S. episode. *Journal of the Air & Waste Management Association (1995)*, *54*(12), 1478–93. Retrieved from http://www.ncbi.nlm.nih.gov/pubmed/15648386

Zhang, Y., Wen, X.-Y., Wang, K., Vijayaraghavan, K., & Jacobson, M. Z. (2009). Probing into regional O 3 and particulate matter pollution in the United States: 2. An examination of formation mechanisms through a process analysis technique and

sensitivity study. *Journal of Geophysical Research*, *114*(D22), D22305. doi:10.1029/2009JD011900

Zhao, W., Hopke, P. K., & Zhou, L. (2007). Spatial distribution of source locations for particulate nitrate and sulfate in the upper-midwestern United States. *Atmospheric Environment*, *41*, 1831–1847. doi:10.1016/j.atmosenv.2006.10.060

Zheng, M., Cass, G. R., Ke, L., Wang, F., Schauer, J. J., Edgerton, E. S., & Russell, A. G. (2007). Source Apportionment of Daily Fine Particulate Matter at Jefferson Street, Atlanta, GA, during Summer and Winter. *Journal of Air & Waste Management Association*, (January 2002), 228–242.

Chapter 3.

Evaluating Isoprene Epoxydiol Aerosol Production in an Urban Region

Chapter adapted from Karambelas, A., H.O.T. Pye, S.H. Budisulistiorini, J.S. Surratt, and R.W. Pinder. *Isoprene epxoydiol contribution to urban aerosol: evidence from modeling and measurements*. In preparation for submission.

For this experiment, I was responsible for conducting the model simulations using input data generated by Dr. Robert Pinder (U.S. EPA) and performing analysis using measurement data taken and prepared by Sri H. Budisulistiorini (UNC-Chapel Hill).

Introduction

Isoprene is the most abundant non-methane organic compound emitted globally (Guenther et al., 2006) and is believed to be an important contributor to global secondary organic aerosol (SOA) formation, contributing approximately 50% of total $PM_{2.5}$ in the U.S on average (Kleindienst et al., 2007). Much of the SOA produced in the atmosphere is of biogenic origin, indicated by large modern carbon contributions of 36±7% in urban European locations (Glasius et al., 2011) and more than two thirds of the total carbon in near-urban and remote locations across the U.S. (Schichtel et al., 2008). Biogenic sources of isoprene include plants and trees with certain synapses (Sharkey et al., 2008) that are regulated by a variety of conditions including temperature and ozone (O_3) levels. Concentrations of isoprene in the U.S. are highest in the summer, indicated by both ground-based (Lee et al., 1998) and satellite (Palmer et al., 2003) observations of formaldehyde, a gas-phase isoprene oxidation product leading to O_3 formation, where isoprene emissions are enhanced under the warm, sunny conditions of northern hemisphere summer.

In addition to contributing to O_3 formation, isoprene can undergo oxidation processes

to contribute to fine particulate matter less than 2.5 μm in diameter ($PM_{2.5}$) in the form of SOA. Isoprene-derived SOA is produced via pathways consisting of gas-phase oxidation and heterogeneous reaction into the particle phase (Carlton et al., 2009) and is outlined in Figure 3.1. Gas-phase isoprene is first oxidized by the hydroxyl radical (OH) to yield isoprene peroxy radicals ($ISOPO_2$) that then react and form methyl vinyl ketone (MVK) or methacrolein (MACR) (Liu et al., 2013), which can contribute to aerosol formation (Surratt et al., 2010); or yield hydroperoxy-aldehydes (HPALDS), which may or may not directly contribute to SOA formation (Crounse et al., 2011; J Peeters et al., 2009). Two distinct aerosol-forming pathways exist; one occurring in a low-NO_X environment and the other in a high-NO_X environment. The latter environment causes $ISOPO_2$ to react with NO, oxidize once more, and ultimately produce methacrylic acid epoxide (MAE), a gas-phase SOA precursor with an epoxide ring structure. In this chapter, we focus on an oxidation pathway that occurs in low-NO_X environments, which begins with the oxidation of isoprene to $ISOPO_2$. From there, $ISOPO_2$ preferentially reacts with HO_2 to yield ISOPOOH with a greater than 70% yield versus the reaction with NO as quantified in laboratory studies (Paulot et al., 2009). Oxidizing once more, ISOPOOH reacts with OH to form a second gas-phase compound with an epoxide ring structure, isoprene epoxydiol (IEPOX) (Paulot et al., 2009). From here, gas-phase IEPOX will then undergo acid-catalyzed reactions that open the epoxide ring structure and attach a nucleophile species to form an aerosol.

To form IEPOX-derived aerosol, dissolved aqueous IEPOX reacts with a nucleophile and an acid in the particle phase. This reaction may produce a variety of different aerosol compounds depending on the nucleophile, including organo-sulfates and organo-nitrates (Darer et al., 2011; Eddingsaas et al., 2010), dimer species, and larger order oligomer

compounds consisting of many first-generation species of IEPOX aerosol products (Piletic et al., 2013). Another aerosol species uniquely associated with isoprene (Edney et al., 2005; Surratt et al., 2010) and IEPOX (Y. Lin et al., 2012) are the 2-methyltetrol compounds. Comprised of the sum of 2-methylthritol and 2-methylthreitol, the 2-methyltetrol species are likely the largest known contributor to IEPOX SOA, contributing between 37.2-46.0% to total isoprene-derived aerosols as found on $PM_{2.5}$ filters in Yorkville, Georgia (Y. Lin et al., 2012).

Recent laboratory experiments (Kleindienst et al., 2006; Surratt et al., 2006, 2010), field measurements (Claeys et al., 2004; Y.-H. Lin et al., 2013) and modeling studies (Carlton et al., 2010a; Pye et al., 2013; Zhang et al., 2007) have made significant advances in determining the aforementioned isoprene derived aerosol pathway, however to what extent these compounds contribute to ambient aerosols remains unclear. Ambient measurements of tracer compounds such as 2-methyltetrols have been used to quantify the contribution of isoprene SOA to total ambient aerosol*s* (Chan et al., 2010; Offenberg et al., 2007). Filter-based measurements indicate that 2-methyltetrols contribute just 5.2-8.9% of the total organic aerosol (OA) mass in Yorkville, GA (Y.-H. Lin et al., 2013). However, summertime isoprene as a whole contributes significantly to total organic carbon (OC) in filter samples taken at various locations in the Midwest U.S. (52% of total OC) (Lewandowski et al., 2008) and Research Triangle Park, North Carolina (25% of total OC) (Kleindienst et al., 2007). This suggests that there are many unknown isoprene-derived aerosol species that contribute to $PM_{2.5}$ in the troposphere.

Ambient measurement approaches employing high time resolution mass spectrometry using Aerosol Mass Spectrometer (AMS) techniques in Borneo forests (Robinson et al.,

2011) and Aerosol Chemical Speciation Monitor (ACSM) in Atlanta, GA (Budisulistiorini et al., 2013) have recently attributed a significant fraction of ambient aerosol mass to isoprene. Positive matrix factorization (PMF) analysis (Ulbrich et al., 2009) found 33% of urban organic aerosol in Atlanta, GA had a characteristic mass spectrum closely resembling that of laboratory experiments of IEPOX aerosol (IEPOX-OA) (Budisulistiorini et al., 2013). These instrumentation techniques provide high temporal resolution data and are useful for comparing with model results of current knowledge of aerosol production. In this case, if the IEPOX-OA is isoprene epoxydiol aerosol, this dataset can be used in evaluation of the specific low-NO_X pathway.

In this chapter, the connection between isoprene, IEPOX, and IEPOX-OA is evaluated with the Community Multi-scale Air Quality (CMAQv5.0) model. Model simulations presented here include detailed isoprene photo-oxidation and reactive uptake pathway (Xie et al., 2013) updated from the previously implemented version of SOA production through absorptive partitioning of semi-volatile VOC oxidation products (Annmarie G Carlton et al., 2010a). Recent CMAQ modeling incorporating this former pathway has shown that ambient measurements of 2-methyltetrol species can be simulated by the reactive uptake of isoprene epoxydiols to aerosols (Pye et al., 2013), and these along with organo-sulfates, organo-nitrates, and dimer species are compared with IEPOX-OA measurements. Base case results of IEPOX SOA are shown to better correlate with measurements than aerosol by the absorptive partitioning method, however a significant amount of mass remains missing. A sensitivity simulation is run with a modified uptake coefficient, effectively increasing the amount of gas-phase IEPOX reacted into the aerosol phase. These results prove to yield better results in terms of mass concentration and indicate

that more investigation is needed with respect to reactive uptake aerosol formation and specific isoprene-derived aerosol species that are formed.

Methods and Data

Aerosol Chemical Speciation Monitor Ambient Observations

High-temporal resolution aerosol composition data were collected from August 8th–September 14th, 2011 in Atlanta, Georgia (Budisulistiorini et al., 2013) using an ACSM instrument (Ng et al., 2011). Atlanta is an urban setting in a region known for high levels of both biogenic isoprene and anthropogenic emissions of NO_2 and SO_2. This instrument provides continuous, on-line chemical measurements from the ionization of individual particles of non-refractory particulate matter less than 1 μm in diameter (PM_1). From this, the composition of PM measurements can be logged in terms of mass spectra over time. Data from September 8th-11th is missing due to a tropical storm interfering with measurements.

Positive Matrix Factorization (PMF) analysis was performed by Budisulistiroini et al. (2013) on the organic mass fraction measurements (Ulbrich et al., 2009). Three common organic aerosol contributors were found through the analysis, including low-volatility, semi-volatile, and hydrocarbon-like organic aerosol (26±15% SV-OOA, 23±15% LV-OOA, and 18±10% HOA, respectively). However, a fourth factor contributing 33±10% to total OA was identified as having a unique increase in mass-to-charge ratio at 82, something characteristic of IEPOX-derived aerosol mass spectra (Robinson et al., 2011; Slowik et al., 2011). The time-series of the factor found in Atlanta correlated with 24-hour integrated filter-based measurements of sulfate (r^2=0.48), a known IEPOX SOA precursor, and 2-methyltetrols

(r^2=0.59), a low-NO_X IEPOX SOA product. The mass spectra of IEPOX-OA is strongly correlated with IEPOX SOA from laboratory experiments using synthetic IEPOX (r^2=0.74) (Y. Lin et al., 2012) as well as measurements of a similar factor found in the forests of Borneo (r^2=0.86) (Robinson et al., 2011). These correlations suggest that this fourth factor is an aerosol product of IEPOX. Comparisons of IEPOX-OA measurements with CMAQ-predicted IEPOX SOA products are used to evaluate the current understanding in isoprene reactive uptake mechanisms.

Air Quality Modeling

The air quality model, CMAQ v5.0, is used in this study (Byun & Schere, 2006). Generally, CMAQ is known to compare very well with ground-based (e.g. Foley et al., 2010; Godowitch et al., 2008; Spak & Holloway, 2009; Zhang et al., 2004), satellite (e.g. Zhang et al., 2009), and aircraft measurements (e.g. Carlton et al., 2008; Yu et al., 2010; Yu et al., 2007). Prior versions of CMAQ have been known to consistently overestimate summertime $PM_{2.5}$ concentrations due to biases in predicting NO_2^-, NH_4^+, organic matter, and unspeciated fine mass (Spak & Holloway, 2009). However, in the southeastern U.S., CMAQ has been shown to accurately simulate secondary inorganic aerosols such as sulfate (Foley et al., 2010) as well as primary organic aerosol (Bhave et al., 2007), where CMAQ is utilized as a tool to understand the composition of and source contributions to $PM_{2.5}$.

Model simulations were run from July 27 to September 14, 2011, and the first twelve days are discarded for model spin-up, and August 8th through September 14th, 2011 are used for analysis. This time period was selected to coordinate with the ACSM measurement data set collected by Budisulistiorini et al. (2013) during this time. The model domain includes

the continental U.S. (CONUS) as well as southern Canada and Northern Mexico. Simulations are conducted at a 12 km x 12 km horizontal resolution and 24 vertical layers from the surface to 50 hPa.

Model Input Data

Inputs to the CMAQ model include emissions sources, lateral boundary inflow, and meteorology. Meteorological data for the simulation time period are from the Weather Research Forecasting (WRF) model, and are nudged to re-analysis fields to reduce error. This data is converted to CMAQ inputs using the Meteorology-Chemistry Interface Processor (MCIP) (Otte & Pleim, 2010). Chemical lateral boundary conditions for the simulation time period are from the GEOS-Chem global chemical transport model (Henderson et al., 2013). These data are in hourly format suitable to simulated dynamic global inflow to the CONUS domain.

Emissions sources include biogenic and anthropogenic sources including but not limited to area sources, on- and off-road motor vehicles, non-road motor vehicles, electricity generating units, industrial sources, forest fires, and lightning NO_X. For these simulations, biogenic emissions, including isoprene, were processed in-line using the Biogenic Emissions Inventory System (BEIS) (Kinnee et al., 1997). Emissions from large power plants are from Continuous Emission Monitors (CEMS). Motor vehicle emissions are simulated using MOVES and include year specific estimates of vehicle miles traveled and fleet characteristics. Simulation-specific meteorology is used to process biogenic, power plants, and motor vehicle emissions. All other emissions, such as area sources and non-electricity generating units, are from the National Emission Inventory (US EPA, 2012).

Updated Isoprene Photochemistry

Simulations in this chapter include the detailed isoprene photochemistry described above that has been recently included in versions of the SAPRC-07 chemical mechanism employed at the EPA. Current aerosol chemistry distributed with updated versions of CMAQ involve gas-phase oxidation of VOCs to result in two semi-volatile gas-phase products that would then undergo vapor pressure-dependent absorptive partitioning into the aerosol phase (Annmarie G Carlton et al., 2010a; Odum et al., 1996). However, aerosol formation can also occur when aerosol water and organic aerosol behave as partitioning phases, causing gas-phase compounds to react on the aerosol surface and form accumulation more aerosols in regions affected by both anthropogenic and biogenic VOC emissions (X. Zhang et al., 2012). Updates were made to the base version of the SAPRC-07 chemical mechanism (Hutzell et al., 2012) that incorporate advances in isoprene oxidation chemistry with regards to HO_X recycling and account for excess OH in areas high in isoprene (Jozef Peeters & Müller, 2010); isoprene oxidation and the relationship to nitrogen species (Lockwood et al., 2010; Rollins et al., 2009); and understanding intermediate steps in isoprene oxidation (Crounse et al., 2011; Paulot et al., 2009). These updates are important for capturing the variability in isoprene SOA formation and precursors like aerosol water and sulfate in the southeastern U.S. (Xie et al., 2013).

The schematic of both the absorptive partitioning and reactive uptake aerosol pathways are shown in Figure 3.2. The absorptive partitioning aerosol formation pathway (Figure 3.2, enclosed in the orange box) is initiated by the gas-phase oxidation of volatile organic compounds (VOC) such as isoprene to form two semi-volatile gas-phase compounds, for example the CMAQ intermediate species SV_ISO1 and SV_ISO2. These compounds

then undergo vapor pressure-dependent absorptive partitioning to yield aerosol products such as AISO1 and AISO2. The 2-product organic aerosol production pathway for SOA formation remains in all up-to-date versions of CMAQ.

In the model version used in these experiments, only the isoprene aerosol pathway has been updated. Major updates to the chemical mechanism include detailed gas-phase oxidation of isoprene to epoxide compounds via low-NO_X (IEPOX) and high-NO_X (MAE) pathways (Figure 3.2, mechanism not enclosed). Both IEPOX and MAE then participate in acid-catalyzed reactions, which break open the epoxide ring-structure and attached a nucleophile species to form an aerosol in the accumulation mode. Aerosol species formed in CMAQ from the reactive uptake of IEPOX include 2-methyltetrols (AIETET), organo-sulfates (AIEOS), organo-nitrates (AIEON), and dimer species that consist of IEPOX combined with an existing IEPOX-derived aerosol (ADIM). These species represent the current knowledge of isoprene-derived aerosol chemistry.

Reactive uptake of isoprene-derived epoxide compounds onto accumulation mode aerosols is incorporated into CMAQ through a series of equations leading to the formation of aerosols and the elimination of gas-phase precursor. All equations referenced are from updates introduced in Pye et al. (2013). The change of gas-phase IEPOX during a model timestep, Δt, is calculated using

$$\Delta IEPOX = IEPOX_i \left[exp\left(\frac{-A}{\frac{r_p}{D_g} + \frac{4}{v_i \gamma_{IEPOX}}} \Delta t \right) - 1 \right], \quad (1)$$

where $IEPOX_i$ is the initial gas-phase IEPOX concentration at the beginning of the model timestep, A is the aerosol surface area, r_p is the effective particle radius, D_g is the gas-phase diffusivity, v_i is the mean molecular speed, and γ_i is the IEPOX uptake coefficient. The uptake coefficient, γ_i, parameterizes the heterogeneous uptake into the aerosol phase, and the general γ_{IEPOX} is calculated using

$$\gamma_{IEPOX} = \left(\frac{1}{\alpha} + \frac{v}{4HRT\sqrt{D_a k_{particle\ IEPOX}}}\frac{1}{f(q)}\right)^{-1} \quad (2)$$

$$f(q) = \coth(q) - \frac{1}{q} \quad (3)$$

$$q = r_p\sqrt{\frac{k_{particle\ IEPOX}}{D_a}} \quad (4)$$

whereD_a is the aerosol phase diffusivity, $k_{particle\ IEPOX}$ is the pseudo first-order rate constant for the reaction of IEPOX into the aerosol phase, q is the diffuso-reactive parameter, T is temperature, R is the gas constant, H is the Henry's Law coefficient ($2.7x10^6$ M/atm for IEPOX), and α is the mass accumulation coefficient. The pseudo first-order particle phase reaction rate is calculated at each model timestep using the concentrations of aerosol acidity and available nucleophiles and the third order particle phase reaction rate constant ($k_{i,j}$) in the equation

$$k_{particle\ IEPOX} = \sum_{i=1}^{N}\sum_{j=1}^{M} k_{ij}[nuc_i][acid_j] \quad (5)$$

for N nucleophiles and M acids. Equation 5 is deemed pseudo first-order because concentration of the acid, where acid is either the hydrogen ion (H^+) or bisulfate ion (HSO_4^-), outweighs that of the nucleophile. Accumulation mode nucleophile species (nuc_i) used in

equation (5) are aerosol water, sulfate, and nitrate, and nucleophile concentrations are calculated along with accumulation-mode acidity concentrations using ISORRPIA II (Fountoukis & Nenes, 2007), a thermodynamic equilibrium model that calculates equilibrium gas, solid, and liquid phase concentrations according to timestep temperature and relative humidity, and concentrations of the following species: Na, Cl, K, Mg, H_2SO_4, HNO_3, NH_3, and HCl. The equilibrated aerosol nucleophile and acid concentrations are then used in equation (5) to propagate the reactive uptake of IEPOX.

The third-order particle phase rate constant (k_{ij}) in equation 5 was determined through laboratory analysis of epoxide-ring opening reactions (Eddingsaas et al., 2010). As of this study, k_{ij} terms remain uncertain, however Pye et al. (2013) conducted a series of sensitivity tests with varying parameters. Parameters used in Pye et al. (2013) that lead to the best agreement with observed IEPOX SOA tracer measurements were used in this simulation and are included in Table 3.1. Additionally, k_{ij} constants used in CMAQ are identical for nucleophilic addition of both sulfate and nitrate due to lack of laboratory measurements

Model results from the grid box containing Atlanta, Georgia are compared to surface measurements taken there during this time period. The correlation between the IEPOX-OA measured factor and the detailed CMAQ simulation of 2-methyltetrols and other IEPOX SOA species are examined. Additionally, modeled correlations between IEPOX-OA and other compounds are analyzed, including that of semi-volatile isoprene SOA. Comparing a variety of predicted aerosol species to measured IEPOX-OA will help determine if isoprene epoxydiols are the best explanation for the IEPOX-OA factor seen in the ACSM measurements in Atlanta, GA. Finally, since 2-methyltetrols are only one compound contributing to IEPOX-OA, a sensitivity simulation was conducted to attempt to explain high

concentrations of IEPOX-OA mass and identify additional sources of IEPOX aerosol. In this scenario, a factor multiplier is applied to γ_{IEPOX} to increase the uptake of gas-phase IEPOX into the aerosol phase and simulate an unknown isoprene-derived aerosol species.

Results

Low-NO_x Isoprene-derived Aerosol Spatial Analysis

Across the continental United States, isoprene is most prevalent in the southeastern U.S. (Figure 3.3a). The lush environment and summertime conditions are ideal for isoprene emissions. Significant concentrations greater than 12 ppbv are seen around the southern half of the Mississippi River, and the rest of the southeast experiences concentrations greater than 5 ppbv. Additional regions of high isoprene concentrations in the domain include coastal California, southern Minnesota, and western Mexico. Gas-phase IEPOX follows a similar spatial pattern as isoprene, but at a fraction of the concentration of isoprene (Figure 3.3b). Concentrations less than 1 ppbv on average exist in the southeast, with maximum concentrations along the border of Texas and Louisiana and across Mississippi, Alabama, and Georgia. Additional IEPOX production is seen in northern California and western Mexico.

The highest concentrations of IEPOX-derived aerosol products is downwind of the highest concentrations of both isoprene and IEPOX (Figure 3.3c and 3.3d, respectively). Production of 2-methyltetrols is greatest in the Virginias and along the Atlantic coast of South Carolina. In these areas, concentrations remain just about 0.5 $\mu g/m^3$ (Figure 3.3c). Elsewhere in the southeast, 2-methyltetrol concentrations remain around 0.25 $\mu g/m^3$. Including organo-sulfates, organo-nitrates, and dimer species increases the IEPOX-derived

aerosol concentration just slightly more than those of the 2-methyltetrols individually, but the spatial pattern remains the same (Figure 3.3d). No other region within the domain experiences IEPOX-derived aerosol production to the extent of the southeast.

Simulated IEPOX-derived Aerosol Driven by Aerosol Acidity

Gas-phase oxidation and particle-phase reactions are two key components that drive IEPOX-OA production, and aerosol acidity is strongly connected to the formation of IEPOX-derived aerosol. The average diurnal model-predicted concentrations of isoprene and relevant oxidation products from August 8th to September 14th, 2011 are shown in Figure 3.4, where the black line represents a model variable (left y-axis) and the red line is the observed IEPOX-OA concentration derived from the PMF factorization (right y-axis). Gas-phase IEPOX is a tertiary oxidation product of isoprene, where the greatest isoprene oxidation occurs during the daytime (Figure 3.4a). A decline in isoprene concentrations is seen corresponding with an increase in the production of the first isoprene oxidation product, $ISOPO_2$, which is only produced via isoprene oxidation (Figure 3.4b). The decline in isoprene concentrations and maximum daytime concentration of $ISOPO_2$ both occur simultaneously with an increase in IEPOX-OA measurements. The peroxy radical reacts with HO_2 to form ISOPOOH (Figure 3.4c), which reacts to form gas-phase IEPOX (Figure 3.4d). Model predicted concentrations of $ISOPO_2$ and ISOPOOH are small fractions of isoprene concentrations on average in Atlanta. Gas-phase IEPOX concentrations, shown in mass concentration, compare well with the mass concentrations of measured IEPOX-OA. This indicates an abundance of gas-phase IEPOX available for reaction into the aerosol phase.

The equations for γ_{IEPOX} and $k_{particle\ IEPOX}$ state that aerosol acidity, nucleophiles, and IEPOX are necessary for the successful reactive uptake of IEPOX onto the accumulation mode. In the base case simulations, nucleophiles are aerosol water, sulfate, nitrate, and the first-order IEPOX SOA products of 2-methyltetrols, organo-sulfates, and organo-nitrate. Gas-phase IEPOX is predicted to be abundant in Atlanta (Figure 3.4d). Additionally, predicted aerosol water concentrations are abundant and are not expected to inhibit formation of 2-methyltetrols. Organo-sulfates and nitrates exhibit weak concentrations compared with 2-methyltetrols, and therefore the nucleophile additions of sulfate and nitrate are less important than the nucleophilic addition of water.

The maximum concentration of IEPOX-derived aerosols (Figure 3.4f) occurs coincident with the maximum $k_{particle\ IEPOX}$ (Figure 3.4e) and a slight reduction in IEPOX (Figure 3.4d). This is evident both in the early morning when CMAQ predicts a slight increase in IEPOX SOA and around noon when maximum concentration occurs. Predicted IEPOX SOA concentrations from CMAQ (left y-axis) exhibit a diurnal structure very similar to that of the IEPOX-OA measurements (right y-axis). Peak concentration occurs in both the model and measurements between the late morning and noon local time. However CMAQ under predicts IEPOX SOA formation by about a factor of 10 despite ample gas-phase IEPOX. The average measurement concentration is 3.45 $\mu g/m^3$, while the average modeled aerosol concentration is 0.290 $\mu g/m^3$.

The isoprene reactive uptake pathway in CMAQ is dependent on $k_{particle\ IEPOX}$ and γ_{IEPOX}, which are strongly regulated by concentrations of aerosol acidity. From equation (2), $k_{particle\ IEPOX}$ is used to solve for γ_{IEPOX} and is calculated using the concentration of H^+ and HSO_4^-. Figure 3.5 indicates a strong connection between acidity (Figure 3.5a, black line)

and the subsequent constants $k_{particle\ IEPOX}$ (Figure 3.5b, black line) and γ_{IEPOX} (Figure 3.5c, black line) as evidenced by the nearly identical diurnal pattern shared between all three variables. IEPOX-OA measurements (red line) indicated CMAQ-estimated acidity, $k_{particle\ IEPOX}$, and γ_{IEPOX} resemble the diurnal structure of measured IEPOX-derived aerosol. The diurnal average of peak aerosol concentration in the measurements (Figure 3.4f) occurs coincident with the diurnal average peak acidity, $k_{particle\ IEPOX}$, and γ_{IEPOX}.

IEPOX-OA Factor Correlated with Simulated IEPOX-derived Aerosol

Although CMAQ significantly under-predicts IEPOX SOA, the reactive uptake pathway proves to better correlate with the diurnal pattern seen in the Atlanta, GA measurements than the 2-product SOA production approach originally included in the model. Measured IEPOX-OA is compared with two representations of isoprene aerosol from CMAQ, reactive uptake of IEPOX to form 2-methyltetrols as described in Pye et al. (2013), and 2-product aerosol approach via vapor pressure-dependent absorptive partitioning of oxidized isoprene products (Annmarie G Carlton et al., 2010b). Diurnal average and temporal plots are shown in (Figure 3.6a). The IEPOX-OA measurements (solid red line) show an average steady decline of 1 $\mu g/m^3$ from midnight until approximately 9AM EST. IEPOX-OA production occurs on average just after 9AM until about 3PM. Concentrations increase during this time from a daily average minimum of 2.67 $\mu g/m^3$ to remain steady around 4 $\mu g/m^3$ through the evening. IEPOX-OA production mainly occurs during the most active photochemical time of day, but there also appears to be enough production during the evening to compensate for loss processes.

Isoprene aerosol by the 2-product absorptive partitioning mechanism shows a noticeably different diurnal structure than that of the IEPOX-OA measurements (blue dashed line, concentrations on left y-axis). Concentrations remain low and peak in the middle of the day just before noon local time, however concentrations exhibit a much larger evening increase around 9PM EST before declining again by midnight. This diurnal pattern represents the semi-volatile partitioning of isoprene gas-phase products to particulate phase, and the diurnal average does not correspond significantly well with the measurements ($r=0.49$).

Predicted 2-methyltetrols (black solid line, concentrations on right y-axis), however, exhibit a very similar diurnal pattern to the IEPOX-OA measurements. Concentrations are considerably lower in the early morning compared to IEPOX-OA, but there is an indication of a small amount of morning production just before 6AM. Daily IEPOX SOA production begins just before 9AM EST and concentrations increase until approximately 1PM local time, after which point concentrations steadily decline through the evening. Although the pattern seen in the IEPOX-OA measurements is also evident in the modeled 2-methyltetrol concentrations, there are a few noticeable differences. Most important is the decline in predicted 2-methyltetrol concentrations in the evening versus the steady IEPOX-OA measurements reflecting the fact that both acidity and aerosol water decline. In addition, CMAQ seems to predict IEPOX SOA production about an hour sooner than shown in the measurements. This can be a result of a number of things, including but not limited to predicting the occurrence of gas-phase oxidation earlier than actually occurs in nature.

The temporal plot for the simulation time period shows that both the 2-product and the reactive uptake aerosol pathways compare fairly similarly with the pattern in the IEPOX-

OA measurements (Figure 3.6b). Both measured and predicted concentrations accumulate every few days before rapidly declining due to reduced relative humidity or increased wind speed. However, the variability in IEPOX-OA measurements (red solid line) is more accurately represented by the IEPOX SOA concentrations (black solid line) than the Odum 2-product isoprene aerosol (blue dashed line). During most periods of aerosol accumulation, the Odum 2-product aerosol concentration consistently increases while IEPOX SOA exhibit fluctuations akin to the measurements. The temporal plot indicates the extent to which CMAQ greatly under predicts both varieties of isoprene aerosol products. The Odum 2-product aerosol is about a factor of 3 less than the IEPOX-OA measurements, while the IEPOX SOA are under predicted by about a factor of 10. Despite the large difference between predicted IEPOX SOA and IEPOX-OA measurements, a slightly higher correlation coefficient between the diurnal average model and measured data (r=0.53) indicates the epoxide pathway is a better representation of isoprene-derived aerosol in a low-NO_X environment.

Enhanced Reactive Uptake to Explain Observed IEPOX-OA Mass

To attempt to account for the missing IEPOX SOA mass in the base case simulation, a sensitivity simulation was conducted where γ_{IEPOX} was increased by a factor of 10. In order to increase gas-phase uptake, it is assumed that an unknown IEPOX-derived aerosol species exists and is produced similarly to 2-methyltetrols. For this simulation, 2-methyltetrols, organo-sulfates and organo-nitrates were not included as nucleophiles, which causes a slight decrease in maximum $k_{particle\ IEPOX}$, though γ_{IEPOX} increases significantly from the factor of 10

increase. From the exclusion of the aforementioned nucleophile species, dimer species are not incorporated into the sensitivity simulation for simplification.

Ultimately, increasing the uptake coefficient significantly increases the amount of IEPOX SOA predicted in CMAQ. As a consequence of more aerosol production, gaseous IEPOX decreases slightly (not shown, from 2.86 $\mu g/m^3$ to 2.56 $\mu g/m^3$ on average), but the amount depleted is very small in comparison to the factor of 5 increase in aerosol formation. Base case concentrations of 2-methyltetrols, organo-sulfates, and organo-nitrates are shown with a factor of 10 increase (Figure 3.7a, blue dashed line), and sensitivity concentrations of the IEPOX aerosol including 2-methyltetrols, organo-sulfates, organo-nitrates, and a fourth unknown species are shown with a factor of 2 increase (Figure 3.7a, solid black line). Concentrations of IEPOX derived aerosol increase from a base case average of 0.280 $\mu g/m^3$ to 1.53 $\mu g/m^3$ in the sensitivity case. From the increased uptake of gas-phase IEPOX, IEPOX SOA in the sensitivity simulation is five times greater than the base case and only a factor of 2 less than the IEPOX-OA measurements (Figure 3.7a, solid red line), a substantial improvement against the base case IEPOX SOA concentrations.

Near identical features are exhibited in both the base and sensitivity scenarios (Figure 3.7a). Early morning concentrations are still not on trend with the measurements, but overall the diurnal shape in the sensitivity case remains highly unchanged from the base case. Differences in the diurnal pattern between the sensitivity simulation and the base case arise at the times of peak concentrations. The maximum sensitivity IEPOX SOA concentration is dampened slightly between 3AM and 6AM and again at 12PM in comparison to the maximum base case concentrations. This is attributed to the slight decrease in maximum $k_{particle\ IEPOX}$ from not including dimer formation in the sensitivity run. The slight reduction in

maximum $k_{particle\ IEPOX}$ yields a similar reduction in maximum γ_{IEPOX}, thus the inconsistent magnitude difference between the two simulations throughout the day is understandable.

From the hourly distribution (Figure 3.7b), the new IEPOX aerosol (black solid line) predicts the magnitude of aerosol substantially better than the base case (blue dashed line) in comparison to the IEPOX aerosol measurements (solid red line). Similar to the diurnal average, the new IEPOX-OA concentrations maintain a very similar shape to the base case simulation, suggesting modifications to the uptake coefficient did not alter IEPOX aerosol formation mechanisms but only the amount of IEPOX aerosol formed from gaseous IEPOX.

Discussion

From the base case and sensitivity simulation, two conclusions can be made. First, the CMAQ predicted IEPOX-derived aerosols have a stronger correlation with IEPOX-OA measurements than do the Odum 2-product isoprene aerosol concentrations (r=0.53 for the former, r=0.49 for the latter). In addition, correlations of the IEPOX-OA measurements and 2-methylglyceric acid, the high-NOx isoprene aerosol pathway, are weak at r=0.394. These suggest that the IEPOX-OA factor from the ACSM observations is consistent with known 2-methyltetrol formation mechanisms as predicted in CMAQ. The diurnal profile is well represented by the model but predicted concentrations are more than a factor of 10 lower than the measurements, suggesting an unknown IEPOX-derived aerosol may not be included in the model.

The 2-methyltetrols, the most abundant IEPOX-derived aerosol product, form from the reaction of IEPOX and aerosol water. Aerosol water (not shown) peaks in the early morning and decreases until the early evening in the model and is partially responsible for

the decrease in modeled IEPOX aerosol later in the day. As the concentration of water decreases, reaction of IEPOX with other particle-phase nucleophiles becomes more favorable.

Pye et al. 2013 considers the oligomerization of IEPOX-derived aerosol monomers (2-methyltetrols, organo-sulfates, and organo-nitrates) with IEPOX that form 2-methyltetrol dimers, but oligomerization of dissolved IEPOX with other organic aerosol constituents is not treated. Piletic et al. (2013) indicate that these other oligomerization reactions not included are kinetically favorable over IEPOX reaction with water. Assuming that all preexisting organic aerosol can oligomerize with dissolved IEPOX in the particle, the formation of oligomers to 2-methyltetrols can be estimated using the ratio of total organic species to aerosol water along with estimated particle-phase rate constants. Estimates of the average diurnal rates of oligomerization versus 2-methyltetrol formation indicate evening oligomer formation could outweigh 2-methyltetrol formation and thus may account for the decline in IEPOX SOA production after the 3PM peak in concentration. However this does not account for the major discrepancy in mass concentration between the measurements and the model throughout the entire day.

Despite the base case CMAQ simulation under-predicting IEPOX SOA concentrations by more than a factor of 10 when compared with the measurements, modeled and measured acidity remain comparable between 15-20 nmol/m^3. Enhancing the acidity in the model would unnecessarily introduce more acidity into the model environment. In addition, CMAQ systematically over predicts 2-methyltetrols by a factor of 2 (Pye et al., 2013), which could be due to a lack of competitive IEPOX loss pathways or further 2-methyltetrol processing. Based on this, it is highly likely that the large underestimation when

compared with IEPOX-OA measurements arises from an unknown IEPOX aerosol species that is not included in the reactive uptake mechanism and not from inadequate aerosol acidity calculations driving the reactive uptake mechanism in CMAQ.

Assuming an unknown IEPOX-derived aerosol forms and behaves as 2-methyltetrols, we increased the reactive uptake coefficient, γ_{IEPOX}, to account for the missing mass attributed to the unknown IEPOX aerosol species. Here, we increased the coefficient by a factor of 10 to account for base case concentrations 10 times lower than the measurements and found that increasing the reactive uptake coefficient increase the IEPOX-derived aerosol concentration without modifying the diurnal structure. Resulting concentrations of 2-methyltetrols, organo-sulfates, and organo-nitrates increased by a factor of 5 in response to a 10 times larger uptake coefficient. Recent modeling analysis of the 82fac aerosol component found in Borneo (Robinson et al., 2011) concluded IEPOX SOA yields should be about 5 times greater than laboratory-based SOA yields (e.g. Y. Lin et al., 2012) in order to account for the IEPOX-derived aerosol (Janssen et al., 2013). Since we predict only a subset of IEPOX-derived aerosol in CMAQ, the factor of 10 increase applied in this study is realistic for better comparison with measurements while accounting for an unknown aerosol species.

It is clear the reactive uptake pathway implemented in CMAQ compares well temporally with a continuous set of IEPOX-OA measurements, especially in comparison to the prior implemented absorptive partitioning aerosol formation mechanism. However, unknown aerosol species can yield poor model results in comparison to measurements. More research of isoprene-derived aerosol formation is necessary to understand aerosol formation and to implement in air quality models for better performance. Additionally, for more accurate comparisons between model and measurement data of the entire reactive uptake

pathway, a complete set of measurements of gas-phase species along the pathway are necessary to monitor from isoprene concentration to isoprene-derived aerosol to understand if CMAQ accurately simulates isoprene reactive uptake to the aerosol phase in low-NOx conditions. Through better understanding of the aerosol mechanism in nature and taking more measurements of different species, air quality model simulations can be improved for research and air quality management purposes.

Figures

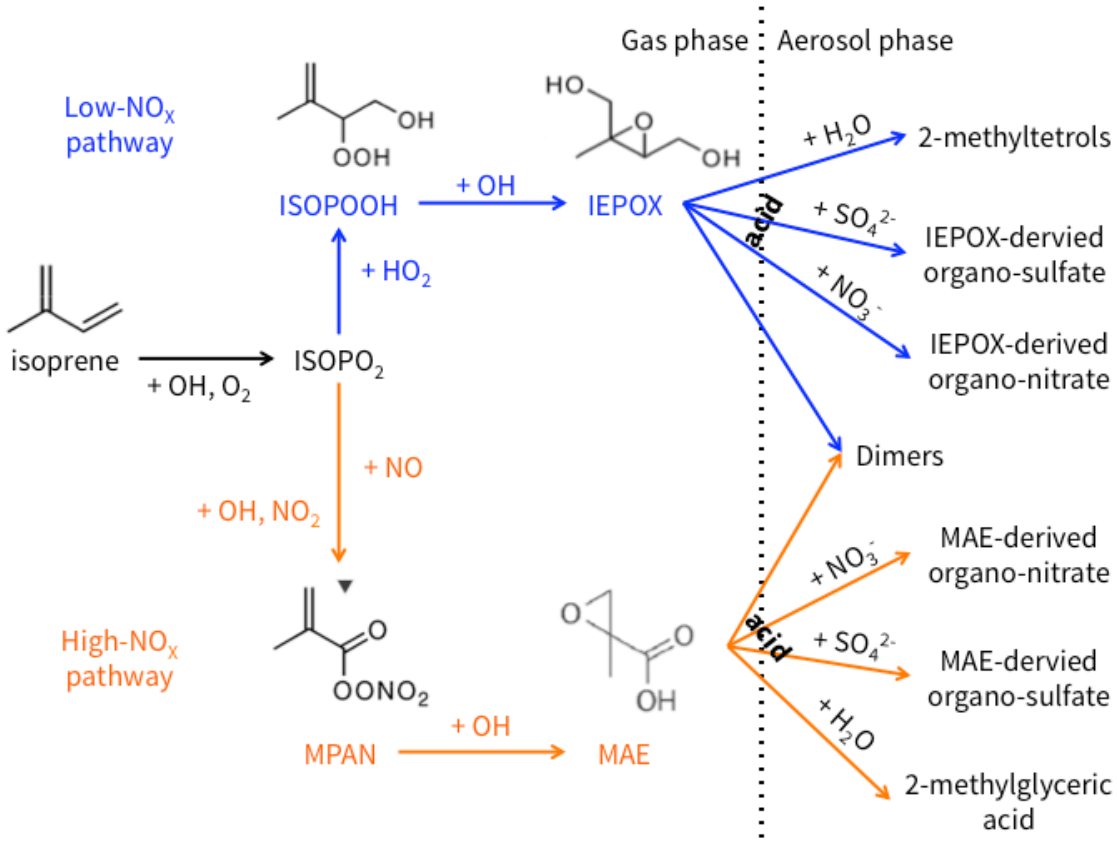

Figure 3.1 Isoprene reactive uptake pathway for both low-NOx (blue) and high-NOx (orange) environments. Isoprene is oxidized to form $ISOPO_2$ that can react with NO (high NO_X) or HO_2 (low NO_X) to further oxidize and yield MAE or IEPOX, respectively. From there, acid-catalyzed reactions form aerosols through the addition of a nucleophile species.

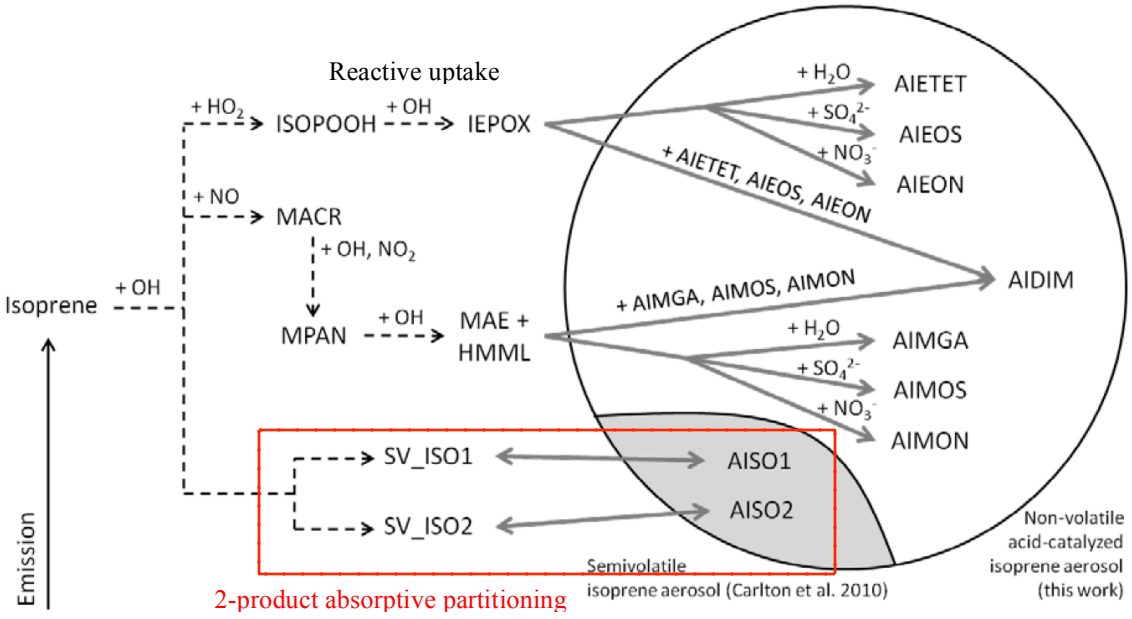

Figure 3.2 Schematic of model isoprene aerosol pathways. The red box indicates the isoprene 2-product vapor pressure-dependent absorptive partitioning aerosol formation pathway used in CMAQ. This pathway involves the oxidation of isoprene by OH to form two semi-volatile isoprene compounds that partition between the aerosol phase and the gas phase. The reactive uptake pathway included in these model simulations (not enclosed within a box) involves the initial oxidation reaction with OH and subsequent reactions with either HO_2 or NO in low-NO_X or high-NO_X environments respectively. From there, further oxidation reactions yield epoxide structures that undergo acid-catalyzed reactions with nucleophiles to form aerosols. Aerosol species produced in CMAQ are enclosed in the circle and are 2-methyltetrols (AIETET), 2-methylglyceric acid (AIMGA), organo-sulfates (AIEOS, AIMOS), organo-nitrates (AIEON, AIMON), and dimers (AIDIM). Source: Pye et al., (2013) supplemental material.

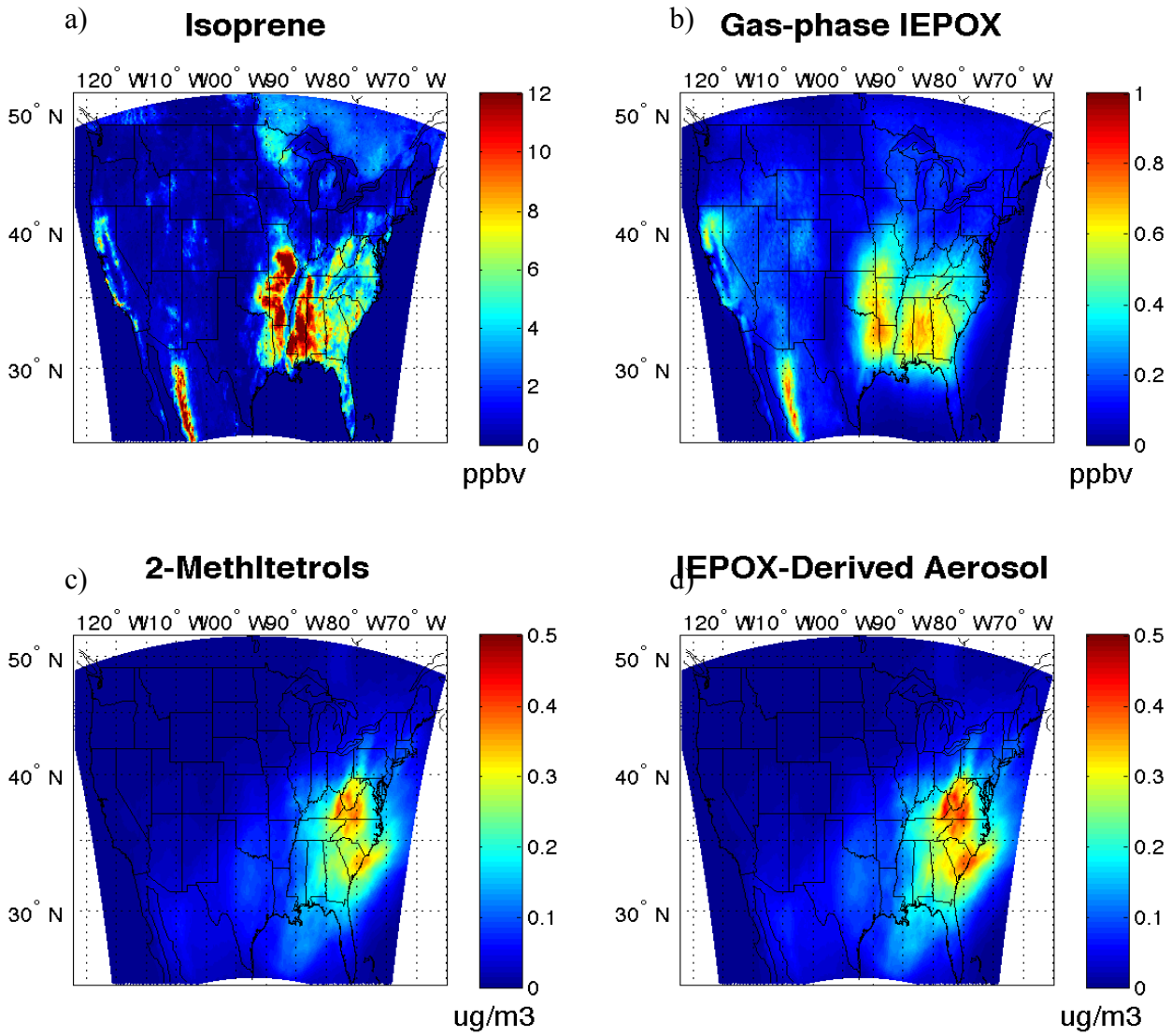

Figure 3.3 Plots of base case isoprene (a), IEPOX (b), 2-methyltetrols (c), and the sum of 2-methyltetrols, organo-sulfates, organo-nitrates, and dimer aerosol species (d). Regions of high IEPOX concentrations coincide with regions of high isoprene concentrations with the largest concentrations seen in the southern Mississippi River region, and IEPOX-derived aerosol production occurs east of largest concentrations of IEPOX with maximum concentrations over the Virginias and South Carolina.

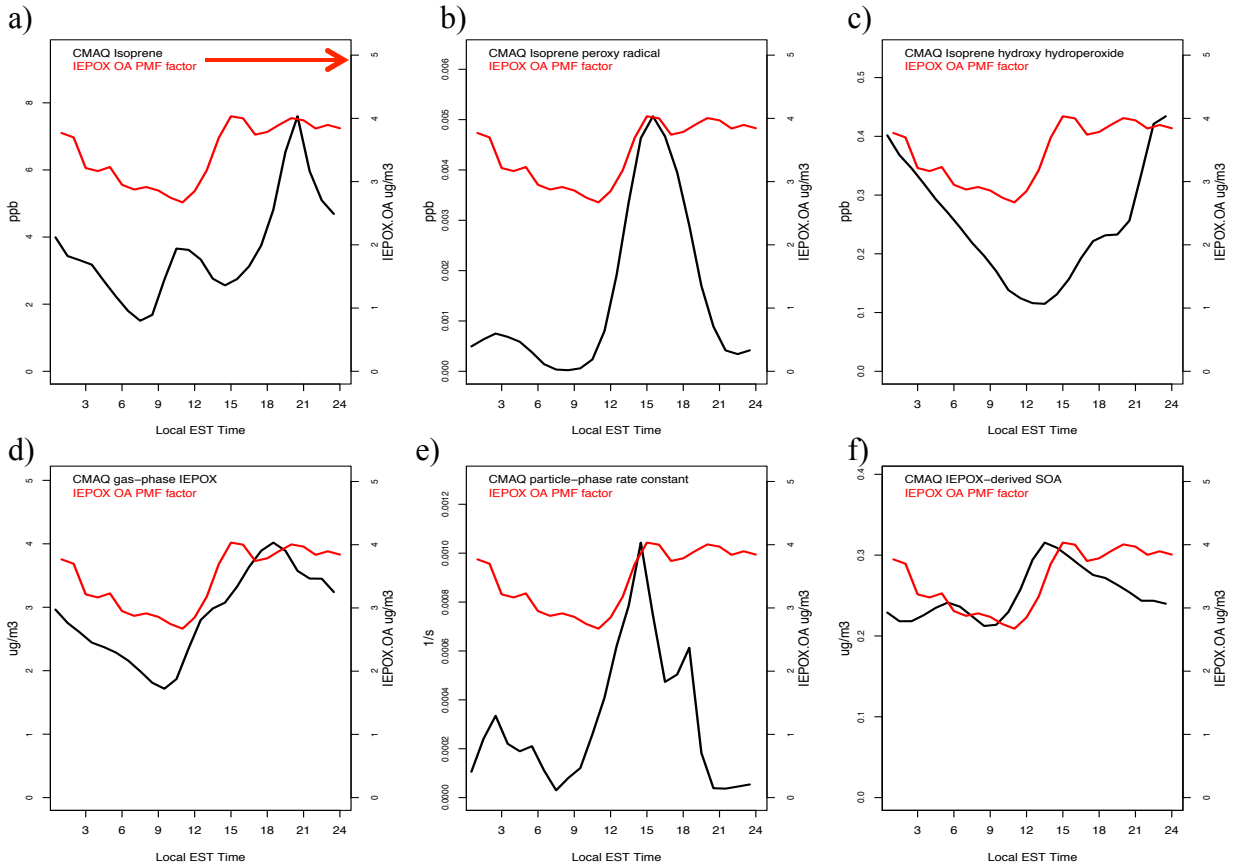

Figure 3.4 CMAQ output (black line) of isoprene oxidation pathway (a-isoprene, b-isoprene peroxy radical, c-isoprene hydroxy hydroperoxide, d-IEPOX), the pseudo-first order particle-phase rate constant $k_{particle\ IEPOX}$ (e) and sum of IEPOX-derived aerosol species (f) compared with IEPOX-OA measurements (red line). CMAQ predicts large amounts of gas-phase IEPOX (d) but fails to reproduce comparable amounts of IEPOX-derived aerosol (f) although the diurnal pattern of measurements if simulated well.

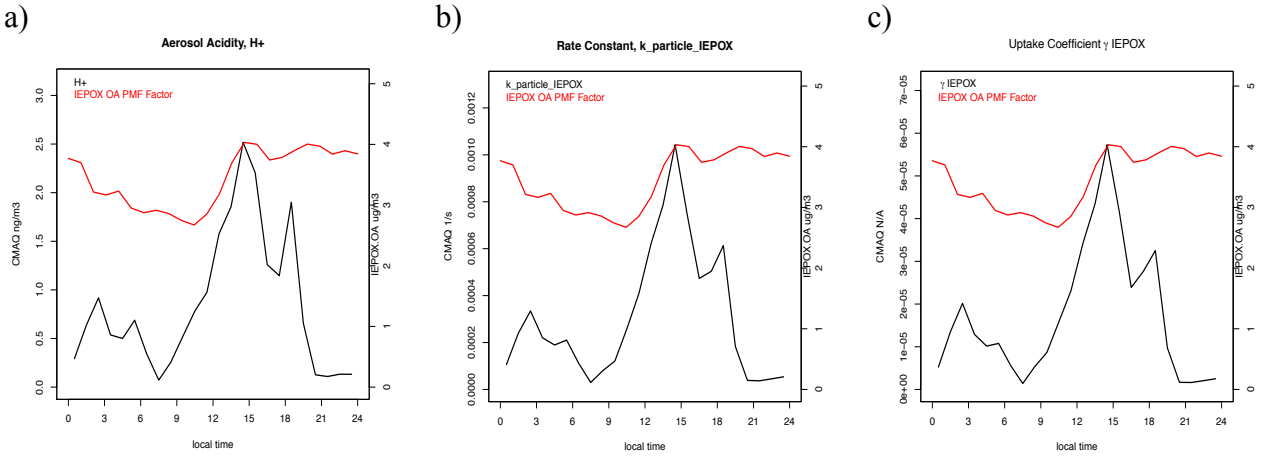

Figure 3.5 Comparison of CMAQ predicted (black line) acidity H+ (a), $k_{particle\ IEPOX}$ (b), and uptake coefficient γ_{IEPOX} (c) and IEPOX-OA measurements (red line). $k_{particle\ IEPOX}$ is calculated in equation (1) and γ_{IEPOX} is calculated using equation (2). The peak in H+, $k_{particle\ IEPOX}$ and γ_{IEPOX} correspond with the peak seen in IEPOX-OA measurements around 3PM eastern time.

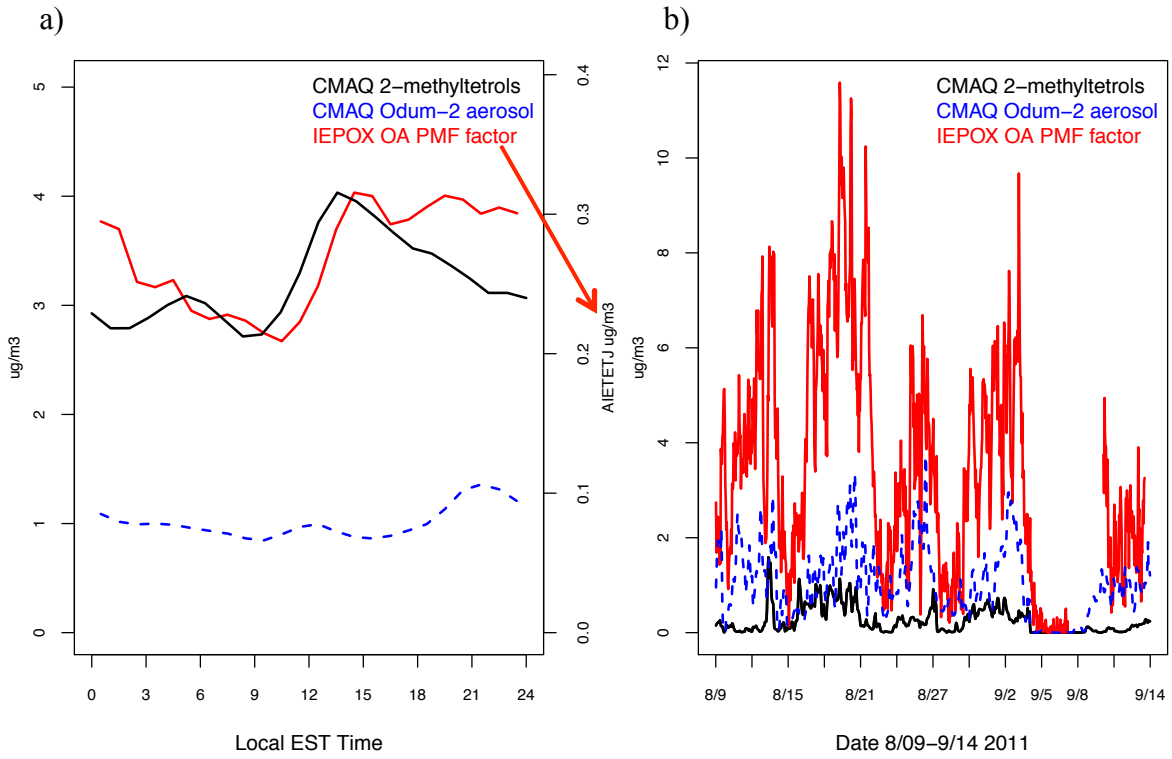

Figure 3.6 IEPOX-derived SOA (black line), IEPOX-OA measurements (red line), Odum 2-product aerosol (dashed blue line). (a) Diurnal average from August 9th to September 14th 2011. Left-hand y-axis for IEPOX-OA measurements and Odum 2-product aerosol concentrations, right-hand y-axis for IEPOX-derived SOA concentrations. Note the similarities in diurnal variability between measurements and IEPOX-derived SOA versus Odum 2-product aerosol. (b) Hourly concentrations over the time period. Again, IEPOX-derived SOA matches trends in measurements better than the Odum 2-product.

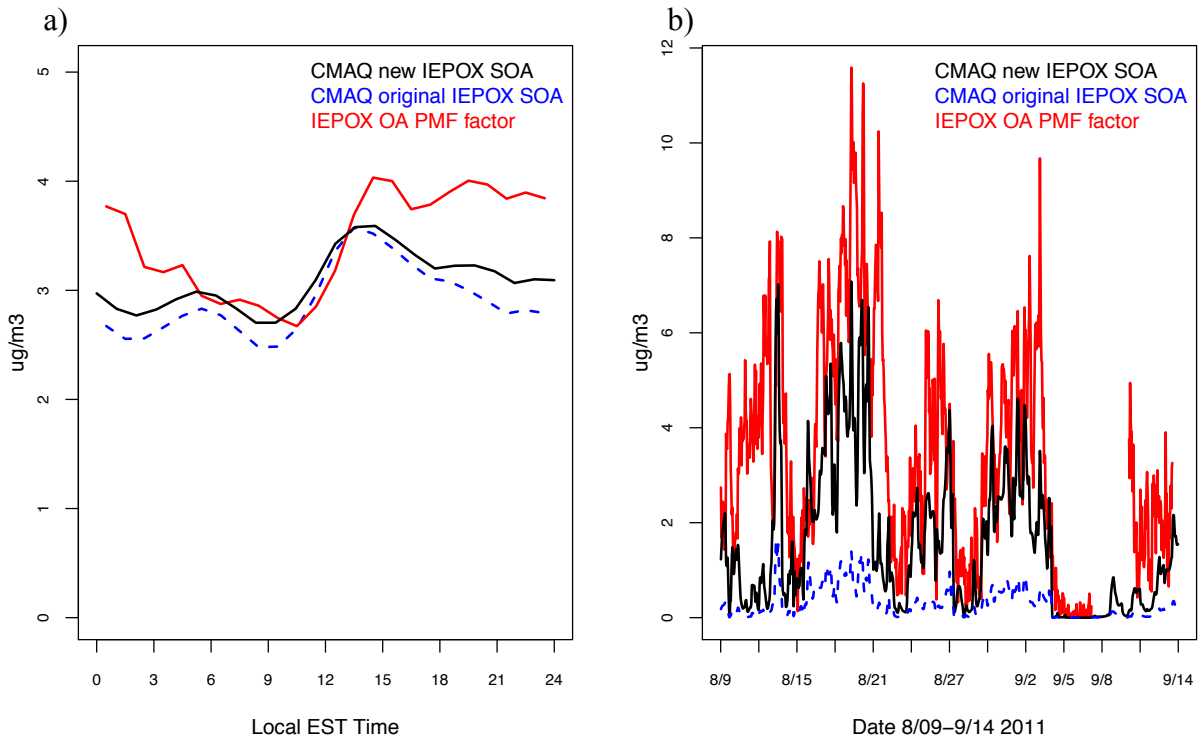

Figure 3.7 CMAQ predicted IEPOX SOA from the sensitivity simulation (black line) and base case simulation (dashed blue line) compared with IEPOX-OA measurements (red line). (a) Diurnal average concentrations during the simulation time period. (b) Hourly concentrations for the simulation period. Concentrations from the sensitivity simulation increase by a factor of 5 from a factor of 10 increase in gas-phase uptake coefficient, γ_{IEPOX}.

Tables

Aerosol species	Nucleophile (i)	$K_{i,H+}$ [m^{-2} s^{-1}]	$K_{i,HSO4-}$ [m^{-2} s^{-1}]
2-methyltetrols	Water	9.0×10^{-4}	1.3×10^{-5}
Organo-sulfates	Sulfate	2.0×10^{-4}	2.9×10^{-6}
Organo-nitrates	Nitrate	2.0×10^{-4}	2.9×10^{-6}
Dimers	2-methyltetrols	2.0×10^{-4}	2.9×10^{-6}
	Organo-sulfate	2.0×10^{-4}	2.9×10^{-6}
	Organo-nitrate	2.0×10^{-4}	2.9×10^{-6}

Table 3.1 Third order particle phase reaction rate constants used in the CMAQ simulations for the reactive uptake of isoprene for the formation of specific aerosol species from individual nucleophile species. $K_{i,j}$ constants used are the same for the formation of organo-sulfates, organo-nitrates, and dimers due to lack of experimental-derived data available. Constants derived from experiments by Eddingsaas et al., (2010) and were first used in model simulations by Pye et al., (2013).

References

Bhave, P. V, Pouliot, G. a, & Zheng, M. (2007). Diagnostic model evaluation for carbonaceous PM2.5 using organic markers measured in the southeastern U.S. *Environmental Science & Technology*, *41*(5), 1577–83. Retrieved from http://www.ncbi.nlm.nih.gov/pubmed/17396644

Budisulistiorini, S. H., Canagaratna, M. R., Croteau, P. L., Marth, W. J., Baumann, K., Edgerton, E. S., … Surratt, J. D. (2013). Real-time continuous characterization of secondary organic aerosol derived from isoprene epoxydiols in downtown atlanta, georgia, using the aerodyne aerosol chemical speciation monitor. *Environmental Science & Technology*, *47*(11), 5686–94. doi:10.1021/es400023n

Byun, D., & Schere, K. L. (2006). Review of the Governing Equations, Computational Algorithms, and Other Components of the Models-3 Community Multiscale Air Quality (CMAQ) Modeling System. *Applied Mechanics Reviews*, *59*(2), 51. doi:10.1115/1.2128636

Carlton, A. G., Wiedinmyer, C., & Kroll, J. H. (2009). A review of Secondary Organic Aerosol (SOA) formation from isoprene. *Atmospheric Chemistry and Physics*, *9*(2), 8261–8305. doi:10.5194/acpd-9-8261-2009

Carlton, Annmarie G, Bhave, P. V, Napelenok, S. L., Edney, E. O., Sarwar, G., Pinder, R. W., … Houyoux, M. (2010a). Model representation of secondary organic aerosol in CMAQv4.7. *Environmental Science & Technology*, *44*(22), 8553–60. doi:10.1021/es100636q

Carlton, Annmarie G, Bhave, P. V., Napelenok, S. L., Edney, E. O., Sarwar, G., Pinder, R. W., … Houyoux, M. (2010b). Model Representation of Secondary Organic Aerosol in CMAQv4.7 Supporting Information. *Environmental Science & Technology*.

Carlton, Annmarie G, Turpin, B. J., Altieri, K. E., Mathur, R., Roselle, S. J., & Weber, R. J. (2008). CMAQ Model Performance Enhanced When In-Cloud Secondary Organic Aerosol is Included : Comparisons of Organic Carbon Predictions with Measurements. *Environmental Science & Technology*, *42*(23), 8798–8802.

Chan, M. N., Surratt, J. D., Claeys, M., Edgerton, E. S., Tanner, R. L., Shaw, S. L., … Seinfeld, J. H. (2010). Characterization and quantification of isoprene-derived epoxydiols in ambient aerosol in the southeastern United States. *Environmental Science & Technology*, *44*(12), 4590–6. doi:10.1021/es100596b

Claeys, M., Graham, B., Vas, G., Wang, W., Vermeylen, R., Pashynska, V., … Maenhaut, W. (2004). Formation of secondary organic aerosols through photooxidation of isoprene. *Science*, *303*(5661), 1173–6. doi:10.1126/science.1092805

Crounse, J. D., Paulot, F., Kjaergaard, H. G., & Wennberg, P. O. (2011). Peroxy radical isomerization in the oxidation of isoprene. *Physical Chemistry Chemical Physics*, *13*(30), 13607–13. doi:10.1039/c1cp21330j

Darer, A. I., Cole-filipiak, N. C., Connor, A. E. O., & Elrod, M. J. (2011). Formation and Stability of Atmospherically Relevant Isoprene-Derived Organosulfates and Organonitrates. *Environmental Science & Technology*, 1895–1902.

Eddingsaas, N. C., VanderVelde, D. G., & Wennberg, P. O. (2010). Kinetics and products of the acid-catalyzed ring-opening of atmospherically relevant butyl epoxy alcohols. *Journal of Physical Chemistry A*, *114*(31), 8106–13. doi:10.1021/jp103907c

Edney, E. O., Kleindienst, T. E., Jaoui, M., Lewandowski, M., Offenberg, J. H., Wang, W., & Claeys, M. (2005). Formation of 2-methyl tetrols and 2-methylglyceric acid in secondary organic aerosol from laboratory irradiated isoprene/NOX/SO2/air mixtures and their detection in ambient PM2.5 samples collected in the eastern United States. *Atmospheric Environment*, *39*(29), 5281–5289. doi:10.1016/j.atmosenv.2005.05.031

Foley, K. M., Roselle, S. J., Appel, K. W., Bhave, P. V, Pleim, J. E., Otte, T. L., … Sarwar, G. (2010). Incremental testing of the Community Multiscale Air Quality (CMAQ) modeling system version 4 . 7. *Geoscientific Model Development*, *3*, 205–226.

Fountoukis, C., & Nenes, A. (2007). ISORROPIA II : a computationally efficient thermodynamic equilibrium model for K+-Ca2+-Mg2+-NH4+-Na+-SO42--NO3--Cl--H2O aerosols. *Atmospheric Chemistry and Physics*, 4639–4659.

Glasius, M., la Cour, A., & Lohse, C. (2011). Fossil and nonfossil carbon in fine particulate matter: A study of five European cities. *Journal of Geophysical Research*, *116*(D11), D11302. doi:10.1029/2011JD015646

Godowitch, J. M., Gilliland, a. B., Draxler, R. R., & Rao, S. T. (2008). Modeling assessment of point source NOx emission reductions on ozone air quality in the eastern United States. *Atmospheric Environment*, *42*(1), 87–100. doi:10.1016/j.atmosenv.2007.09.032

Guenther, A., Karl, T., Harley, P., Wiedinmyer, C., Palmer, P. I., & Geron, C. (2006). Estimates of global terrestrial isoprene emissions using MEGAN (Model of Emissions of Gases and Aerosols from Nature). *Atmospheric Chemistry and Physics Discussions*, *6*(1), 107–173. doi:10.5194/acpd-6-107-2006

Henderson, B. H., Akhtar, F., Pye, H. O. T., Napelenok, S. L., & Hutzell, W. T. (2013). A database and tool for boundary conditions for regional air quality modeling: description

and evaluation. *Geoscientific Model Development Discussions*, *6*(3), 4665–4704. doi:10.5194/gmdd-6-4665-2013

Hutzell, W. T., Luecken, D. J., Appel, K. W., & Carter, W. P. L. (2012). Interpreting predictions from the SAPRC07 mechanism based on regional and continental simulations. *Atmospheric Environment*, *46*, 417–429. doi:10.1016/j.atmosenv.2011.09.030

Janssen, R. H. H., Vilà-Guerau de Arellano, J., Jimenez, J. L., Ganzeveld, L. N., Robinson, N. H., Allan, J. D., … Pugh, T. a. M. (2013). Influence of boundary layer dynamics and isoprene chemistry on the organic aerosol budget in a tropical forest. *Journal of Geophysical Research: Atmospheres*, *118*, n/a–n/a. doi:10.1002/jgrd.50672

Kinnee, E., Geron, C., & Pierce, T. (1997). United States Land Use Inventory for Estimating Biogenic Ozone Precursor Emissions. *Ecological Applications*, *7*(1), 46–58.

Kleindienst, T. E., Edney, E. O., Lewandowski, M., Offenberg, J. H., & Jaoui, M. (2006). Secondary Organic Carbon and Aerosol Yields from the Irradiations of Isoprene and a-Pinene in the Presence of NOx and SO2. *Environmental Science & Technology*, *40*(12), 3807–3812.

Kleindienst, T. E., Jaoui, M., Lewandowski, M., Offenberg, J. H., Lewis, C. W., Bhave, P. V., & Edney, E. O. (2007). Estimates of the contributions of biogenic and anthropogenic hydrocarbons to secondary organic aerosol at a southeastern US location. *Atmospheric Environment*, *41*(37), 8288–8300. doi:10.1016/j.atmosenv.2007.06.045

Lee, Y., Zhou, X., Kleinman, L. I., Nunnermacker, L. J., Springston, S. R., Newman, L., … Ryerson, T. B. (1998). Atmospheric chemistry and distribution of formaldehyde and several multioxygenated carbonyl compounds during the 1995 Nashville/Middle Tennessee Ozone Study. *Journal of Geophysical Research*, *103*(98).

Lewandowski, M., Jaoui, M., Offenberg, J. H., Kleindienst, T. E., Edney, E. O., Sheesley, R. J., & Schauer, J. J. (2008). Primary and Secondary Contributions to Ambient PM in the Midwestern United States. *Environmental Science & Technology*, *42*(9), 3303–3309.

Lin, Y., Zhang, Z., Docherty, K. S., Zhang, H., Budisulistiorini, S. H., Rubitschun, C. L., … Surratt, J. D. (2012). Isoprene Epoxydiols as Precursors to Secondary Organic Aerosol Formation : Acid-Catalyzed Reactive Uptake Studies with Authentic Compounds. *Environmental Science & Technology*, *46*, 250–258.

Lin, Y.-H., Knipping, E. M., Edgerton, E. S., Shaw, S. L., & Surratt, J. D. (2013a). Investigating the influences of SO2 and NH3 levels on isoprene-derived secondary organic aerosol formation using conditional sampling approaches. *Atmospheric Chemistry and Physics*, *13*, 8457–8470. doi:10.5194/acp-13-8457-2013

Lin, Y.-H., Knipping, E. M., Edgerton, E. S., Shaw, S. L., & Surratt, J. D. (2013b). Investigating the influences of SO_2 and NH_3 levels on isoprene-derived secondary organic aerosol formation using conditional sampling approaches. *Atmospheric Chemistry and Physics Discussions*, *13*(2), 3095–3134. doi:10.5194/acpd-13-3095-2013

Liu, Y. J., Herdlinger-Blatt, I., McKinney, K. a., & Martin, S. T. (2013). Production of methyl vinyl ketone and methacrolein via the hydroperoxyl pathway of isoprene oxidation. *Atmospheric Chemistry and Physics*, *13*(11), 5715–5730. doi:10.5194/acp-13-5715-2013

Lockwood, a. L., Shepson, P. B., Fiddler, M. N., & Alaghmand, M. (2010). Isoprene nitrates: preparation, separation, identification, yields, and atmospheric chemistry. *Atmospheric Chemistry and Physics*, *10*(13), 6169–6178. doi:10.5194/acp-10-6169-2010

Ng, N. L., Herndon, S. C., Trimborn, a., Canagaratna, M. R., Croteau, P. L., Onasch, T. B., … Jayne, J. T. (2011). An Aerosol Chemical Speciation Monitor (ACSM) for Routine Monitoring of the Composition and Mass Concentrations of Ambient Aerosol. *Aerosol Science and Technology*, *45*(7), 780–794. doi:10.1080/02786826.2011.560211

Odum, J. R., Hoffmann, T., Bowman, F., Collins, D., Flagan, R. C., & Seinfeld, J. H. (1996). Gas/Particle Partitioning and Secondary Organic Aerosol Yields. *Environmental Science & Technology*, *30*(8), 2580–2585. doi:10.1021/es950943+

Offenberg, J. H., Lewis, C. W., Lewandowski, M., Jaoui, M., Kleindienst, T. E., & Edney, E. O. (2007). Contributions of toluene and alpha-pinene to SOA formed in an irradiated toluene/alpha-pinene/NO(x)/air mixture: comparison of results using 14C content and SOA organic tracer methods. *Environmental Science & Technology*, *41*(11), 3972–6. Retrieved from http://www.ncbi.nlm.nih.gov/pubmed/17612177

Otte, T. L., & Pleim, J. E. (2010). The Meteorology-Chemistry Interface Processor (MCIP) for the CMAQ modeling system: updates through MCIPv3.4.1. *Geoscientific Model Development*, *3*(1), 243–256. doi:10.5194/gmd-3-243-2010

Palmer, P. I., Jacob, D. J., Fiore, A. M., Martin, R. V, Chance, K., & Kurosu, T. P. (2003). Mapping isoprene emissions over North America using formaldehyde column observations from space. *Journal of Geophysical Research*, *108*. doi:10.1029/2002JD002153

Paulot, F., Crounse, J. D., Kjaergaard, H. G., Kürten, A., St Clair, J. M., Seinfeld, J. H., & Wennberg, P. O. (2009). Unexpected epoxide formation in the gas-phase photooxidation of isoprene. *Science*, *325*(5941), 730–3. doi:10.1126/science.1172910

Peeters, J, Nguyen, T. L., & Vereecken, L. (2009). HOx radical regeneration in the oxidation of isoprene. *Physical chemistry chemical physics : PCCP*, *11*(28), 5935–9. doi:10.1039/b908511d

Peeters, Jozef, & Müller, J.-F. (2010). HO(x) radical regeneration in isoprene oxidation via peroxy radical isomerisations. II: experimental evidence and global impact. *Physical Chemistry Chemical Physics*, *12*(42), 14227–35. doi:10.1039/c0cp00811g

Piletic, I. R., Edney, E. O., & Bartolotti, L. J. (2013). A computational study of acid catalyzed aerosol reactions of atmospherically relevant epoxides. *Physical Chemistry Chemical Physics*, *15*(41), 18065–76. doi:10.1039/c3cp52851k

Pye, H. O. T., Pinder, R. W., Piletic, I. R., Xie, Y., Capps, S. L., Lin, Y.-H., … Edney, E. O. (2013). Epoxide Pathways Improve Model Predictions of Isoprene Markers and Reveal Key Role of Acidity in Aerosol Formation. *Environmental Science & Technology*. doi:10.1021/es402106h

Robinson, N. H., Hamilton, J. F., Allan, J. D., Langford, B., Oram, D. E., Chen, Q., … Coe, H. (2011). Evidence for a significant proportion of Secondary Organic Aerosol from isoprene above a maritime tropical forest. *Atmospheric Chemistry and Physics*, *11*(3), 1039–1050. doi:10.5194/acp-11-1039-2011

Rollins, A. W., Fry, J. L., Brauers, T., Brown, S. S., Dorn, H., & Dub, W. P. (2009). Isoprene oxidation by nitrate radical: alkyl nitrate and secondary organic aerosol yields. *Atmospheric Chemistry and Physics*, (3), 6685–6703.

Schichtel, B. a., Malm, W. C., Bench, G., Fallon, S., McDade, C. E., Chow, J. C., & Watson, J. G. (2008). Fossil and contemporary fine particulate carbon fractions at 12 rural and urban sites in the United States. *Journal of Geophysical Research*, *113*(D2), D02311. doi:10.1029/2007JD008605

Sharkey, T. D., Wiberley, A. E., & Donohue, A. R. (2008). Isoprene emission from plants: why and how. *Annals of botany*, *101*(1), 5–18. doi:10.1093/aob/mcm240

Slowik, J. G., Brook, J., Chang, R. Y.-W., Evans, G. J., Hayden, K., Jeong, C.-H., … Abbatt, J. P. D. (2011). Photochemical processing of organic aerosol at nearby continental sites: contrast between urban plumes and regional aerosol. *Atmospheric Chemistry and Physics*, *11*(6), 2991–3006. doi:10.5194/acp-11-2991-2011

Spak, S. N., & Holloway, T. (2009). Seasonality of speciated aerosol transport over the Great Lakes region. *Journal of Geophysical Research*, *114*(D8), D08302. doi:10.1029/2008JD010598

Surratt, J. D., Chan, A. W. H., Eddingsaas, N. C., Chan, M., Loza, C. L., Kwan, A. J., … Seinfeld, J. H. (2010). Reactive intermediates revealed in secondary organic aerosol formation from isoprene. *Proceedings of the National Academy of Sciences of the United States of America*, *107*(15), 6640–5. doi:10.1073/pnas.0911114107

Surratt, J. D., Murphy, S. M., Kroll, J. H., Ng, N. L., Hildebrandt, L., Sorooshian, A., … Seinfeld, J. H. (2006). Chemical composition of secondary organic aerosol formed from the photooxidation of isoprene. *Journal of Physical Chemistry A*, *110*(31), 9665–90. doi:10.1021/jp061734m

Ulbrich, I. M., Canagaratna, M. R., Zhang, Q., Worsnop, D. R., & Jimenez, J. L. (2009). Interpretation of organic components from Positive Matrix Factorization of aerosol mass spectrometric data. *Atmospheric Chemistry and Physics*, *9*, 2891–2918.

USEPA. (2012). *Our Nation's Air Status and Trends Through 2010*. *Tech. Rep.* (p. EPA–454/R–12–001).

Xie, Y., Paulot, F., Carter, W. P. L., Nolte, C. G., Luecken, D. J., Hutzell, W. T., … Pinder, R. W. (2013). Understanding the impact of recent advances in isoprene photooxidation on simulations of regional air quality. *Atmospheric Chemistry and Physics*, *13*(16), 8439–8455. doi:10.5194/acp-13-8439-2013

Yu, S., Mathur, R., Sarwar, G., Kang, D., Tong, D., Pouliot, G., & Pleim, J. (2010). Eta-CMAQ air quality forecasts for O_3 and related species using three different photochemical mechanisms (CB4, CB05, SAPRC-99): comparisons with measurements during the 2004 ICARTT study. *Atmospheric Chemistry and Physics*, *10*(6), 3001–3025. doi:10.5194/acp-10-3001-2010

Yu, Shaocai, Bhave, P. V., Dennis, R. L., & Mathur, R. (2007). Seasonal and Regional Variations of Primary and Secondary Organic Aerosols over the Continental United States : Semi-Empirical Estimates and Model Evaluation. *Environmental Science & Technology*, *41*(13), 4690–4697.

Zhang, X., Liu, J., Parker, E. T., Hayes, P. L., Jimenez, J. L., de Gouw, J. a., … Weber, R. J. (2012). On the gas-particle partitioning of soluble organic aerosol in two urban atmospheres with contrasting emissions: 1. Bulk water-soluble organic carbon. *Journal of Geophysical Research: Atmospheres*, *117*(D21). doi:10.1029/2012JD017908

Zhang, Y., Huang, J.-P., Henze, D. K., & Seinfeld, J. H. (2007). Role of isoprene in secondary organic aerosol formation on a regional scale. *Journal of Geophysical Research*, *112*(D20), 1–13. doi:10.1029/2007JD008675

Zhang, Y., Pun, B., Wu, S.-Y., Vijayaraghavan, K., & Seigneur, C. (2004). Application and evaluation of two air quality models for particulate matter for a southeastern U.S. episode. *Journal of the Air & Waste Management Association (1995)*, *54*(12), 1478–93. Retrieved from http://www.ncbi.nlm.nih.gov/pubmed/15648386

Zhang, Y., Vijayaraghavan, K., Wen, X.-Y., Snell, H. E., & Jacobson, M. Z. (2009). Probing into regional ozone and particulate matter pollution in the United States: 1. A 1 year

CMAQ simulation and evaluation using surface and satellite data. *Journal of Geophysical Research*, *114*(D22), D22304. doi:10.1029/2009JD011898

Chapter 4.
Conclusions and Future Work

Results presented here explore the connection between anthropogenic and biogenic emissions with respect to the formation of tropospheric aerosols. The U.S. Environmental Protection Agency (EPA) Community Multi-scale Air Quality (CMAQ) model was employed in two studies: 1) To understand the role biogenic emissions play in inorganic sulfate (SO_4^{2-}) and nitrate (NO_3^-) aerosol formation; 2) To evaluate the latest understanding in the isoprene-derived aerosol formation pathway. Model simulations were evaluated to understand contributions of biogenic secondary organic aerosol (SOA) and anthropogenic secondary aerosols SO_4^{2-} and NO_3^- to summertime fine particulate matter ($PM_{2.5}$). Observational data including ground-based aerosol and dry deposition flux measurements from the Clean Air Status and Trends Network (CASTNet), satellite observations of the gas-phase precursor nitrogen dioxide (NO_2), and ion measurements from the Aerosol Chemical Speciation Monitor (ACSM) were compared with model results to validate the model simulations, and to evaluate how model processes relate to observed atmospheric behavior. Understanding aerosol formation in the troposphere is essential for air quality management, and this chapter discusses how our study results contribute to policy-relevant scientific analysis.

Biogenic Impact on Sulfate and Nitrate Aerosol

Anthropogenic sources of $PM_{2.5}$ include motor vehicles and electricity generating units that are large contributors to gas-phase precursors NO_2 and sulfur dioxide (SO_2), respectively. In the atmosphere, these compounds contribute to aerosol mass through gas and aqueous phase oxidation processes and reaction with ammonia (NH_3) to form aerosol

ammonium salts. A set of two of simulations was conducted to evaluate the contributions of individual source sectors to $PM_{2.5}$, and it was found that removing biogenic emissions negatively impacted total $PM_{2.5}$ concentrations in the eastern U.S. while positively contributing in the west. Closer inspection revealed that inorganic aerosols including SO_4^{2-} and NO_3^- increased in concentration when biogenic sources were removed, even though inorganic aerosol concentrations decreased as expected when their respective largest contributors (electricity generating units and motor vehicles, respectively) were removed (not shown). Increases were most prominent in Aitken and accumulation mode aerosols for both SO_4^{2-} and NO_3^-, while coarse mode mass remained approximately unchanged when biogenic emissions were removed. Spatially, changes to SO_4^{2-} and NO_3^- concentrations were unique to the emissions of anthropogenic precursor species, with largest changes to SO_4^{2-} occurring near large SO_2 emissions in the Ohio River Valley, and larges changes to NO_3^- occurring in regions with large emissions of NO_X and NH_3, such as the Great Lakes and rural stretches of large interstates.

Increased inorganic aerosol formation as caused by the removal of biogenic emissions was found to be related to gas-phase oxidation processes in the model mechanism. In CMAQ, SO_4^{2-} aerosol preferentially occurs through the aqueous phase oxidation of sulfuric acid (H_2SO_4) by hydrogen peroxide (H_2O_2) and subsequent reactions with NH_3. However, Aitken mode SO_4^{2-} in CMAQ forms from direct oxidation of SO_2 by the hydroxyl radical (OH) to yield H_2SO_4 vapor that nucleates into new, ultrafine particles. Similarly, NO_2 can be oxidized by the OH radial to yield nitric acid (HNO_3), though this does not nucleate as SO_4^{2-} does in CMAQ or the atmosphere. Instead, dissolved HNO_3 readily reacts with NH_3 to form ammonium nitrate aerosol. A surplus of OH results from the removal of biogenic emissions.

In the base case simulation, biogenic gases undergo oxidation by the OH radical to yield semi-volatile compounds, which occurs preferentially to gas-phase oxidation of anthropogenic emissions. Once OH reacts, it is efficiently removed from the model system with very little regeneration by the current mechanism, CB05. However, measurements in low-NO_X environments have concluded that isoprene oxidation is effective at OH-recycling (Lelieveld et al., 2008). If an updated chemical mechanism including OH-recycling were used in these model simulations, we would expect an increase in inorganic aerosol concentrations.

In the CB05 chemical mechanism used in simulations presented in Chapter 2, OH is not recycled through isoprene oxidation, therefore with the removal of biogenic gases the OH radical in CMAQ is "free" to react with anything else, including SO_2 and NO_X. By this mechanism, more H_2SO_4 and HNO_3 are produced and react to form more Aitken and accumulation mode particulates. Further, increasing fine-mode particulates has a profound influence on the dry deposition of each individual species, where NO_3^- deposition increases due to increased aerosol concentration, but SO_4^{2-} dry deposition decreases downwind of the Ohio River Valley due to increased Aitken mode aerosols that are too small to be dry deposited out of the atmosphere. Although biogenics largely contribute to $PM_{2.5}$ through SOA formation, removing them from the environment causes $PM_{2.5}$ to increase due to an increased formation of inorganic aerosols.

Chapter 2 has shown that a unique and complex relationship exists between biogenic and anthropogenic gases with respect to aerosol formation. Biogenic sources contribute negatively to total $PM_{2.5}$ in the eastern half of the U.S., even though the oxidation of biogenic VOC emissions yields aerosol products. From the model results presented in Chapter 2, it

seems that biogenic sources effectively "clean" particulate pollution by prohibiting the oxidation of anthropogenic gases. However, this is unique to the eastern U.S., a broad area subject to ample NO_X and SO_2 precursor pollution. In the western U.S. where there is little to no SO_2 emissions and NO_X emissions are largely localized to urban areas, biogenic SOA is a positive contributor to total $PM_{2.5}$. The relationship that biogenic emissions have with inorganic aerosol formation relies on the emissions from not just biogenic source but from anthropogenic sources as well.

The influence biogenic emissions have on aerosol formation poses an interesting air quality management problem when regulating pollution across broad-scale regions. Air quality regulations are enforced for anthropogenic emissions, but what happens when aerosol formation as a whole is connected to both anthropogenic and biogenic emission interactions? Populated urban areas experience large amounts of particulate pollution from anthropogenic sources and are not subject to the influence biogenic emissions have on particulate formation, but in between cities biogenic contributions play a substantial role in prohibiting inorganic aerosol formation as evidenced by the large increases in SO_4^{2-} and NO_3^- aerosol concentrations from the removal of biogenic emissions. In this study, we have shown that biogenic SOA formation interferes with anthropogenic aerosol formation. Since there is a connection between anthropogenic and biogenic pollutants, aerosol formation may not remain unique to each of these respective sources. For existing air quality mitigation techniques, it is necessary to confidently know what sources are contributing most heavily to poor air quality in a region.

Isoprene Aerosol Formation Pathway

Isoprene is known to be the largest source of biogenic precursor contributing to SOA formation. In Chapter 3, CMAQv.5.0.1 model simulations were performed using a recently updated isoprene-derived aerosol formation pathway consisting of detailed photo-oxidation and the reactive uptake of gas-phase isoprene epoxydiol (IEPOX) (Xie et al., 2013), a third-generation isoprene-derived product, into the aerosol phase. Aerosol uptake occurs through acid-catalyzed reactions involving IEPOX and a nucleophile species to yield an aerosol compound. The success of this reaction is dependent on the availability of gas-phase IEPOX, aerosol water, aerosol acidity, and a nucleophile such as water, SO_4^{2-}, NO_3^-, or an existing IEPOX-derived aerosol compound. Base case model results were compared with measurements taken in Atlanta, GA (Budisulistiorini et al., 2013b), and indicated that CMAQ was missing about a factor of 10 in aerosol mass derived from gas-phase IEPOX. The large amount of missing IEPOX-derived aerosol mass was not due to any of the aforementioned necessities: there was abundant IEPOX and aerosol water, and the acidity conditions modeled in CMAQ were comparable to that estimated from an ion-calculation of the measurements. Despite the significant discrepancy in mass concentration between the model results and the measurements, isoprene-derived aerosol via this new reactive uptake method correlates better (r=0.531) with the measurements than the previous absorptive partitioning aerosol pathway (r=0.488).

However, not all resultant IEPOX-aerosol species are currently known. Calculations driving the heterogeneous reactive uptake were driven by constants derived in laboratory studies for IEPOX-derived aerosol tracer species such as 2-methyltetrols, which may not account for all aerosol species produced. Additionally, constants derived in chamber

experiments may not hold true in all environments. A sensitivity simulation, in which the reactive uptake coefficient, γ_{IEPOX}, was increased by a factor of 10, drastically improved the amount of IEPOX-derived aerosol produced. This simulation was conducted assuming that new aerosol mass was formed similarly to 2-methyltetrols, and as such any new mass was simply accumulated in the 2-methyltetrol variable. Aerosol concentrations increased from a base case average of 0.290 $\mu g/m^3$ to an average of 1.53 $\mu g/m^3$ in the sensitivity simulation results, although they still remain a little more than a factor of 2 less than the average measurement concentration of 3.45 $\mu g/m^3$. Aerosol-phase reactions that produce larger oligomer species were not included in either simulation, and as such the total organic mass (OM) to organic carbon (OC) ratio in the model is 2.1, however the OM/OC ratio calculated from the measurements is 4 (Budisulistiorini et al., 2013a). The discrepancy between modeled and measured OM/OC ratios implies that additional IEPOX-derived aerosol species exist and are currently unknown, and therefore they are not accounted for in the model.

Model evaluation of the low-NO_X isoprene-derived aerosol pathway show a large difference in mass concentrations between the model predicted and measured concentrations, indicative of the possibility that unknown aerosol species not included in the model. Without understanding what these aerosols are and how they form may hinder adequate air quality management procedures, particularly if the formation of these unknown aerosols is influenced or enhanced by anthropogenic pollution similar to other isoprene-derived aerosol species. If this is the case, mitigating anthropogenic emissions of NO_X and SO_2 may have a two-fold positive effect on air quality through the reduced formation of inorganic aerosols, SO_4^{2-} and NO_3^-, and SOA.

The aerosol mechanism evaluation as presented in Chapter 3 suggests that more laboratory experiments must be performed and/or new aerosol measurement techniques must be used in the field to improve the current knowledge of SOA formation. These experiments and techniques would be able to solve for unknowns found in model simulations, such as the possible unknown aerosol species assumed in the sensitivity simulation in Chapter 3, or more accurate reaction rate constants and coefficients. New updates to the pathway can then be evaluated in model simulations, and further laboratory and field studies can solve for more unknowns and so on. Continuous improvements to and understanding of the SOA formation mechanism will in turn improve air quality management techniques that require accurate air quality model simulations.

Future Direction in Understanding Biogenic-Anthropogenic Interactions

Aerosols form from both biogenic and anthropogenic gas-phase precursors, though until recently the relationship they share in aerosol formation and growth has been overlooked. Understanding how anthropogenic gas-phase compounds influence biogenic SOA formation and how biogenic gas-phase compounds influence inorganic aerosol formation is necessary for the comprehensive knowledge of aerosols. This knowledge is imperative for proper air quality management techniques in regions susceptible to this unique biogenic-anthropogenic relationship, such as the eastern U.S. Proper particulate pollution mitigation requires substantial knowledge on aerosols and their formation processes, therefore it important to know how emission sources may interact to yield aerosol, especially downwind of extremely polluted areas such as cities. Results presented here on the

connection between biogenic and anthropogenic emissions and subsequent aerosol formation will have positive implications for successful air quality management.

Model simulations provide an experimental tool where manipulations can be implemented into the model environment to simulate unique environments. This would be one such technique to verify if the results from Chapter 2 are linear, and inorganic aerosol formation would continually increase when biogenic emissions decrease. In addition, detailed aerosol formation mechanisms can be implemented into air quality models similar to the simulations used in Chapter 3 as a way to study aerosol formation from individual precursor emissions. Such experiments can lead to additional model studies that attempt to evaluate how individual gas-phase compounds interact with one another versus broadly generalizing contributions from whole emission sectors as presented in Chapter 2 of this thesis. Future simulations expanding on the results presented here include a wintertime simulation quantifying the biogenic contribution to aerosol formation and how biogenic emissions influence inorganic aerosol formation, especially that of NO_3^-, in the wintertime. Seasonal simulations over the duration of summer and winter seasons would provide a more robust dataset to indicate when biogenic sources exhibit the most and least influence on inorganic aerosol formation. Further, simulations incorporating future climate and emission scenarios can quantify the amount aerosol formation changes with increased temperatures and emissions. Climate evaluations such as these will reduce the uncertainty associated with aerosols and their influence as short-term climate drivers. Overall, the work presented in this thesis may have implications for a variety of related experiments.

Further understanding of aerosol formation processes requires integration of model simulations, *in situ* measurements, and chamber experiments across a broad range of

environments. It is important to understand chemical formation processes and quantity yields found in chamber experiments, and then to be able to apply these to model simulations that can be validated against ground, aircraft, and satellite measurements. Incorporating a variety of tools is essential to thorough understanding of atmospheric processes and to provide a comprehensive spatial and temporal analysis.

References

Budisulistiorini, S. H., Canagaratna, M. R., Croteau, P. L., Baumann, K., Kollman, M. S., Ng, N. L., … Alto, P. (2013). Intercomparison of an Aerosol Chemical Speciation Monitor (ACSM) with Ambient Fine Aerosol Measurements in Downtown Atlanta , Georgia. *in prep*, 1–36.

Budisulistiorini, S. H., Canagaratna, M. R., Croteau, P. L., Marth, W. J., Baumann, K., Edgerton, E. S., … Surratt, J. D. (2013). Real-time continuous characterization of secondary organic aerosol derived from isoprene epoxydiols in downtown atlanta, georgia, using the aerodyne aerosol chemical speciation monitor. *Environmental Science & Technology*, *47*(11), 5686–94. doi:10.1021/es400023n

Lelieveld, J., Butler, T. M., Crowley, J. N., Dillon, T. J., Fischer, H., Ganzeveld, L., … Williams, J. (2008). Atmospheric oxidation capacity sustained by a tropical forest. *Nature*, *452*(7188), 737–40. doi:10.1038/nature06870

Xie, Y., Paulot, F., Carter, W. P. L., Nolte, C. G., Luecken, D. J., Hutzell, W. T., … Pinder, R. W. (2013). Understanding the impact of recent advances in isoprene photooxidation on simulations of regional air quality. *Atmospheric Chemistry and Physics*, *13*(16), 8439–8455. doi:10.5194/acp-13-8439-2013